Investigating the Substrate Selectivity and Regulation of Histone Deacetylases

by

Katherine Welker Leng

A dissertation submitted in partial fulfillment
of the requirements for the degree of
Doctor of Philosophy
(Chemistry)
in the University of Michigan
2019

Doctoral Committee:

Professor Carol A. Fierke, Chair
Professor Robert T. Kennedy
Professor Anna K. Mapp
Professor Zaneta Nikolovska-Coleska

Katherine Rebecca Welker Leng

krleng@umich.edu

ORCID iD: 0000-0001-6021-5159

DEDICATION

This dissertation is dedicated to all of my friends and family who have supported and guided me towards achieving my goals as a scientist and as a person.

ACKNOWLEDGEMENTS

I thank my advisor and mentor, Dr. Carol A. Fierke for her guidance and support.
I thank my committee members Dr. Anna K. Mapp, Dr. Robert T. Kennedy, and Dr. Zaneta Nikolovska-Coleska for providing guiding commentary and suggestions for my research.
I thank the members of the Fierke lab, both past and present, including Andrea Stoddard, Dr. Desireé Garcia Torres, Dr. Nancy Wu, and Dr. Benjamin Jennings for their help and companionship.
I thank the past members of the HDAC subgroup for paving the way to allow for the research described in this dissertation.
I thank the current and recent members of the HDAC subgroup, including Kelsey Diffley, Hannah Foley, Dr. Jeff Lopez, Dr. Eric Sullivan, Dr. Carol Ann Castañeda, Dr. Noah Wolfson, and Dr. Byung Chul Kim, for their moral and technical support and their friendship which has helped me through many challenges.
I thank my family, including my parents Ronald and Patricia Leng, my grandparents Douglas and Marguerite Leng, my brother Ryan Leng, my sister Jessica Sturgeon, and my husband, Raymond Welker, for their endless confidence and love. Even though they might not understand what I do, I would not have been able to do it without their presence in my life.

TABLE OF CONTENTS

LIST OF TABLES

LIST OF FIGURES

ABSTRACT

Lysine acetylation regulates thousands of proteins and nearly every cellular process from cell replication to cell death. Dysregulated acetylation has been implicated in diseases including cancer, neurodegenerative disorders, and infectious diseases. For this reason, the enzymes that regulate acetylation, including the histone deacetylases (HDACs), are targeted for drug development, and understanding their biological function is of the utmost importance. Unfortunately, few HDAC-specific substrates have been identified, and how HDACs recognize and select for their substrates, a key aspect of their biological function, is poorly understood. HDAC8, a unique member of class I, is phosphorylated at S39, which affects HDAC8 substrate selectivity *in vitro* and may be used by the cell to regulate HDAC8 biological function. Measuring HDAC8 phosphomimetic mutant S39E-catalyzed deacetylation of various peptides demonstrates altered HDAC8 activity and importantly substrate selectivity. Structural analyses indicate this alteration is due to changes in the substrate binding pocket and active-site architecture. Moreover, wild-type HDAC8 substrate selectivity is influenced by both substrate sequence and structure *in vitro*. Comparing HDAC8-catalyzed deacetylation of histone H3 K9ac, K14ac, and K56ac peptides and proteins reveals that protein structure enhances activity from 40- to over 300-fold, and local sequence determines substrate selectivity, particularly in less structured regions. These data support the use of peptide substrates to determine relative activity and to identify HDAC substrates. To expand on these results, HDAC6-catalyzed deacetylation of a library of peptides was tested to develop a structure-based model of HDAC6 activity. The results reveal HDAC6 distinguishes between sequences, catalyzing deacetylation of peptides with k_{cat}/K_M values from 10 to 10^6 $M^{-1}s^{-1}$. These data demonstrate the usefulness of a prediction model based on peptides. Together, these investigations reveal that phosphorylation, local sequence, and protein structure affect HDAC substrate selectivity and activity *in vitro* and likely play key roles in the biological function and dysfunction of HDACs in the cell. Finally, development of structure-based models combined with peptide-based experiments can be used to identify HDAC substrate candidates for study *in vivo*.

CHAPTER I

Introduction

Post-Translational Modifications, Epigenetics, and Protein Acetylation

Post-Translational Modifications Diversify the Proteome

The central dogma of molecular biology dictates that DNA is transcribed to RNA which is then translated to protein. Out of approximately 20,000 genes in the human genome[1-2] consisting of four deoxyribonucleic acids that code for 20 amino acids, arise all of the building blocks to create life. The fascinating complexity of the human species boils down to a mere 20,000 coding segments of genetic information. Even more perplexing than this is the fact that humans share 96% of their genetic information with chimpanzees[3] and over 40% with fruit flies.[4] It only takes a casual observation to note that there are major differences between fruit flies, chimpanzees, and humans. Even within the human species, where 99.9% of genetic information is shared, there is incredible diversity.[5] In a 2016 TED talk, physicist and entrepreneur Riccardo Sabatini explained that if your entire genetic code was written down, it would fill around 262,000 pages or 175 large books, and that out of all of those pages, only about 500 would be unique to you.[6] The key to this incredible diversity, the differences seen among humans and between humans and other species, lies, in part, with post-translational modifications (PTMs), chemical additions to proteins that alter their functionality.

Currently, over 400 different types of post-translational modifications have been observed, the most abundant and famous of these being phosphorylation.[7] Phosphorylation occurs on serine, threonine, and tyrosine residues within proteins and alters the size, charge, and therefore function of the amino acids. Phosphorylation was first described in the 1950s by Edwin Krebs and Edmond Fischer, who were awarded the Nobel prize in 1992 for their work.[8] Since that time, phosphorylation research has grown to become the most studied PTM. Phosphorylation was found as an integral regulator of countless biological pathways, most

notably metabolism and signal transduction, and a special class of proteins known as kinases were identified as the enzymes responsible for the addition of this PTM.[9-10]

The History of Acetylation and the Birth of Epigenetics

Only a few years after the discovery of phosphorylation, a less conspicuous post-translational modification, and the central topic of this dissertation, was discovered on the tails of histone proteins: acetylation (Figure I.1).[11-12] In comparison to phosphorylation with its unique phosphorous atom and charged oxygens, the acetyl moiety consisting of two carbons, four hydrogens, and an oxygen garnered less attention. However, in the 1960s, researchers started to investigate acetylation more deeply and began to suspect this modest PTM was an important modulator of cellular processes. Although little was known about histones, it was hypothesized that these complex proteins may somehow be responsible for controlling RNA synthesis, and that the chemical groups, including acetylation, peppering the long, unstructured tails of the histones were a key aspect to this regulation. In 1963, following the discoveries of coenzyme A and acetyl CoA in the 1940s and 1950s by Fritz Lipmann, Konrad Bloch, and Feodor Lynen,[13-15] who also received Nobel Prizes for their research (Lipmann together with Hans Kreb for acetyl-CoA and the citric acid cycle in 1954 and Bloch and Lynen for fatty acid metabolism in 1964), Phillips reported the presence of acetyl groups on histones isolated from calf thymus.[11] A year later, in 1964, Allfrey, Faulkner, and Mirsky described the process of acetylation, along with methylation, as a reversible, post-translational mechanism for regulating RNA synthesis.[16]

Fast forward thirty years, and the field of phosphorylation has expanded dramatically as researchers took advantage of methods to visualize and study the PTM's unique phosphorous atom. Without similar strategies available to study acetate, the field of acetylation moved more slowly. However, several important discoveries were made during that time including identification of n-butyrate as an inhibitor of deacetylation in the 1970s[17-20] and acetylation of α-tubulin on residue K40 and the development of residue-specific antibodies in the 1980s.[21-24] Eventually, in the mid-1990s and early 2000s, enzymes were identified and isolated that added, removed, and read acetylation PTMs, and as more information was uncovered about the histone proteins, research in the field of epigenetics rapidly expanded.[12, 25-26] With new advancements in information and protein science, the hypotheses purported by the scientists in the 1960s were confirmed. Histone tail modifications do indeed regulate transcription, and they do so by promoting chromatin condensation (heterochromatin) or relaxation (euchromatin) through direct

alterations of the DNA-protein interactions and/or through the recruitment of chromatin-binding factors and transcriptional remodeling machinery.[27] This selective gene activation and silencing allows cells, which all contain the same genetic information, to differentiate themselves and carry out their discrete and necessary functions.[26] The complex combinations of multiple histone tail modifications have been referred to as *the histone code*, and is currently under heavy investigation.[28-29] It was soon discovered that the histone code is essential for cellular processes and physiological homeostasis, and when these finely tuned systems go awry, the cells quickly degrade, or worse, quickly divide.[26] Numerous diseases are linked to aberrant epigenetics, the most notable of which is cancer.[26] Aberrant acetylation, in particular, is linked to a plethora of diseases, including various types of cancer, neurodegenerative and autoimmune disorders, and infectious disease, among others.[12, 30-34] The enzymes regulating acetylation, the writers known as histone acetytransferases (HATs) and the erasers known as histone deacetylases (HDACs), and the proteins containing acetylation reader *bromodomains* became targets of interest in drug discovery research.[12, 26] Acetylation was observed, predominantly by means of site-specific antibodies, on several dozen additional proteins, including human transcriptional factors p53[35], YY1[36], HMG[37], STAT3[38], GATA[39], EKLF[40], MyoD[41], nuclear androgen[42] and estrogen receptors[43], and NF-κB[44], as well as molecular chaperone Hsp90[45] and viral HIV-Tat,[46] among others, alluding to a broader role for acetylation in the cell.[47]

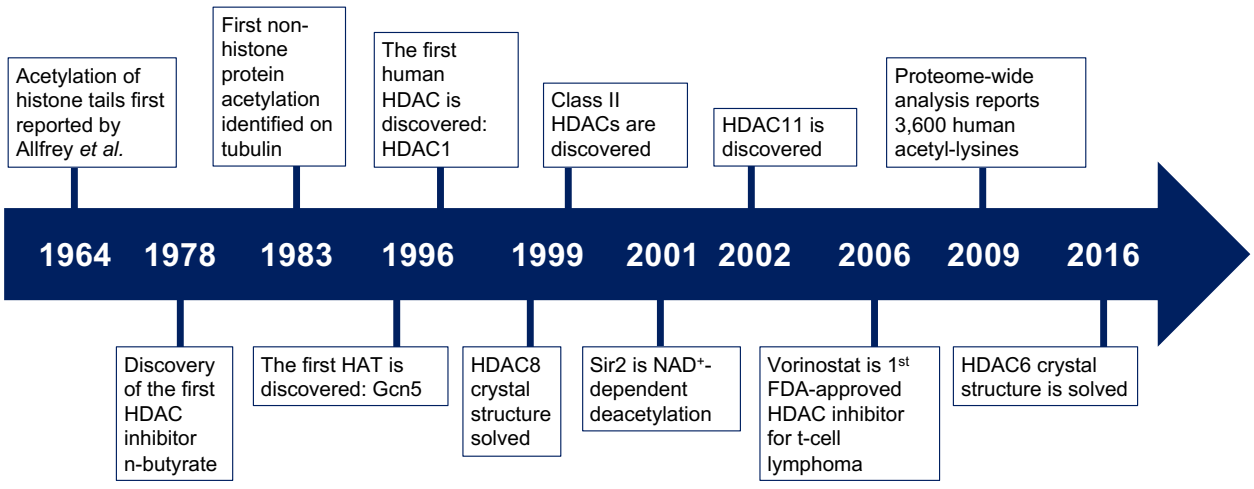

Figure I.1 Timeline of Key Events in Acetylation Research

Summary timeline of acetylation research indicating major discoveries that have occurred over the past 50 years.

Protein Acetylation

Fast forward another 10 years to the last decade, during which new and improved techniques paved the way for the field of research called proteomics and opened the door to study this unobtrusive PTM in miniscule detail. Mass spectrometry advancements allowed researchers to sort through thousands of proteins and differentiate, identify, and measure specific acetylated residues within proteins from other acetylated or non-acetylated residues.[29, 48] In proteome-wide searches, acetylation was observed on significantly greater numbers of proteins than previously identified, thus revealing the broad impact acetylation has in biological pathways ranging from metabolism to cell signaling, a role second only to phosphorylation in significance (Figure I.2).[49-50] Today, using a wide variety of *in silico*, *in vitro*, and *in vivo* tools, researchers are uncovering more information each day about protein acetylation, including the proteins and pathways that are regulating and regulated by acetylation and the ways misacetylation is linked to disease.

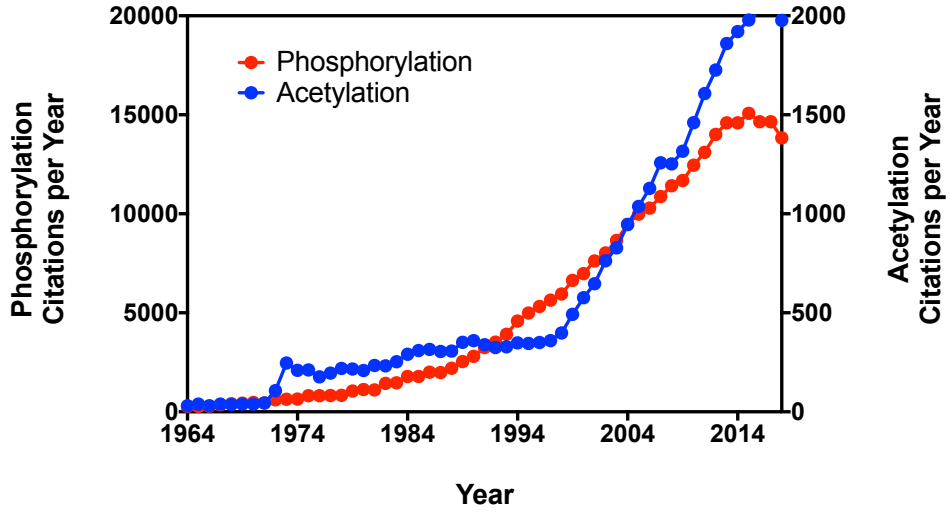

Figure I.2 Acetylation Versus Phosphorylation Publication Growth

Comparison of phosphorylation and acetylation publication growth. Values indicate the number of citations on PubMed referencing the terms 'phosphorylation' or 'acetylation'. Acetylation citation number is plotted on the right-hand y-axis and phosphorylation citation number is plotted on the left-hand y-axis. Data presented in previous review.[51]

Bromodomains, Histone Acetyltransferases, and Histone Deacetylases

Acetylation Readers and Writers

Canonical acetylation occurs on the ε-amino group of lysine residues within proteins. The PTM is enzymatically added and removed. Although spontaneous (chemical) acetylation has been observed under certain circumstances, namely in the mitochondria where high acetyl-CoA concentrations and pH conditions favor the reaction, acetylation is irreversible without enzymatic intervention.[52] Acetylation also occurs on the N-termini of nascent proteins where it is important for protein stability, folding, and binding.[53] Acetylation can occur on proteins in the nuclear, cytoplasmic, and mitochondrial compartments of the cell leading to a wide variety of outcomes.[48] On histones, acetylation is generally associated with euchromatin and active transcription, whereas deacetylation is associated with heterochromatin and lack of transcription (Figure I.3). This phenomenon was originally attributed to the neutralization of lysine's positive charge and consequently the interruption of electrostatic interactions between the histones and negatively charged DNA. However, the process has proved to be significantly more complicated, involving recruitment of transcription factors and chromatin remodeling complexes, and this mechanism is not fully understood.

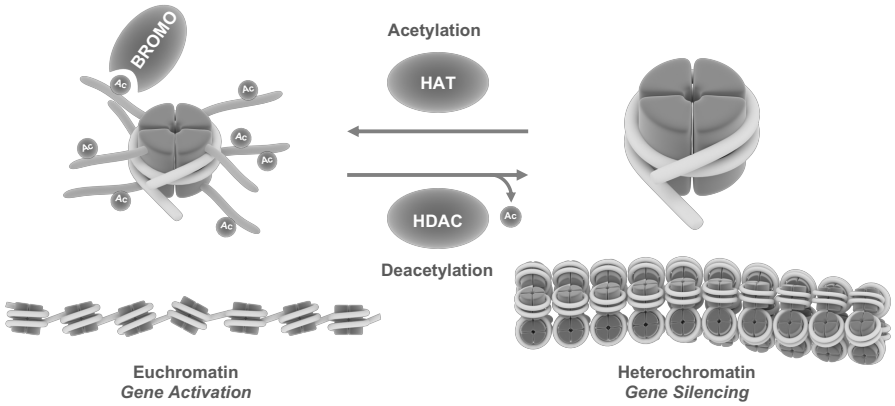

Figure I.3 Histone Acetylation and Transcriptional Regulation[1]

Lysine acetylation by histone acetyltransferases (HAT) on the N-terminal tails of histones regulates transcription through altering the charge state of lysine and recruiting chromatin remodeling machinery that allow for chromatin relaxation and transcription activation. Acetylation PTMs are read by bromodomains (BROMO) and deacetylated by histone deacetylases (HDAC) returning chromatin to its condensed state and silencing transcription.

[1] Figure created using media from the Library of Science and Medical Illustrations provided by somersault 18:24 (www.somersault1824.com) and protected under the Creative Commons license CC BY-NC-SA 4.0.

Shortly before the discovery of acetylation writers and erasers, a *reader* domain was reported.[54] Bromodomains recognize and bind to acetylated lysine residues and are generally structurally conserved with four α-helices forming a hydrophobic cavity and a few conserved residues including an asparagine residue that facilitates acetyl-lysine recognition.[55] Bromodomains have very little sequence homology due to a wide range of acetyl-lysine residue-specific selectivity for acetyl-lysine.[55] Currently, over 40 proteins have been identified with over 60 putative bromodomains, and only half of those have been verified to bind specific acetyl-lysine residues.[55] These proteins have varying functions serving as scaffolds, transcription factors, transcriptional co-regulators, and biological catalysts, and due to their dysregulation in a number of diseases, are targeted with small molecule inhibitors.[55]

The enzymes responsible for adding acetylation to lysine residues within proteins are known as histone acetyltransferases (HATs), named for their first, and at the time presumed only, substrate or more appropriately lysine acetyltransferases (KATs). In 1996, a protozoan enzyme was isolated and shown to be homologous to yeast Gcn5 and capable of catalyzing lysine acetylation.[56] Since then, the number of histone acetyltransferases (HATs or KATs) has grown to over 20 widely varied proteins identified from different species.[57] This family of enzymes is currently divided into five sub-families: HAT1, Gcn5/PCAF, MYST, CBP/p300 and Rtt109.[58] Like kinases, this divergent family of enzymes share a structurally homologous core made up of three β-sheets flanked by an acetyl-CoA binding α-helix.[59] Interestingly, these enzymes share very little sequence homology within this catalytic domain as well as within their N- and C-terminal domains.[60] Furthermore, although these enzymes catalyze the same acetylation reaction, they do so by using multiple mechanisms.[60] This diversity has led researchers to suggest that more structurally and mechanistically diverse HATs remain to be discovered, as currently known enzymes were identified through having at least some homology to other known acetyltransferases.[58] Although HAT substrates are far from being fully characterized, some HATs recognize specific lysine residues, particularly on histones, and small molecule modulators are of clinical interest due to aberrant HAT activity in cancer, autoimmune disorders, diabetes, and infectious disease.[58]

Acetylation Erasers and Disease

The histone deacetylase (HDAC) family of enzymes is responsible for removing acetyl-lysine post translational modifications. This family of enzymes, also known as lysine deacetylases

(KDACs) or more appropriately acetyl-lysine deacetylases (AcKDACs), consists of 18 enzymes divided into four classes, based on phylogenetic similarities (Figure I.4).[61-62] Class I, II, and IV are mechanistically similar relying on a catalytic divalent ion to perform deacetylation. Class III, the sirtuins, are mechanistically dissimilar from the other classes, relying on an NAD^+ co-substrate to carry out deacetylation. HDACs have been linked to human disease, and HDAC inhibition has proven to be promising in indications ranging from neurogenerative disorders to cancer.[63] Although genetic deletions of all class I HDACs as well as HDAC4, HDAC7, and both HDAC5 and HDAC9 are lethal in mice, conditional deletions after development are non-fatal, underscoring the importance of HDACs in development and explaining the surprising efficacy of global inhibition of metal-dependent HDACs in certain indications.[63]

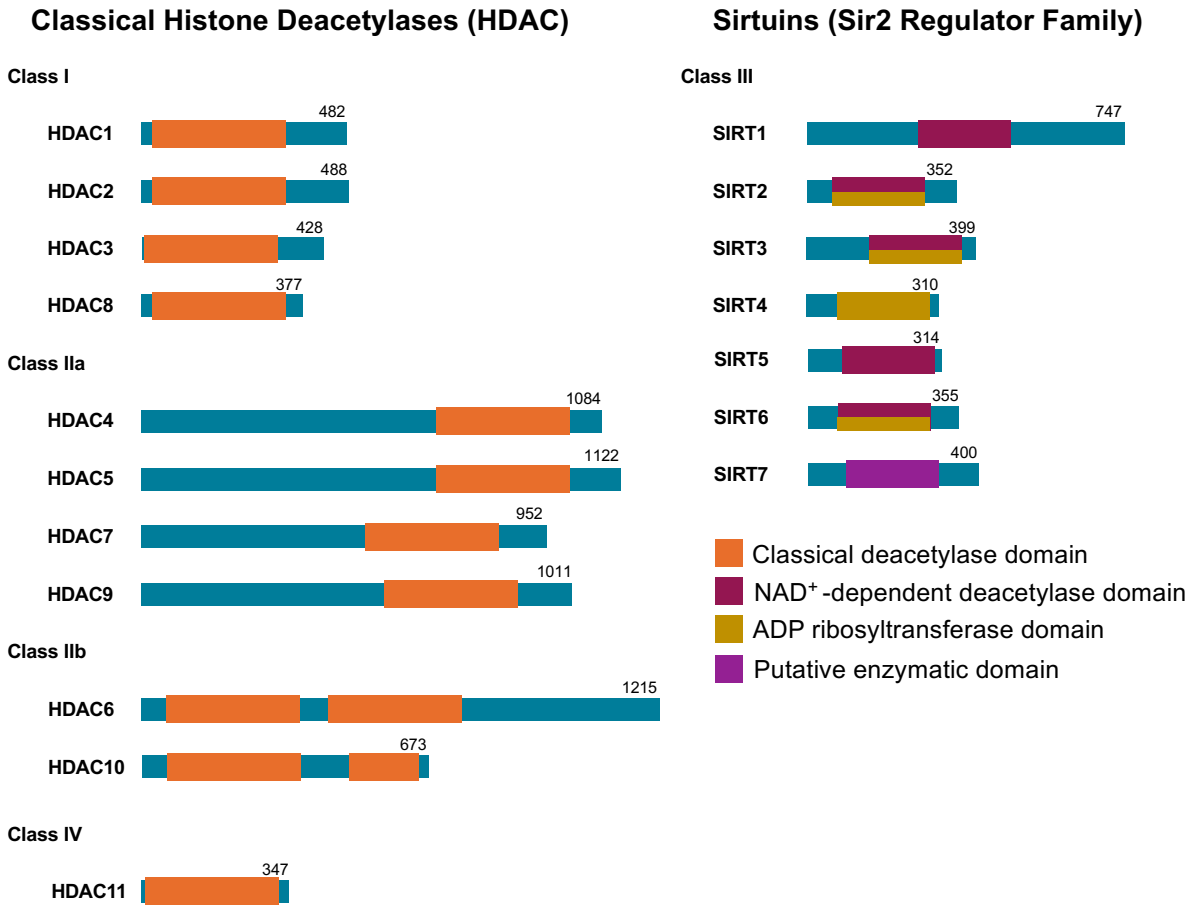

Figure I.4 Family of Histone Deacetylases

Structural representation of histone deacetylase classes I-IV indicating amino acid length, functional (and putative) catalytic domains. Figure adapted from Seto and Yoshida, 2014.[64]

To date, there are four FDA-approved inhibitors targeting HDACs (Figure I.5): Merck's Zolinza (vorinostat/suberoylanilide hydroxamic acid or SAHA),[65-67] Celgene's Istodax (romidepsin),[68-69] and Onxeo's Beleodaq (belinostat)[70-71] for T-cell lymphoma and Novartis's Farydak (panobinostat) for multiple myeloma.[72-73] Unfortunately, since these compounds are non-selective and target most of the metal-dependent deacetylases to some extent, they are often treated as the drug of last resort due to toxicity and adverse side effects including fatigue, weight loss, nausea, diarrhea, and low blood cell count.[74] Additional compounds are currently undergoing clinical trials with many more inhibitors in development.[75] A recent survey reported patents filed for over 70 HDAC inhibitors between 2013-2017.[76] Most of these compounds were isozyme-specific, and while over 100 clinical trials were currently underway, less than 5% have reached stage III, emphasizing an ongoing need for the development of more effective therapeutics.[76]

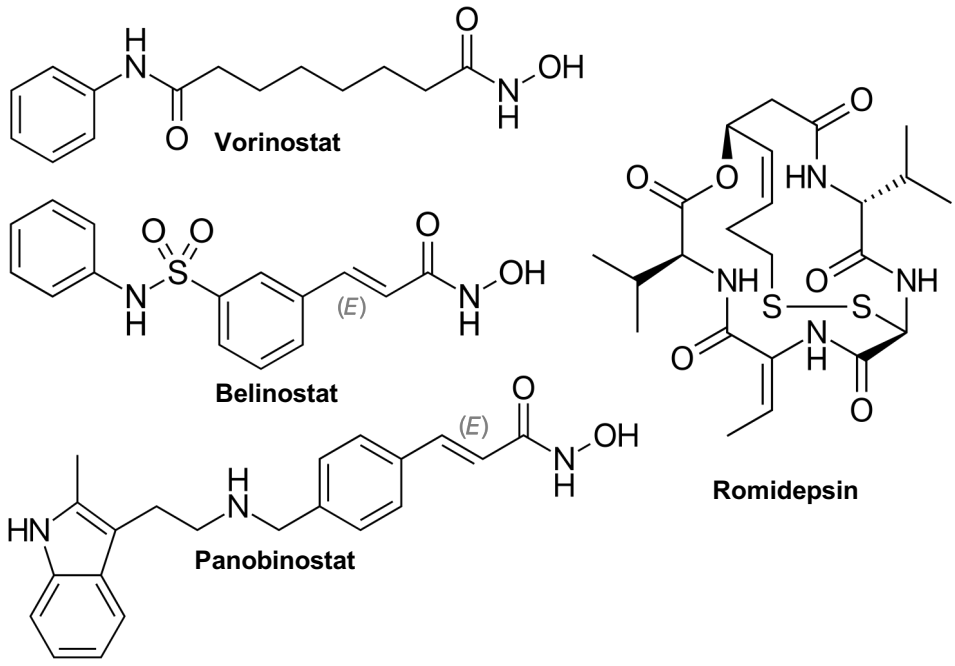

Figure I.5 FDA-approved pan-HDAC inhibitors

Chemical structures of the four FDA-approved histone deacetylase inhibitors, hydroxamic acids vorinostat, belinostat, and panobinostat and depsipeptide romidepsin, for treatment of t-cell lymphoma (vorinostat, belinostat, romidepsin) and multiple myeloma (panobinostat).

Class I HDACs

Class I HDACs (HDAC1[77], HDAC2[78], HDAC3[79-80], and HDAC8[81-82]) share similarities with the yeast deacetylase Rpd3 (reduced potassium dependency 3). In 1996, the first human HDAC was purified (aptly named HDAC1), and whose sequence similarity with Rpd3, a known gene regulator, quickly spurred the search and subsequent identification of other isozymes.[12, 77] Class I HDACs are predominantly nuclear, although HDAC8 and HDAC3 have been observed in both the nucleus and the cytoplasm and contain nuclear localization and export signals.[83] HDAC1 and HDAC2 are nearly identical sharing 82% sequence identity and often displaying functional redundancy.[84] HDAC1 and HDAC2 are components of large chromosomal remodeling complexes including Sin3, NuRD, and CoREST. Additionally, HDAC1 and HDAC2 are post-translationally phosphorylated, which regulates their activity and facilitates protein-protein interactions. The functions of HDAC3 and HDAC8, sharing 34% sequence identity with each other, are more varied and less well defined.[84] HDAC3, in association with class II HDACs -4, -5, and -7, was found to be linked to two co-repressor complexes N-CoR (nuclear receptor co-repressor) and SMRT (silencing mediator of retinoic acid and thyroid hormone receptors).[85-87] HDAC8 is not observed to associate with any known complexes in cells, and activity is retained in the absence of any cofactors when recombinantly expressed and purified.[88] Class I HDACs are ubiquitously expressed, however, expression levels change depending on cell type and disease.[89] All four isozymes have been linked to a variety of diseases including cancer, neurodegeneration, and autoimmunity.[31]

Class II HDACs

Class II HDACs (HDAC4[85], HDAC5[85], HDAC6[85], HDAC7[86], HDAC9[90], and HDAC10[91-92]) share homology with the yeast deacetylase Hda1. Larger than class I isozymes with molecular weights ranging from 80-131 kDa, these enzymes are divided into sub-classes IIa and IIb. Class IIa HDACs (HDAC4, HDAC5, HDAC7, and HDAC9) contain one deacetylase domain, while Class IIb HDACs, HDAC6 and HDAC10, contain two fully intact deacetylase domains and one intact and one partial deacetylase domain, respectively.[64] Generally speaking, class IIa HDACs shuttle between the nucleus and cytoplasm and have low deacetylase activity when purified and have been proposed to have predominantly non-deacetylation roles in the cell.[64, 84-85] In contrast, class IIb HDACs catalyze deacetylation and are predominantly cytoplasmic, although HDAC6 has been observed in the nucleus in complex with HDAC11.[84, 93]

The activity of class II HDACs can be regulated through post-translational modifications and protein-protein interactions. For example, HDAC4, HDAC5, and HDAC7 are phosphorylated which regulates their interaction with 14-3-3 proteins that anchor the HDACs in the cytoplasm.[94] Complex disassociation allows for these enzymes to translocate to the nucleus where they interact with HDAC3.[85, 94] Additionally, HDAC4 and other class II HDACs have been shown to interact with MEF2 proteins.[95] HDAC4, HDAC5, and HDAC7 have divergent N and C-terminal extensions that presumably facilitate isozyme-specific functions.[62] The N-terminal domains of these isozymes share homology, except HDAC7 lacks a nuclear export signal.[84] HDAC10 is one of the least studied deacetylases and its function is not well understood.[64] Recently, however, HDAC10 was shown to function as a polyamine deacetylase.[96] In contrast, HDAC6 has become one of the most studied isozymes due to its predominantly cytoplasmic role and involvement in a separate set of cellular functions and disease.[84]

Class III HDACs

Class III HDACs, the sirtuins SIRT1-7, unlike their metalloenzyme cousins, use NAD^+ as a cosubstrate.[97] The sirtuins, like the classic HDACs, bind a zinc(II) ion, however, the ion serves a structural rather than catalytic role.[98] The sirtuins are named for their homology to yeast Sir2 (silent information regulator 2), a transcriptional regulator first described in the 1970s and heavily investigated for its apparent role in starvation and longevity.[97, 99] Human sirtuins were identified as deacetylases due to their homology to Sir2 and their ability to catalyze deacetylation of core histones, transcription factors, and other acetylated proteins.[97, 100-101] Sirtuins have a conserved catalytic core with varying N- and C-terminal sequences and use NAD^+ as a cosubstrate to form nicotinamide, adenine diphosphate ribose, acetate, and the deacetylated protein product.[100, 102-103] Although there is some functional redundancy, the sirtuins vary in subcellular localization, substrate selectivity, and cellular function.[97] SIRT1, the closest homologue to Sir2, is primarily nuclear, although it shuttles between the nucleus and cytoplasm.[97] SIRT1 deacetylates core histones and various transcription factors.[64] SIRT2, shares similar functions to SIRT1, although it resides primarily in the cytoplasm.[97] Additionally, SIRT2 has been shown to have demyristoylase and mono-ADP-ribosyltransferase activity in addition to deacetylation.[64, 104] SIRT3 is localized to the mitochondria and catalyzes deacetylation and other deacylation reactions.[97] Mitochondrial SIRT4 and SIRT5 display lower activity and also catalyze alternative deacylation reactions.[97] Finally, SIRT6 and SIRT7 are localized to the nucleus with

activity similar to that of SIRT4 and SIRT5.[97, 103] The sirtuins are also implicated in various human diseases including cancer and metabolic and neurodegenerative disorders, among others and are targeted for inhibitor and activator development in drug discovery research.[97]

Class IV HDACs

Class IV contains the remaining human isozyme HDAC11, which is classified separately despite sharing sequence homology with class I HDACs, including 28% sequence homology with HDAC8.[105] Phylogenetic analysis supports three separate sub-families of metal-dependent HDACs with human HDAC11 and other HDAC11-type enzymes falling into the third category.[61] This evidence supports the existence of non-redundant functions for each class in basic cellular processes. Notably, while class I and II are found in all fully-sequenced eukaryotic organisms, there are no class IV enzymes in fungi.[61] Described in 2002, HDAC11 is the most recently identified, and at only 347 residues and 39 kDa, is the smallest classical HDAC.[105] HDAC11 is ubiquitously expressed with increased expression levels in the brain, kidney, heart, skeletal muscle, and testis, suggesting HDAC11 may have tissue-specific roles.[105] Relatively little is known about HDAC11 function in comparison with its class I and II brothers, however abnormally overexpressed HDAC11 has been implicated in breast, kidney, and liver cancers, where inhibition was shown to decrease cancer cell viability, although with some apparent overlap with HDAC1 and HDAC2.[106] An additional role for HDAC11 in the adaptive immune response has been proposed due to its regulation of interleukin-10 expression.[107] Moreover, inhibition of HDAC11 led to enhanced Foxp3+ Treg cell function and Treg-dependent suppression of allograft rejection in a model of organ reperfusion, presumably due to deacetylation of Foxp3.[108] HDAC11 has relatively low deacetylase activity *in vitro*, however, recently HDAC11 has been proposed to have myristoyl-lysine hydrolase functionality.[109] The next section focuses on HDAC8 and HDAC6 as model enzymes from class I and II and the foci of this dissertation.

HDAC8 Function, Regulation, and Physiological Role

HDAC8 Discovery and Structure

HDAC8 was first described in 2000 when three groups published separate analyses of a new class I deacetylase capable of *in vitro* deacetylation of histones.[81-82, 110] Shortly thereafter, in 2004, the crystal structure of human HDAC8 was solved,[111-112] the first reported human

deacetylase structure and the first of many HDAC8 structures. At 377 amino acid residues and 42 kDa and containing little more than a deacetylase domain, HDAC8 is the smallest class I isozyme and the second smallest HDAC (next to HDAC11) (Figure I.7). Since its discovery, HDAC8 has become arguably the best mechanistically and structurally characterized HDAC.[113] HDAC8 displays an arginase-like fold consisting of a single α/β domain arranged with a central eight-stranded β-sheet flanked by eleven α-helices.[68, 111-112, 114-123] The substrate binding surface is characterized by 9 flexible loops and an 11 Å substrate binding tunnel terminating in the active site divalent metal coordinated by a His/Asp/Asp triad.[118, 124] In addition to its catalytic divalent ion, HDAC8 also binds two monovalent ions (K^+ or Na^+) with an activating binding site distal to the active site and an inhibitory site near the active site.[125] These ions allow for regulation of the enzyme depending on cellular conditions and explain the sensitivity of HDAC8 activity to salt concentrations.[125]

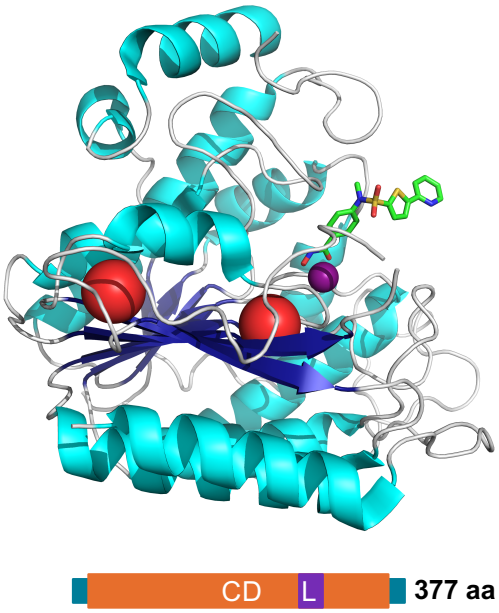

Figure I.6. HDAC8 Structure

HDAC8 crystal structure bound to a hydroxamic acid inhibitor (PDB ID 1W22) and graphical representation highlighting the catalytic domain (CD), nuclear localization signal (L), and amino acid length. Potassium ions are shown in red, the zinc(II) ion is shown in purple, and the inhibitor molecule is shown in green.

HDAC8 Catalytic Mechanism and Metal Activation

The proposed mechanism for HDACs is general acid-base catalysis (GABC), where the active site metal ion coordinates the substrate and a water molecule, and two conserved histidine residues serve as the general acid and/or general base (Figure I.7).[118] In HDAC8, the divalent metal ion is bound to the protein by interactions with D178, D267, and H180, and coordinates the substrate carbonyl and a water molecule. Structural and biochemical data support one catalytic histidine residue, H143, acting as both general acid and general base. This side chain initiates catalysis by deprotonating and activating a water molecule for attack on the carbonyl oxygen of the acetyl moiety to form a tetrahedral intermediate. The second histidine residue H143 is proposed to remain protonated throughout the catalytic cycle, serving as an electrostatic catalyst.[118] Another conserved residue, Y306, enhances catalytic activity, and is proposed to stabilize the oxyanion of the transition state through hydrogen-bonding with the tetrahedral intermediate.[118] Breakdown of the tetrahedral intermediate occurs simultaneously with donation of a proton from protonated H143, now serving as the general acid, to the product amine resulting in free acetate and deacetylated lysine.[118]

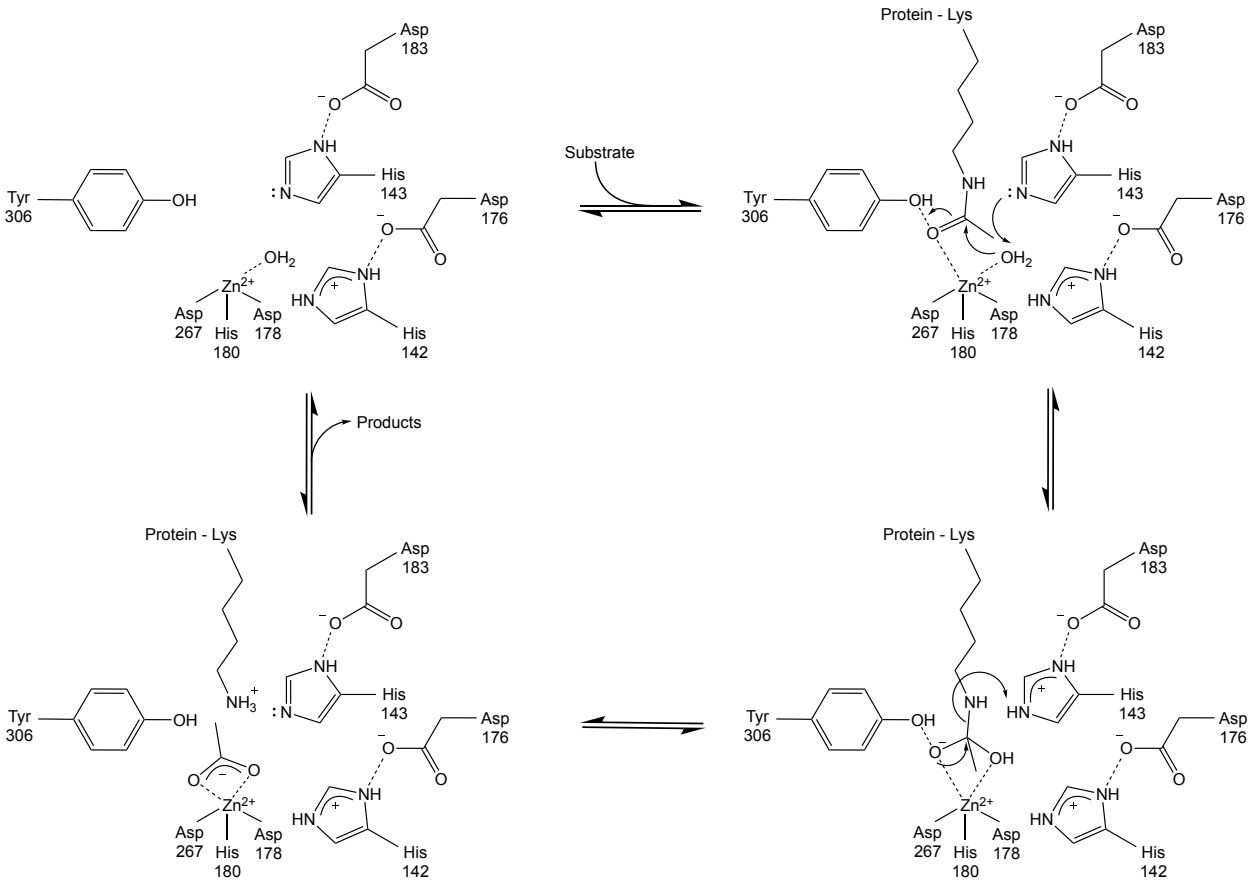

Figure I.7. HDAC8 Mechanism

Proposed catalytic cycle and mechanism of HDAC8 whereby Tyr306 and a zinc(II) ion, coordinated by His180, Asp276, and Asp178, orient the carbonyl oxygen of the acetyl-lysine substrate in the active site to be acted on by catalytic acid/base H143, while protonated H142 serves as an electrostatic catalyst. Figure adapted from Gantt *et al.* 2016.[118]

HDAC8 is activated by multiple catalytic divalent ions including zinc(II), the canonical active site metal, cobalt(II), iron(II), nickel(II), and manganese(II).[88] HDAC8 is most active when bound to cobalt with a $k_{cat}/K_M = 7500 \pm 300$ $M^{-1}s^{-1}$ for deacetylation of the coumarin-tagged test substrate, a p53-derived tetrapeptide.[88] However, cellular levels of cobalt(II) preclude this ion from being the physiologically relevant catalytic metal ion.[88] The next most activating ion is iron(II) at 2300 ± 160 $M^{-1}s^{-1}$ followed by zinc(II) at 800 ± 50 $M^{-1}s^{-1}$.[88] HDAC8 metal affinities (K_D) for these two ions compare to their putative readily exchangeable cellular concentrations, with Zn(II) binding more tightly than the more abundant Fe(II); therefore, both zinc and iron have the potential to be physiologically relevant.[126] Although HDAC8 is bound to zinc when overexpressed, the active site metal of HDAC8 under normal expression conditions

has yet to be determined. Interestingly, HDAC8 is maximally activated by zinc at 1:1 stoichiometry, and excess zinc(II) is inhibitory likely due to a secondary metal binding site.[88] In certain cases, HDAC8 has displayed oxygen sensitivity suggesting HDAC8, or a portion of HDAC8, may be bound to iron(II) *in vivo*.[88] Since HDAC8 is inactive with iron(III), allowing for oxidative regulation of activity, and inhibited by excess zinc(II), the cellular metal ion concentrations may play a crucial role in regulating HDAC8 activity.[88] Additionally, HDAC8 has been shown to have different substrate selectivity depending on the identity of the active site metal ion.[127] HDAC8 may potentially bind either metal ion in cells and be regulated by a metal-switching mechanism, as seen with other metalloenzymes such as the *E. coli* deacetylase LpxC.[128]

HDAC8 Regulation by Localization and Post-Translational Modifications

Unlike nuclear class I HDACs 1-3, HDAC8 has been observed in the nucleus and cytoplasm of cells. In HEK293 cells, HDAC8 is localized in the nucleus, but in smooth muscle cells, skin fibroblasts, and NIH3T3 cells, HDAC8 has been observed in both the nucleus and cytoplasm.[129-130] HDAC8 contains a putative nuclear localization sequence suggesting that HDAC8 may shuttle between the nucleus and cytoplasm. HDAC8 is post-translationally phosphorylated at residue Ser39 by protein kinase A (PKA), which effects enzyme structure and function (see Chapter II). Although other HDACs are post-translationally acetylated, ubiquitinated, and sumoylated, the only PTM reported for HDAC8 is phosphorylation of S39.

HDAC8 Protein-Protein Interactions

While other class I and class II isozymes have known functions in protein complexes that regulate their activity and function, HDAC8 has not been observed in any known functional protein complexes. Furthermore, HDAC8 is purified and is catalytically active *in vitro* in the absence of binding partners, suggesting HDAC8 acts predominantly as a monomer *in vivo*. If protein-protein interactions are weak or short-lived, regardless of their importance, such complexes may escape detection by current methods. However, HDAC8 does interact with other proteins that may regulate HDAC8 activity and selectivity.

For example, in HEK293 cells, overexpressed HDAC8 co-immunoprecipitates with nuclear cAMP responsive element-binding protein (CREB) and its phosphatase PP1, resulting in CREB dephosphorylation and inactivation.[131] Additionally, HDAC8 colocalizes with α-actin in

the cytoskeleton of human smooth muscle NIH-3T3 fibroblast cells, and HDAC8 RNAi decreased cell spreading thus suggesting a role for HDAC8 in smooth muscle cytoskeleton regulation and contraction.[129-130] Moreover, HDAC8 co-immunoprecipitates with Hsp20, cofilin, α-actin, and myosin heavy chain in myometrial smooth muscle cells and impacts Hsp20 acetylation and muscle contraction.[132] Another study demonstrated that overexpressed HDAC8 in HeLa cells coimmunoprecipitates with overexpressed human Ever-Shorter Telomeres 1B (hEST1B) and HOP1 and endogenous levels of HOP1 interacting partners Hsp70 and Hsp90.[133] As Hsp90 is a known modulator of α-actin and α-tubulin, this provides further evidence of HDAC8 regulation of cytoskeletal dynamics.[133]

In a comprehensive study to elucidate and characterize the interaction network or 'interactome' of histone deacetylases, over a dozen protein interactions, including SMC1A and SMC3, were identified for HDAC8 by immunoprecipitation in CEM T-cells stably expressing HDAC8.[134] Over half of the proteins identified had a non-canonical or unknown role in biological processes, while the other half was split between cell-cycle and transportation processes.[134] This study was limited to identifying the most stable complexes under one set of experimental conditions and was unable to measure the stoichiometry and composition of the complexes. Although there is strong evidence that SMC3 is an HDAC8 substrate,[135-136] little information exists to implicate the remaining proteins as HDAC8 substrates, some of which have not been identified as acetylated. The role of HDAC8 in these protein-protein interactions is difficult to identify. HDAC8 may provide scaffolding or other activity-independent functions in these interactions, or HDAC8 may directly deacetylate or initiate a cascade that results in deacetylation of its interacting partner(s). As HDAC8 substrate disassociation is proposed to be rapid to facilitate turnover, interactions that survive pull-downs or are long lasting enough to be visualized in another manner are likely not HDAC8 substrates. Interestingly, the proteins that immunoprecipitated with HDAC8 were predominantly specific for this isozyme, unlike the complex network of overlapping protein-protein interactions between HDAC1 and HDAC2.[134] This study underscores the significance of protein complexes for HDAC1 and HDAC2 and suggests lower significance of protein complexes for the cellular function of HDAC8, further emphasizing the functional differences between isozymes.

In efforts to capture transient interactions and identify potential HDAC8 substrates, non-natural amino acid incorporation was used to insert a photocrosslinker into specific sites within

HDAC8, including one near the active site, to covalently link HDAC8 with any interactors in HEK293 cell lysates.[137] The study reported the identification of numerous protein interactors by mass spectrometry. Hits from photocrosslinkers distal to the active site were identified as binding partners, while hits from the active site photocrosslinker, including Hsp90 and α-tubulin, were identified as putative substrates.[137] Furthermore, acetylated peptide substrates corresponding to those proteins showed reactivity with HDAC8 *in vitro*.[137] Other substrate-enzyme interactions were proposed by an acetylome-wide survey of proteins affected by treatment with an HDAC8-specific inhibitor, PCI-34051, in MCF-7 cells. Using stable isotope labeling in cell culture coupled with mass spectrometry (SILAC-MS), about a dozen proteins, including previously reported SMC3 as well as novel proteins such as ARID1A, RAI1, NCOA3, and KAT14, were identified with differentially increased acetylation upon HDAC8i compared to controls.[138] Although the study could only provide evidence of HDAC8-mediated hyperacetylation and not direct deacetylation of these proteins by HDAC8, acetylated peptides corresponding to the putative substrates demonstrated reactivity with HDAC8 *in vitro*.[138]

HDAC8 in Development and Cornelia de Lange Syndrome

The physiological role of HDAC8 is poorly understood, however HDAC8 has been connected to a number of cellular processes. First, HDAC8 appears to be integral to development. Embryonic knockout of HDAC8 leads to perinatal death in mice due to skull defects leading to brain hemorrhage.[139] The skull defects result from improper neural crest patterning, a phenomenon seen upon overexpression of transcription factors Otx2 and Lhx1, suggesting HDAC8 may be involved either directly or indirectly in regulation of these proteins.[139] Conditional deletions of HDAC8 are non-lethal; however, mutations to HDAC8 have been linked to a rare genetic disorder called Cornelia de Lange syndrome (CdLS) caused by defects in the cohesin complex.[121-122, 135, 139-142] The cohesin complex regulates the separation of sister chromatids during cell division, and errors in this process lead to the developmental disorder characterized by physical and intellectual impairments. While the majority of CdLS cases arise due to mutations in proteins within this complex, including SMC3 (structural maintenance of chromosomes 3), a number of HDAC8 loss-of-function mutations led to the same phenotype.[135, 142] As SMC3 is post-translationally acetylated and assists in complex formation, it is hypothesized that HDAC8-catalyzed deacetylation of SMC3 promotes complex disassociation leading to separation of sister chromatids under normal conditions, and impaired

HDAC8 leads to hyperacetylated SMC3 and prolonged complex association.[135] Moreover, HDAC8 is implicated in neural-crest derived childhood neuroblastoma (described in the next section), which also indicates a prominent role for HDAC8 in development and developmental-related disorders.[143]

HDAC8 in cancer

HDAC8 has been implicated in numerous types of cancer including lymphoma/leukemia, childhood neuroblastoma, and breast cancers, among others, although HDAC8 function in pathology is not fully understood. [144] For this reason, HDAC8 is an attractive target for drug development. Higher expression levels of HDAC8 mRNA are reported in numerous cancer cell lines and tissues including leukemia, neuroblastoma, and female reproductive system cancers, compared to normal cells and tissues.[89] Analysis of protein expression levels of class I HDACs by immunoblot and immunostaining reported that while the enzymes, including HDAC8, were expressed in the selected cancerous cell types, they were only slightly overexpressed in comparison with the corresponding normal cell types and tissues.[145] However, in a study focusing on liver cancer, HDAC8 mRNA and protein expression were elevated in several hepatocellular carcinoma (HCC) tissues and cell lines compared to paired normal tissues and cells, and RNAi knockdown of HDAC8 decreased cell growth and proliferation.[146] Moreover, HDAC8 dysregulation may play a predominant role in disease progression, despite normal expression levels,

Vannini *et al.* reported HDAC8 RNAi-mediated growth inhibition of lung (A549), colon (HCT-116), and cervical (HeLa) cancer cell lines.[111] In contrast, a study reporting on the activity of HDAC8-specific inhibitor PCI-34051 demonstrated poor growth inhibition and no apoptosis of these cells and other solid tumor lines at the dosage tested.[147] The difference could be due to the difference between RNAi- and PCI-34051-mediated inhibition the analysis used. However, PCI-34051 effectively inhibited growth and induced apoptosis of T-cell derived cell lines (Jurkat, HuT78, HSB-2, and Molt-4).[147] This is in agreement with another study that placed HDAC8, along with transcription factors SOX4 and FRA-2/JUND, in an oncogenic cascade implicated in promoting cell growth of acute t-cell leukemia/lymphoma (ATL).[148] SOX4, activated by FRA-2/JUND, in turn upregulates HDAC8 expression by activation of the HDAC8 promoter.[148] RNAi knockdown of members of this cascade, including HDAC8, suppresses ATL cell growth.[148]

In acute myeloid leukemia (AML), approximately 8% of cases harbor the inversion(16) chromosomal translocation and resulting chimera protein inv(16). The fusion protein interacts with HDAC8 and mSin3a (and mSin3a-associated HDACs) separately to promote the inv(16)-mediated transcriptional repression linked to AML pathology.[149] HDAC8 is further implicated in inv(16)$^+$ AML through regulation of p53 acetylation, where hypoacetylated p53 promotes leukemia stem cell transformation and maintenance.[150] HDAC8i treatment with compound 22d[151] led to apoptosis in inv(16)$^+$ CD34$^+$ cells and decreased AML tumorigenesis and propagation. Furthermore, HDAC8 regulates mRNA and protein expression of p53 in colon and pancreatic cancer cell lines, suggesting HDAC8i may be a therapeutic approach to treatment of mutant p53-directed cancers.[152] Since the p53 gene is the most frequently mutated gene in cancer, these findings underscore the clinical significance and potential for HDAC8 inhibition.[153]

In triple negative breast cancer (TNBC), HDAC8 mRNA overexpression was observed in 24% of tested clinical tissues samples compared to controls, and HDAC8 overexpression correlated with late stage disease and poor prognosis in early-stage.[154] Breast cancer is the 2nd leading cause of cancer-related mortality in the United States, and TNBC, a highly malignant form, is often metastatic and difficult to treat due to the lack of targetable hormone receptors. Inhibition of HDAC8 by RNAi or PCI-34051 treatment yielded impaired TNBC cell migration, and altered the expression of numerous cell-movement- and cancer-related genes. In a similar study, RNAi of HDAC1, HDAC8, and HDAC6 repressed TNBC cell migration and invasion, and induced cell-cycle arrest and apoptosis.[155]

HDAC8 also appears to play a prominent role in childhood neuroblastoma, a solid tumor cancer that accounts for 10% of childhood cancers, 15% of childhood mortality from cancer, and 50% of infant cancers.[156] Neuroblastoma, a cancer arising from neural crest-derived cells, most often affects infants (<18 months) where it generally results in good outcomes, even in late stages (>90% survival).[139] However, in older children (>18 months), neuroblastoma tumors are particularly malignant and metastatic resulting in poor prognosis (<30% survival).[74] As mentioned in the previous section, global deletion of HDAC8 in mice results in perinatal lethality due to morphological errors in skull development attributed aberrant HDAC8 in cranial neural crest cells.[139] HDAC8 was identified as the only classical HDAC whose expression correlated significantly with late stage disease and metastasis.[143] Interestingly, downregulation of HDAC8 correlated with stage 4S neuroblastoma, which is associated with spontaneous

regression.[143] Moreover, HDAC8-specific inhibition in neuroblastoma cell lines and xenograft mouse neuroblastoma models led to cell cycle arrest and differentiation without the toxicity associated with pan-HDAC inhibitor SAHA.[157] In addition to HDAC inhibitors and combinatorial treatments, micro RNAs, short non-coding suppressive RNA elements, may prove to be therapeutic approaches for downregulating HDAC8 mRNA expression along with other oncogenes in neuroblastoma.[158-159] Together, these results suggest HDAC8 inhibition is a promising strategy for treatment of these highly malignant and devastating cancers.

HDAC8 in Infectious Disease

HDAC8 is also implicated as a target to treat infectious disease. In the neglected tropical disease schistosomiasis, the HDAC8 orthologue in the parasitic flatworm *Schistosoma mansoni* is an ongoing target for drug discovery.[160] Schistosomiasis affects over 200 million people resulting in up to 200,000 deaths per year worldwide. Currently, praziquantel is the primary drug for treatment of schistosomaisis. While effective, praziquantel is at risk for resistance development due to lack of alternative treatments and praziquantel's widespread use, as it is often administered as a preventive measure in at-risk communities. The HDAC pan-inhibitor TSA leads to larvae and adult flatworm death. HDAC8 is the least conserved and most abundant HDAC orthologue in *S. mansoni*. Therefore HDAC8-specific inhibitors may prove to be effective treatment options without the side-effects caused by TSA.[161-163] HDAC8 has also been implicated in influenza A infection, where cellular HDAC8 promotes viral mechanisms including endocytosis, acidification, and penetration, and HDAC8 RNAi resulted in reduced viral infection rates.[164]

HDAC6 structure and physiological role

HDAC6 Discovery, Structure, and Mechanism

Histone deacetylase 6 (HDAC6), first described in 1999 by Grozinger and colleagues, is unique among the family of HDACs.[85] HDAC6 is the largest of the HDACs at 1,215 amino acid residues and contains two active catalytic domains (CD1 and CD2) with different substrate specificity and selectivity.[62, 85, 165-166] Along with HDAC10, which contains one active and one partial, inactive catalytic domain, HDAC6 belongs to class IIb.[91] While class I HDACs (HDAC1-3, 8) are primarily localized in the nucleus and are ubiquitously expressed to differing levels depending on tissue type, class II HDACs (HDAC4-7,9-10) are predominantly

cytoplasmic and appear to have more tissue-specific roles.[79, 82, 84, 167] Class IIa HDACs have modest to no activity, and it is proposed that these enzymes may perform other functions within the cell.[62] On the other hand, HDAC6 is robustly active *in vitro.*[165] HDAC6 contains other important and unique structural features (Figure I.8). An N-terminal nuclear localization signal (L) and N- and C-terminal nuclear export signals (E) allow HDAC6 to travel between the nucleus and cytoplasm, and a C-terminal serine glutamate tetradecapeptide repeat (SE14) facilitates cytoplasmic retention.[165, 167] Interestingly, HDAC6 also contains a C-terminal zinc finger ubiquitin binding domain (BUZ) which may participate in both deacetylase dependent and independent functions.[165, 168-169] Several physiological roles have been proposed for HDAC6 mainly in the cytosol, including cytoskeleton dynamics, protein degradation and cellular stress.

Figure I.8 Diagram of HDAC6 structural features

Human HDAC6 (blue) is composed of 1,215 amino acid residues organized into several key domains: N-terminal nuclear localization signal and C-terminal serine-glutamate tetradecapeptide repeat cytoplasmic retention domain (L and SE14, respectively in yellow), N- and C-terminal nuclear export signals (E in teal), catalytic domains 1 and 2 (CD1 and CD2 in orange), and finally the dynein motor binding domain and ubiquitin binding zinc finger domain (DM and BUZ, respectively in red).

HDAC6 and Cytoskeleton Dynamics

HDAC6 plays an important role in cell function through interaction with the cytoskeleton.[170] Alpha- and beta- tubulin polymerize to form microtubules, which along with actin polymers (microfilaments) and fibrillary proteins, form the eukaryotic cytoskeleton.[171] The cytoskeleton is a crucial element of the cell, providing cell structure and flexibility, aiding in tissue organization, and regulating cell cycle through maintenance of cytoskeletal dynamics involved in cell growth, movement, and division.[172] The cytoskeleton is also important in cell signaling where signal uptake and intracellular transport are key components of signal cascades.[173-175] Acetylation of α-tubulin, most notably at K40 within the actin binding domain of cortactin, aids in microtubule and microfilament polymerization. In contrast, deacetylation, catalyzed at least in part by HDAC6, is associated with microtubule depolymerization and consequently cytoskeletal reorganization.[170, 176-179]

HDAC6 in Protein Degradation and Cellular Stress

HDAC6 plays an integral role in protein degradation, where the balance between two protein degradation pathways, the proteasome-ubiquitin system and autophagy, is dependent on HDAC6.[180] Under normal, non-stressed cellular conditions, the proteasome-ubiquitin system clears mis-folded proteins.[181] Under these conditions, HDAC6 is complexed with heat shock protein 90 (Hsp90) and heat shock factor 1 (HSF1), as shown by Hsp90 pull-downs from mouse fibroblasts.[182] When the proteasome is inhibited, or accumulation of mis-folded proteins occurs faster than the proteasome can clear them, proteasome-independent autophagy is triggered.[183] Under these conditions, the complex dissociates as HDAC6 binds to excess ubiquitinated proteins and associates with dynein motor proteins to transport the cargo along the microtubule to undergo autophagy.[184-186] Additionally, release of HSF1 and deacetylation of Hsp90 catalyzed by HDAC6 is proposed to activate chaperone activity aiding in cellular stress response.[45, 182, 187-188]

HDAC6 as a drug target

Over the past 20 years, HDAC6 has risen to be one of the most studied deacetylases as seen in the increase in publications mentioning HDAC6 (Figure I.9). Indeed, many drug discovery efforts have focused on the development of HDAC6-specific inhibitors. Recently, the crystal structures of HDAC6 catalytic domains 1 & 2 were reported.[165, 189] Before the HDAC6 structure was known, rational inhibitor design depended on homology models.[190] The crystal structure of HDAC6 now allows for rationale inhibitor design and the development of more effective compounds. In a recent HDAC inhibitor patent survey, over two thirds of the patents for isozyme-specific inhibitors targeted HDAC6.[76] While class I HDACs, in particular HDAC1 and HDAC2, have been targeted due to an apparent role in chromatin remodeling and overexpression in various cancer subtypes,[191] the role of HDAC6 in disease remains mysterious, as aberrant increased and decreased activity is observed in cancer,[180] neurodegenerative diseases,[169] and autoimmune disorders.[192] Although HDAC6i appears to be antagonistic in certain disease states, data suggest that HDAC6i is a promising therapeutic route in other indications.[193]

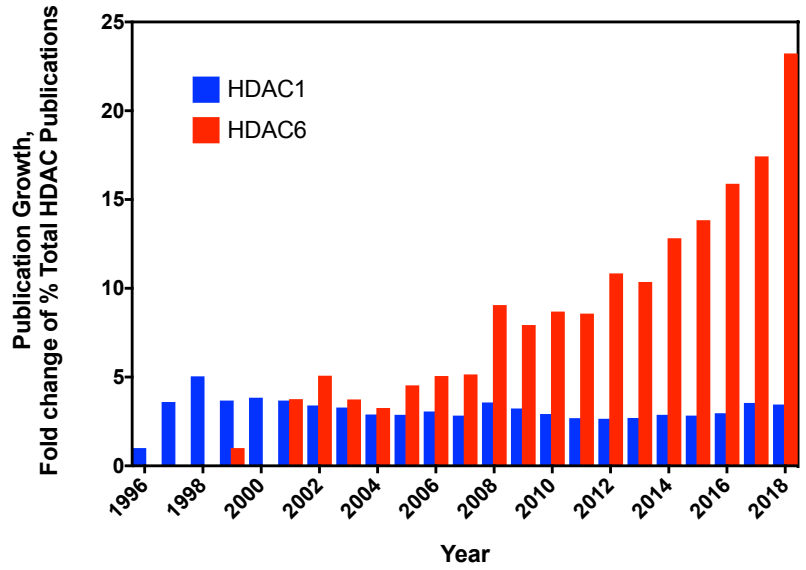

Figure I.9. Publication growth of HDAC6 has drastically increased over the past decade compared to most cited deacetylase: HDAC1

Graph represents fold change in the HDAC1 (blue bars) and HDAC6 (red bars) percentage of total yearly HDAC publications compared to the first year mentioned (1996 for HDAC1, 1999 for HDAC6). Pubmed search input for total HDAC Publications: "HDAC" OR "Histone Deacetylase"; HDAC6 publications: "HDAC6" OR "Histone Deacetylase 6"; HDAC1 publications: "HDAC1" OR "Histone deacetylase 1".

HDAC6 in cancer

HDAC6 is an attractive target in cancer therapeutics since its role in cell cycle regulation, cellular stress response, and cell signaling is often a contributing factor in oncogenic transformation and tumor cell survival (reviewed by Aldana-Masangkay and Sakamoto 2011).[180] HDAC6 misregulation of cortactin, α-tubulin, and cytoskeletal dynamics aids in tumor metastasis,[177, 194] and HDAC6 clearance of misfolded proteins and activation of the heat shock response promotes cell survival.[182, 195] HDAC6 also appears to play a role in Ras/MAPK signaling regulation where it aids in oncogenic transformation through an unknown mechanism.[195-196] In addition, HDAC6 overexpression has been implicated in a variety of cancer types including breast,[155, 197-201] ovarian,[202-204] oral squamous,[205] cutaneous T-cell lymphoma,[206] and acute myloid and lymphoblastic leukemia cancers,[207] among others, underscoring the diverse role of HDAC6 in oncogenic pathologies, the necessity of better understanding those roles, and the therapeutic potential of targeting HDAC6 in cancer.

HDAC6 in neurodegenerative disease

Accumulation of misfolded proteins is the hallmark of many neurodegenerative disease, as seen in the tau neurofibrillary tangles and β-amyloid plaques of Alzheimer's disease, aggregated α-synuclein Lewy bodies of Parkinson's disease, and accumulation of huntingtin in Huntington's disease.[169, 208] While HDAC6 aids in misfolded protein clearance, misregulated HDAC6 can also lead to accumulation of misfolded proteins under certain circumstances.[169] For example, in Alzheimer's disease, HDAC6 activation of Hsp90 by deacetylation leads to increased levels of tau protein, an Hsp90 client, as activated Hsp90 inhibits tau degradation due to increased association with hypoacetylated Hsp90 and decreased tau polyubiquitination leading to proteasomal degradation.[209] Additionally, microtubule degradation is exacerbated by HDAC6 deacetylation of α-tubulin promoting microtubule de-polymerization and cytoskeleton disorganization.[210-211] This in turn leads to impairment of intracellular transport, loss of synapse integrity, and eventually cell death by way of β-amyloid accumulation and tau hyperphosphorylation.

HDAC6 in autoimmune disorders

The adaptive immune response is powered by an army of cells called lymphocytes, also known as B and T cells. While B cells carry the information needed to rapidly produce antibodies against previously encountered pathogens, T cells are responsible for identifying and attacking novel threats, such as a new pathogen.[81] Regulatory T cells, or Tregs, control the activation of T cells in response to an antigen. Tregs are critical in preventing excessive and harmful immune response, as seen in autoimmune disorders.[212] Treg activation and consequently immune response suppression is controlled by the transcription factor Foxp3, which is in turn regulated by HDAC6, potentially through deacetylation of Foxp3 and/or Hsp90.[213] HDAC6 genetic knockout and treatment with HDAC6-specific inhibitors tubacin and tubastatin A in mice, leads to enhanced Treg activation and immune system suppression and is therefore a potential therapeutic avenue in autoimmune disorders and other immune response-related issues such as transplant rejection. It is also possible that HDAC6 inhibition could be used in immunotherapies for cancer.

Challenges and the Future of HDAC Research

The family of HDACs represents a promising avenue for targeting therapeutics and drug discovery due to their widespread impact on physiological processes and disease pathology. Modern technological advancements have equipped researchers with tools to characterize these enzymes in order to better understand their function. Recent studies have uncovered a rich complexity to HDACs including divergent structures, intricate mechanisms, and widely varied substrate selectivity, protein-protein interactions, subcellular localization, and tissue distribution. This research is ongoing, as many questions remain, and the individual roles for these enzymes is not fully understood. This insight is essential for developing the best targeting approaches for HDACs in disease and for providing the most effective treatment options for these diseases. An important task regarding HDAC-specific function is deciphering their individual targets. Thus far, numerous HDAC-specific substrates have been proposed, underscoring the diverse and individual functions for the different members of this family of enzymes. However, with thousands of acetyl-lysine residues reported in the human acetylome, there are still many residues left to characterize and identify the HDAC(s) responsible for their regulation.

HDAC research is both exciting and challenging. Challenges include designing increasingly more sensitive tools to analyze low acetylation levels, developing methods to parse individual and overlapping HDAC activity, and collaborating to create systematic, streamlined, and rapid approaches to compiling and connecting the most relevant and robust information. One thing is evident, there is no one tool, method, or approach that can provide all the answers. For this reason, a barrage of techniques, or a so-called ‘toolbox’ of methodologies, must be implemented to assign substrates, identify biological pathways, detect overlapping function between isozymes, and make relevant connections between studies. Developing robust, well-designed, and high-throughput methods for quickly surveying a continuously expanding pool of targets will be critical for future success in the field.

In the following pages, I describe a set of such experiments used to characterize the impact of post-translational modifications, structure, protein-protein interactions, and substrate specificity and selectivity on the regulation and function of representative class I HDAC8 and class II HDAC6. In chapter 2, the role of HDAC8 phosphorylation in regulating HDAC8 activity and substrate selectivity is investigated. A phosphomimetic S39E HDAC8 mutant catalyzes deacetylation of a library of singly-acetylated peptides more slowly and with altered substrate

selectivity than wild type. For a peptide corresponding to SMC3, the best validated HDAC8 substrate, the glutamate substitution nearly abolishes activity suggesting that phosphorylation could be a mechanism used in the cell to regulate HDAC8-catalyzed deacetylation of this protein. Crystallographic analysis suggests that the altered enzyme activity and substrate selectivity are due to minor structural changes at the site of phosphorylation (S39) that are translated through the protein to affect active site architecture. Molecular dynamics simulations of S39E, wild-type, and pS39 HDAC8 recapitulate the structural observations and suggest additional changes at the substrate binding interface that lead to altered molecular recognition of peptides.

The data in chapter 3 demonstrate the impact of interactions between substrate and HDAC8 distal to the active site. HDAC8-catalyzed deacetylation of full-length histone H3/H4 complexes containing modifications at H3 K9ac, K14ac, or K56ac were measured and compared to reactivity of the corresponding peptides. The results demonstrate that contacts distal to the active site made between substrate and enzyme increase deacetylation rates at least 30-fold. However, when comparing the activities, the protein and peptide substrates showed similar trends in reactivity. For both peptides and proteins, HDAC8 deacetylated histone H3 K9ac more rapidly than H3 K14ac, despite their close proximity and similar structure and sequence environment. This indicates that local sequence impacts substrate selectivity and supports the continued use of peptides as substrate surrogates in future studies.

In chapter 4, a structure-based computational method for determining the substrate specificity and selectivity of HDAC6 is developed. HDAC6-catalyzed deacetylation of a library of over 30 peptides was measured, demonstrating a wide range of activities varying up to 20,000-fold. These data indicate HDAC6 has significant substrate sequence preferences and may be modeled to develop a computational algorithm capable of predicting HDAC6 activity. Using the Rosetta FlexPepBind platform, our collaborators in the lab of Dr. Ora Schueler-Furman have developed a structure capable to predicting good HDAC6 substrates. This computational model will be useful in identifying cellular HDAC6 substrates and enhancing our understanding of the function of this enzyme.

References

1. Willyard, C., New human gene tally reignites debate. *Nature* **2018,** *558* (7710), 354-355.

2. Pertea, M.; Shumate, A.; Pertea, G.; Varabyou, A.; Chang, Y.-C.; Madugundu, A. K.; Pandey, A.; Salzberg, S., Thousands of large-scale RNA sequencing experiments yield a comprehensive new human gene list and reveal extensive transcriptional noise. *bioRxiv* **2018**, 332825.

3. Initial sequence of the chimpanzee genome and comparison with the human genome. *Nature* **2005,** *437* (7055), 69-87.

4. Pandey, U. B.; Nichols, C. D., Human disease models in Drosophila melanogaster and the role of the fly in therapeutic drug discovery. *Pharmacological reviews* **2011,** *63* (2), 411-436.

5. Rosenberg, N. A.; Pritchard, J. K.; Weber, J. L.; Cann, H. M.; Kidd, K. K.; Zhivotovsky, L. A.; Feldman, M. W., Genetic structure of human populations. *Science* **2002,** *298* (5602), 2381-5.

6. Sabatini, R. In *How to read the genome and build a human being*, TED2016, 2016.

7. Khoury, G. A.; Baliban, R. C.; Floudas, C. A., Proteome-wide post-translational modification statistics: frequency analysis and curation of the swiss-prot database. *Scientific reports* **2011,** *1*, 90.

8. Fischer, E. H.; Graves, D. J.; Crittenden, E. R.; Krebs, E. G., Structure of the site phosphorylated in the phosphorylase b to a reaction. *The Journal of biological chemistry* **1959,** *234* (7), 1698-704.

9. Roskoski, R., Jr., A historical overview of protein kinases and their targeted small molecule inhibitors. *Pharmacological research* **2015,** *100*, 1-23.

10. Ubersax, J. A.; Ferrell Jr, J. E., Mechanisms of specificity in protein phosphorylation. *Nature Reviews Molecular Cell Biology* **2007,** *8*, 530.

11. Phillips, D. M., The presence of acetyl groups of histones. *The Biochemical journal* **1963,** *87*, 258-63.

12. Verdin, E.; Ott, M., 50 years of protein acetylation: from gene regulation to epigenetics, metabolism and beyond. *Nature reviews. Molecular cell biology* **2015,** *16* (4), 258-64.

13. Lipmann, F., Development of the acetylation problem, a personal account. *Science* **1954,** *120* (3126), 855-65.

14. Lipmann, F., Enzymatic acetylation and the coenzyme of acetylation. *Biol Bull* **1946,** *91* (02), 239.

15. Bloch, K.; Borek, E., Biological acetylation of natural amino acids. *The Journal of biological chemistry* **1946,** *164*, 483.

16. Allfrey, V. G.; Faulkner, R.; Mirsky, A. E., Acetylation and Methylation of Histones and Their Possible Role in the Regulation of Rna Synthesis. *Proc Natl Acad Sci U S A* **1964,** *51*, 786-94.

17. Hagopian, H. K.; Riggs, M. G.; Swartz, L. A.; Ingram, V. M., Effect of n-butyrate on DNA synthesis in chick fibroblasts and HeLa cells. *Cell* **1977,** *12* (3), 855-60.

18. Riggs, M. G.; Whittaker, R. G.; Neumann, J. R.; Ingram, V. M., n-Butyrate causes histone modification in HeLa and Friend erythroleukaemia cells. *Nature* **1977,** *268* (5619), 462-4.

19. Candido, E. P.; Reeves, R.; Davie, J. R., Sodium butyrate inhibits histone deacetylation in cultured cells. *Cell* **1978,** *14* (1), 105-13.

20. Vidali, G.; Boffa, L. C.; Bradbury, E. M.; Allfrey, V. G., Butyrate suppression of histone deacetylation leads to accumulation of multiacetylated forms of histones H3 and H4 and increased DNase I sensitivity of the associated DNA sequences. *Proc Natl Acad Sci U S A* **1978,** *75* (5), 2239-43.

21. Piperno, G.; Fuller, M. T., Monoclonal antibodies specific for an acetylated form of alpha-tubulin recognize the antigen in cilia and flagella from a variety of organisms. *J Cell Biol* **1985,** *101* (6), 2085-94.

22. L'Hernault, S. W.; Rosenbaum, J. L., Chlamydomonas alpha-tubulin is posttranslationally modified in the flagella during flagellar assembly. *J Cell Biol* **1983,** *97* (1), 258-63.

23. LeDizet, M.; Piperno, G., Identification of an acetylation site of Chlamydomonas alpha-tubulin. *Proc Natl Acad Sci U S A* **1987,** *84* (16), 5720-4.

24. Piperno, G.; LeDizet, M.; Chang, X. J., Microtubules containing acetylated alpha-tubulin in mammalian cells in culture. *J Cell Biol* **1987,** *104* (2), 289-302.

25. Felsenfeld, G., A brief history of epigenetics. *Cold Spring Harbor perspectives in biology 6* (1), a018200.

26. Allis, C. D.; Jenuwein, T., The molecular hallmarks of epigenetic control. *Nature Reviews Genetics* **2016,** *17*, 487.

27. Klemm, S. L.; Shipony, Z.; Greenleaf, W. J., Chromatin accessibility and the regulatory epigenome. *Nature Reviews Genetics* **2019,** *20* (4), 207-220.

28. Jenuwein, T.; Allis, C. D., Translating the Histone Code. *Science* **2001,** *293* (5532), 1074.

29. Janssen, K. A.; Sidoli, S.; Garcia, B. A., Recent Achievements in Characterizing the Histone Code and Approaches to Integrating Epigenomics and Systems Biology. *Methods in enzymology* **2017,** *586*, 359-378.

30. Saha, R. N.; Pahan, K., HATs and HDACs in neurodegeneration: a tale of disconcerted acetylation homeostasis. *Cell death and differentiation* **2006,** *13* (4), 539-50.

31. Falkenberg, K. J.; Johnstone, R. W., Histone deacetylases and their inhibitors in cancer, neurological diseases and immune disorders. *Nature reviews. Drug discovery* **2014,** *13* (9), 673-91.

32. Dubey, H.; Gulati, K.; Ray, A., Recent studies on cellular and molecular mechanisms in Alzheimer's disease: focus on epigenetic factors and histone deacetylase. *Reviews in the neurosciences* **2018,** *29* (3), 241-260.

33. Liu, K. Y.; Wang, L. T.; Hsu, S. H., Modification of Epigenetic Histone Acetylation in Hepatocellular Carcinoma. *Cancers* **2018,** *10* (1).

34. Jones, P. A.; Issa, J. P.; Baylin, S., Targeting the cancer epigenome for therapy. *Nature reviews. Genetics* **2016,** *17* (10), 630-41.

35. Gu, W.; Roeder, R. G., Activation of p53 sequence-specific DNA binding by acetylation of the p53 C-terminal domain. *Cell* **1997,** *90* (4), 595-606.

36. Yao, Y. L.; Yang, W. M.; Seto, E., Regulation of Transcription Factor YY1 by Acetylation and Deacetylation. **2001,** *21* (17), 5979-5991.

37. Sterner, R.; Vidali, G.; Allfrey, V. G., Studies of acetylation and deacetylation in high mobility group proteins. Identification of the sites of acetylation in HMG-1. *The Journal of biological chemistry* **1979,** *254* (22), 11577-83.

38. Wang, R.; Cherukuri, P.; Luo, J., Activation of Stat3 sequence-specific DNA binding and transcription by p300/CREB-binding protein-mediated acetylation. *The Journal of biological chemistry* **2005,** *280* (12), 11528-34.

39. Boyes, J.; Byfield, P.; Nakatani, Y.; Ogryzko, V., Regulation of activity of the transcription factor GATA-1 by acetylation. *Nature* **1998,** *396* (6711), 594-8.

40. Zhang, W.; Bieker, J. J., Acetylation and modulation of erythroid Kruppel-like factor (EKLF) activity by interaction with histone acetyltransferases. *Proc Natl Acad Sci U S A* **1998,** *95* (17), 9855-60.

41. Sartorelli, V.; Puri, P. L.; Hamamori, Y.; Ogryzko, V.; Chung, G.; Nakatani, Y.; Wang, J. Y.; Kedes, L., Acetylation of MyoD directed by PCAF is necessary for the execution of the muscle program. *Mol Cell* **1999,** *4* (5), 725-34.

42. Gaughan, L.; Logan, I. R.; Cook, S.; Neal, D. E.; Robson, C. N., Tip60 and histone deacetylase 1 regulate androgen receptor activity through changes to the acetylation status of the receptor. *The Journal of biological chemistry* **2002,** *277* (29), 25904-13.

43. Wang, C.; Fu, M.; Angeletti, R. H.; Siconolfi-Baez, L.; Reutens, A. T.; Albanese, C.; Lisanti, M. P.; Katzenellenbogen, B. S.; Kato, S.; Hopp, T.; Fuqua, S. A.; Lopez, G. N.; Kushner, P. J.; Pestell, R. G., Direct acetylation of the estrogen receptor alpha hinge region by p300 regulates transactivation and hormone sensitivity. *The Journal of biological chemistry* **2001,** *276* (21), 18375-83.

44. Chen, L.; Fischle, W.; Verdin, E.; Greene, W. C., Duration of nuclear NF-kappaB action regulated by reversible acetylation. *Science* **2001,** *293* (5535), 1653-7.

45. Kovacs, J. J.; Murphy, P. J.; Gaillard, S.; Zhao, X.; Wu, J. T.; Nicchitta, C. V.; Yoshida, M.; Toft, D. O.; Pratt, W. B.; Yao, T. P., HDAC6 regulates Hsp90 acetylation and chaperone-dependent activation of glucocorticoid receptor. *Mol Cell* **2005,** *18* (5), 601-7.

46. Ott, M.; Schnolzer, M.; Garnica, J.; Fischle, W.; Emiliani, S.; Rackwitz, H. R.; Verdin, E., Acetylation of the HIV-1 Tat protein by p300 is important for its transcriptional activity. *Current biology : CB* **1999,** *9* (24), 1489-92.

47. Glozak, M. A.; Sengupta, N.; Zhang, X.; Seto, E., Acetylation and deacetylation of non-histone proteins. *Gene* **2005,** *363*, 15-23.

48. Choudhary, C.; Weinert, B. T.; Nishida, Y.; Verdin, E.; Mann, M., The growing landscape of lysine acetylation links metabolism and cell signalling. *Nature reviews. Molecular cell biology* **2014,** *15* (8), 536-50.

49. Choudhary, C.; Kumar, C.; Gnad, F.; Nielsen, M. L.; Rehman, M.; Walther, T. C.; Olsen, J. V.; Mann, M., Lysine acetylation targets protein complexes and co-regulates major cellular functions. *Science* **2009,** *325* (5942), 834-40.

50. Kim, S. C.; Sprung, R.; Chen, Y.; Xu, Y.; Ball, H.; Pei, J.; Cheng, T.; Kho, Y.; Xiao, H.; Xiao, L.; Grishin, N. V.; White, M.; Yang, X. J.; Zhao, Y., Substrate and functional diversity of lysine acetylation revealed by a proteomics survey. *Mol Cell* **2006,** *23* (4), 607-18.

51. Verdin, E.; Ott, M., 50 years of protein acetylation: from gene regulation to epigenetics, metabolism and beyond. *Nature Reviews Molecular Cell Biology* **2014,** *16* (4), 258-264.

52. Wang, M.-M.; You, D.; Ye, B.-C., Site-specific and kinetic characterization of enzymatic and nonenzymatic protein acetylation in bacteria. *Scientific reports* **2017,** *7* (1), 14790.

53. Ree, R.; Varland, S.; Arnesen, T., Spotlight on protein N-terminal acetylation. *Experimental & Molecular Medicine* **2018,** *50* (7), 90.

54. Haynes, S. R.; Dollard, C.; Winston, F.; Beck, S.; Trowsdale, J.; Dawid, I. B., The bromodomain: a conserved sequence found in human, Drosophila and yeast proteins. *Nucleic acids research* **1992,** *20* (10), 2603-2603.

55. Fujisawa, T.; Filippakopoulos, P., Functions of bromodomain-containing proteins and their roles in homeostasis and cancer. *Nature Reviews Molecular Cell Biology* **2017,** *18*, 246.

56. Brownell, J. E.; Zhou, J.; Ranalli, T.; Kobayashi, R.; Edmondson, D. G.; Roth, S. Y.; Allis, C. D., Tetrahymena histone acetyltransferase A: a homolog to yeast Gcn5p linking histone acetylation to gene activation. *Cell* **1996,** *84* (6), 843-51.

57. Roth, S. Y.; Denu, J. M.; Allis, C. D., Histone acetyltransferases. *Annu Rev Biochem* **2001,** *70*, 81-120.

58. Yuan, H.; Marmorstein, R., Histone acetyltransferases: Rising ancient counterparts to protein kinases. *Biopolymers* **2013,** *99* (2), 98-111.

59. Maksimoska, J.; Segura-Peña, D.; Cole, P. A.; Marmorstein, R., Structure of the p300 Histone Acetyltransferase Bound to Acetyl-Coenzyme A and Its Analogues. *Biochemistry* **2014,** *53* (21), 3415-3422.

60. Friedmann, D. R.; Marmorstein, R., Structure and mechanism of non-histone protein acetyltransferase enzymes. *The FEBS Journal* **2013,** *280* (22), 5570-5581.

61. Gregoretti, I. V.; Lee, Y. M.; Goodson, H. V., Molecular evolution of the histone deacetylase family: functional implications of phylogenetic analysis. *J Mol Biol* **2004,** *338* (1), 17-31.

62. Yang, X. J.; Seto, E., The Rpd3/Hda1 family of lysine deacetylases: from bacteria and yeast to mice and men. *Nature reviews. Molecular cell biology* **2008,** *9* (3), 206-18.

63. Haberland, M.; Montgomery, R. L.; Olson, E. N., The many roles of histone deacetylases in development and physiology: implications for disease and therapy. *Nature reviews. Genetics* **2009,** *10* (1), 32-42.

64. Seto, E.; Yoshida, M., Erasers of histone acetylation: the histone deacetylase enzymes. *Cold Spring Harbor perspectives in biology* **2014,** *6* (4), a018713-a018713.

65. Duvic, M.; Vu, J., Vorinostat: a new oral histone deacetylase inhibitor approved for cutaneous T-cell lymphoma. *Expert opinion on investigational drugs* **2007,** *16* (7), 1111-20.

66. Marks, P. A., Discovery and development of SAHA as an anticancer agent. *Oncogene* **2007,** *26* (9), 1351-6.

67. Mann, B. S.; Johnson, J. R.; Cohen, M. H.; Justice, R.; Pazdur, R., FDA approval summary: vorinostat for treatment of advanced primary cutaneous T-cell lymphoma. *The oncologist* **2007,** *12* (10), 1247-52.

68. Tabackman, A. A.; Frankson, R.; Marsan, E. S.; Perry, K.; Cole, K. E., Structure of 'linkerless' hydroxamic acid inhibitor-HDAC8 complex confirms the formation of an isoform-specific subpocket. *Journal of structural biology* **2016,** *195* (3), 373-378.

69. Guan, P.; Fang, H., Clinical development of histone deacetylase inhibitor romidepsin. *Drug discoveries & therapeutics* **2010,** *4* (6), 388-91.

70. Lee, H. Z.; Kwitkowski, V. E.; Del Valle, P. L.; Ricci, M. S.; Saber, H.; Habtemariam, B. A.; Bullock, J.; Bloomquist, E.; Li Shen, Y.; Chen, X. H.; Brown, J.; Mehrotra, N.; Dorff, S.; Charlab, R.; Kane, R. C.; Kaminskas, E.; Justice, R.; Farrell, A. T.; Pazdur, R., FDA Approval: Belinostat for the Treatment of Patients with Relapsed or Refractory Peripheral T-cell Lymphoma. *Clin Cancer Res* **2015,** *21* (12), 2666-70.

71. Plumb, J. A.; Finn, P. W.; Williams, R. J.; Bandara, M. J.; Romero, M. R.; Watkins, C. J.; La Thangue, N. B.; Brown, R., Pharmacodynamic response and inhibition of growth of human tumor xenografts by the novel histone deacetylase inhibitor PXD101. *Mol Cancer Ther* **2003,** *2* (8), 721-8.

72. Laubach, J. P.; Moreau, P.; San-Miguel, J. F.; Richardson, P. G., Panobinostat for the Treatment of Multiple Myeloma. *Clin Cancer Res* **2015,** *21* (21), 4767-73.

73. Richardson, P. G.; Harvey, R. D.; Laubach, J. P.; Moreau, P.; Lonial, S.; San-Miguel, J. F., Panobinostat for the treatment of relapsed or relapsed/refractory multiple myeloma: pharmacology and clinical outcomes. *Expert review of clinical pharmacology* **2016,** *9* (1), 35-48.

74. Oehme, I.; Deubzer, H. E.; Lodrini, M.; Milde, T.; Witt, O., Targeting of HDAC8 and investigational inhibitors in neuroblastoma. *Expert opinion on investigational drugs* **2009,** *18* (11), 1605-1617.

75. Suraweera, A.; O'Byrne, K. J.; Richard, D. J., Combination Therapy With Histone Deacetylase Inhibitors (HDACi) for the Treatment of Cancer: Achieving the Full Therapeutic Potential of HDACi. *Frontiers in oncology* **2018,** *8*, 92-92.

76. Faria Freitas, M.; Cuendet, M.; Bertrand, P., HDAC inhibitors: a 2013-2017 patent survey. *Expert opinion on therapeutic patents* **2018**, 1-17.

77. Taunton, J.; Hassig, C. A.; Schreiber, S. L., A mammalian histone deacetylase related to the yeast transcriptional regulator Rpd3p. *Science* **1996,** *272* (5260), 408-11.

78. Yang, W. M.; Yao, Y. L.; Sun, J. M.; Davie, J. R.; Seto, E., Isolation and characterization of cDNAs corresponding to an additional member of the human histone deacetylase gene family. *The Journal of biological chemistry* **1997,** *272* (44), 28001-7.

79. Emiliani, S.; Fischle, W.; Van Lint, C.; Al-Abed, Y.; Verdin, E., Characterization of a human RPD3 ortholog, HDAC3. *Proc Natl Acad Sci U S A* **1998,** *95* (6), 2795-800.

80. Dangond, F.; Hafler, D. A.; Tong, J. K.; Randall, J.; Kojima, R.; Utku, N.; Gullans, S. R., Differential display cloning of a novel human histone deacetylase (HDAC3) cDNA from PHA-activated immune cells. *Biochemical and biophysical research communications* **1998,** *242* (3), 648-52.

81. Buggy, J. J.; Sideris, M. L.; Mak, P.; Lorimer, D. D.; McIntosh, B.; Clark, J. M., Cloning and characterization of a novel human histone deacetylase, HDAC8. *The Biochemical journal* **2000,** *350 Pt 1*, 199-205.

82. Van den Wyngaert, I.; de Vries, W.; Kremer, A.; Neefs, J.; Verhasselt, P.; Luyten, W. H.; Kass, S. U., Cloning and characterization of human histone deacetylase 8. *FEBS letters* **2000,** *478* (1-2), 77-83.

83. Yang, W. M.; Tsai, S. C.; Wen, Y. D.; Fejer, G.; Seto, E., Functional domains of histone deacetylase-3. *The Journal of biological chemistry* **2002,** *277* (11), 9447-54.

84. de Ruijter, A. J.; van Gennip, A. H.; Caron, H. N.; Kemp, S.; van Kuilenburg, A. B., Histone deacetylases (HDACs): characterization of the classical HDAC family. *The Biochemical journal* **2003,** *370* (Pt 3), 737-49.

85. Grozinger, C. M.; Hassig, C. A.; Schreiber, S. L., Three proteins define a class of human histone deacetylases related to yeast Hda1p. *Proc Natl Acad Sci U S A* **1999,** *96* (9), 4868-73.

86. Fischle, W.; Dequiedt, F.; Fillion, M.; Hendzel, M. J.; Voelter, W.; Verdin, E., Human HDAC7 histone deacetylase activity is associated with HDAC3 in vivo. *The Journal of biological chemistry* **2001,** *276* (38), 35826-35.

87. Fischle, W.; Dequiedt, F.; Hendzel, M. J.; Guenther, M. G.; Lazar, M. A.; Voelter, W.; Verdin, E., Enzymatic Activity Associated with Class II HDACs Is Dependent on a Multiprotein Complex Containing HDAC3 and SMRT/N-CoR. *Molecular Cell* **2002,** *9* (1), 45-57.

88. Gantt, S. L.; Gattis, S. G.; Fierke, C. A., Catalytic activity and inhibition of human histone deacetylase 8 is dependent on the identity of the active site metal ion. *Biochemistry* **2006,** *45* (19), 6170-8.

89. Uhlen, M.; Zhang, C.; Lee, S.; Sjostedt, E.; Fagerberg, L.; Bidkhori, G.; Benfeitas, R.; Arif, M.; Liu, Z.; Edfors, F.; Sanli, K.; von Feilitzen, K.; Oksvold, P.; Lundberg, E.; Hober, S.; Nilsson, P.; Mattsson, J.; Schwenk, J. M.; Brunnstrom, H.; Glimelius, B.; Sjoblom, T.; Edqvist, P. H.; Djureinovic, D.; Micke, P.; Lindskog, C.; Mardinoglu, A.; Ponten, F., A pathology atlas of the human cancer transcriptome. *Science* **2017,** *357* (6352).

90. Zhou, X.; Marks, P. A.; Rifkind, R. A.; Richon, V. M., Cloning and characterization of a histone deacetylase, HDAC9. *Proc Natl Acad Sci U S A* **2001,** *98* (19), 10572-7.

91. Fischer, D. D.; Cai, R.; Bhatia, U.; Asselbergs, F. A.; Song, C.; Terry, R.; Trogani, N.; Widmer, R.; Atadja, P.; Cohen, D., Isolation and characterization of a novel class II histone deacetylase, HDAC10. *The Journal of biological chemistry* **2002,** *277* (8), 6656-66.

92. Kao, H. Y.; Lee, C. H.; Komarov, A.; Han, C. C.; Evans, R. M., Isolation and characterization of mammalian HDAC10, a novel histone deacetylase. *The Journal of biological chemistry* **2002,** *277* (1), 187-93.

93. Cheng, F.; Lienlaf, M.; Perez-Villarroel, P.; Wang, H. W.; Lee, C.; Woan, K.; Woods, D.; Knox, T.; Bergman, J.; Pinilla-Ibarz, J.; Kozikowski, A.; Seto, E.; Sotomayor, E. M.; Villagra, A., Divergent roles of histone deacetylase 6 (HDAC6) and histone deacetylase 11 (HDAC11) on the transcriptional regulation of IL10 in antigen presenting cells. *Mol Immunol* **2014,** *60* (1), 44-53.

94. Grozinger, C. M.; Schreiber, S. L., Regulation of histone deacetylase 4 and 5 and transcriptional activity by 14-3-3-dependent cellular localization. *Proc Natl Acad Sci U S A* **2000,** *97* (14), 7835-40.

95. Pon, J. R.; Marra, M. A., MEF2 transcription factors: developmental regulators and emerging cancer genes. *Oncotarget* **2015,** *7* (3), 2297-2312.

96. Hai, Y.; Shinsky, S. A.; Porter, N. J.; Christianson, D. W., Histone deacetylase 10 structure and molecular function as a polyamine deacetylase. *Nature communications* **2017,** *8*, 15368.

97. Bedalov, A.; Chowdhury, S.; Simon, J. A., Biology, Chemistry, and Pharmacology of Sirtuins. Elsevier: 2016; pp 183-211.

98. Min, J.; Landry, J.; Sternglanz, R.; Xu, R. M., Crystal structure of a SIR2 homolog-NAD complex. *Cell* **2001,** *105* (2), 269-79.

99. Gottschling, D. E., Gene silencing: Two faces of SIR2. *Current Biology* **2000,** *10* (19), R708-R711.

100. Frye, R. A., Phylogenetic Classification of Prokaryotic and Eukaryotic Sir2-like Proteins. *Biochemical and biophysical research communications* **2000,** *273* (2), 793-798.

101. Frye, R. A., Characterization of five human cDNAs with homology to the yeast SIR2 gene: Sir2-like proteins (sirtuins) metabolize NAD and may have protein ADP-ribosyltransferase activity. *Biochemical and biophysical research communications* **1999,** *260* (1), 273-9.

102. Finnin, M. S.; Donigian, J. R.; Pavletich, N. P., Structure of the histone deacetylase SIRT2. *Nature Structural Biology* **2001,** *8*, 621.

103. Feldman, J. L.; Dittenhafer-Reed, K. E.; Kudo, N.; Thelen, J. N.; Ito, A.; Yoshida, M.; Denu, J. M., Kinetic and Structural Basis for Acyl-Group Selectivity and NAD+ Dependence in Sirtuin-Catalyzed Deacylation. *Biochemistry* **2015,** *54* (19), 3037-3050.

104. Teng, Y. B.; Jing, H.; Aramsangtienchai, P.; He, B.; Khan, S.; Hu, J.; Lin, H.; Hao, Q., Efficient demyristoylase activity of SIRT2 revealed by kinetic and structural studies. *Scientific reports* **2015,** *5*, 8529.

105. Gao, L.; Cueto, M. A.; Asselbergs, F.; Atadja, P., Cloning and functional characterization of HDAC11, a novel member of the human histone deacetylase family. *The Journal of biological chemistry* **2002,** *277* (28), 25748-55.

106. Deubzer, H. E.; Schier, M. C.; Oehme, I.; Lodrini, M.; Haendler, B.; Sommer, A.; Witt, O., HDAC11 is a novel drug target in carcinomas. *Int J Cancer* **2013,** *132* (9), 2200-8.

107. Villagra, A.; Cheng, F.; Wang, H. W.; Suarez, I.; Glozak, M.; Maurin, M.; Nguyen, D.; Wright, K. L.; Atadja, P. W.; Bhalla, K.; Pinilla-Ibarz, J.; Seto, E.; Sotomayor, E. M., The histone deacetylase HDAC11 regulates the expression of interleukin 10 and immune tolerance. *Nature immunology* **2009,** *10* (1), 92-100.

108. Huang, J.; Wang, L.; Dahiya, S.; Beier, U. H.; Han, R.; Samanta, A.; Bergman, J.; Sotomayor, E. M.; Seto, E.; Kozikowski, A. P.; Hancock, W. W., Histone/protein deacetylase 11 targeting promotes Foxp3+ Treg function. *Scientific reports* **2017,** *7* (1), 8626.

109. Moreno-Yruela, C.; Galleano, I.; Madsen, A. S.; Olsen, C. A., Histone Deacetylase 11 Is an epsilon-N-Myristoyllysine Hydrolase. *Cell Chem Biol* **2018**.

110. Hu, E.; Chen, Z.; Fredrickson, T.; Zhu, Y.; Kirkpatrick, R.; Zhang, G. F.; Johanson, K.; Sung, C. M.; Liu, R.; Winkler, J., Cloning and characterization of a novel human class I histone deacetylase that functions as a transcription repressor. *The Journal of biological chemistry* **2000,** *275* (20), 15254-64.

111. Vannini, A.; Volpari, C.; Filocamo, G.; Casavola, E. C.; Brunetti, M.; Renzoni, D.; Chakravarty, P.; Paolini, C.; De Francesco, R.; Gallinari, P.; Steinkuhler, C.; Di Marco, S., Crystal structure of a eukaryotic zinc-dependent histone deacetylase, human HDAC8, complexed with a hydroxamic acid inhibitor. *Proc Natl Acad Sci U S A* **2004,** *101* (42), 15064-9.

112. Somoza, J. R.; Skene, R. J.; Katz, B. A.; Mol, C.; Ho, J. D.; Jennings, A. J.; Luong, C.; Arvai, A.; Buggy, J. J.; Chi, E.; Tang, J.; Sang, B. C.; Verner, E.; Wynands, R.; Leahy, E. M.; Dougan, D. R.; Snell, G.; Navre, M.; Knuth, M. W.; Swanson, R. V.; McRee, D. E.; Tari, L. W., Structural snapshots of human HDAC8 provide insights into the class I histone deacetylases. *Structure (London, England : 1993)* **2004,** *12* (7), 1325-34.

113. Wolfson, N. A.; Pitcairn, C. A.; Fierke, C. A., HDAC8 substrates: Histones and beyond. *Biopolymers* **2013,** *99* (2), 112-26.

114. Vannini, A.; Volpari, C.; Gallinari, P.; Jones, P.; Mattu, M.; Carfi, A.; De Francesco, R.; Steinkuhler, C.; Di Marco, S., Substrate binding to histone deacetylases as shown by the crystal structure of the HDAC8-substrate complex. *EMBO Rep* **2007,** *8* (9), 879-84.

115. Dowling, D. P.; Gattis, S. G.; Fierke, C. A.; Christianson, D. W., Structures of metal-substituted human histone deacetylase 8 provide mechanistic inferences on biological function. *Biochemistry* **2010,** *49* (24), 5048-56.

116. Dowling, D. P.; Gantt, S. L.; Gattis, S. G.; Fierke, C. A.; Christianson, D. W., Structural studies of human histone deacetylase 8 and its site-specific variants complexed with substrate and inhibitors. *Biochemistry* **2008,** *47* (51), 13554-63.

117. Cole, K. E.; Dowling, D. P.; Boone, M. A.; Phillips, A. J.; Christianson, D. W., Structural basis of the antiproliferative activity of largazole, a depsipeptide inhibitor of the histone deacetylases. *Journal of the American Chemical Society* **2011,** *133* (32), 12474-7.

118. Gantt, S. M.; Decroos, C.; Lee, M. S.; Gullett, L. E.; Bowman, C. M.; Christianson, D. W.; Fierke, C. A., General Base-General Acid Catalysis in Human Histone Deacetylase 8. *Biochemistry* **2016,** *55* (5), 820-32.

119. Porter, N. J.; Christianson, N. H.; Decroos, C.; Christianson, D. W., Structural and Functional Influence of the Glycine-Rich Loop G(302)GGGY on the Catalytic Tyrosine of Histone Deacetylase 8. *Biochemistry* **2016,** *55* (48), 6718-6729.

120. Decroos, C.; Clausen, D. J.; Haines, B. E.; Wiest, O.; Williams, R. M.; Christianson, D. W., Variable Active Site Loop Conformations Accommodate the Binding of Macrocyclic Largazole Analogues to HDAC8. **2015,** *54* (12), 2126-2135.

121. Decroos, C.; Bowman, C. M.; Moser, J. A.; Christianson, K. E.; Deardorff, M. A.; Christianson, D. W., Compromised structure and function of HDAC8 mutants identified in Cornelia de Lange Syndrome spectrum disorders. *ACS chemical biology* **2014,** *9* (9), 2157-64.

122. Decroos, C.; Christianson, N. H.; Gullett, L. E.; Bowman, C. M.; Christianson, K. E.; Deardorff, M. A.; Christianson, D. W., Biochemical and structural characterization of HDAC8 mutants associated with Cornelia de Lange syndrome spectrum disorders. *Biochemistry* **2015,** *54* (42), 6501-13.

123. Whitehead, L.; Dobler, M. R.; Radetich, B.; Zhu, Y.; Atadja, P. W.; Claiborne, T.; Grob, J. E.; McRiner, A.; Pancost, M. R.; Patnaik, A.; Shao, W.; Shultz, M.; Tichkule, R.; Tommasi, R. A.; Vash, B.; Wang, P.; Stams, T., Human HDAC isoform selectivity achieved via exploitation of the acetate release channel with structurally unique small molecule inhibitors. *Bioorg Med Chem* **2011,** *19* (15), 4626-34.

124. Kunze, M. B.; Wright, D. W.; Werbeck, N. D.; Kirkpatrick, J.; Coveney, P. V.; Hansen, D. F., Loop interactions and dynamics tune the enzymatic activity of the human histone deacetylase 8. *Journal of the American Chemical Society* **2013,** *135* (47), 17862-8.

125. Gantt, S. L.; Joseph, C. G.; Fierke, C. A., Activation and inhibition of histone deacetylase 8 by monovalent cations. *The Journal of biological chemistry* **2010,** *285* (9), 6036-43.

126. Kim, B.; Pithadia, A. S.; Fierke, C. A., Kinetics and thermodynamics of metal-binding to histone deacetylase 8. *Protein science : a publication of the Protein Society* **2015,** *24* (3), 354-65.

127. Castaneda, C. A.; Lopez, J. E.; Joseph, C. G.; Scholle, M. D.; Mrksich, M.; Fierke, C. A., Active Site Metal Identity Alters Histone Deacetylase 8 Substrate Selectivity: A Potential Novel Regulatory Mechanism. *Biochemistry* **2017,** *56* (42), 5663-5670.

128. Gattis, S. G.; Hernick, M.; Fierke, C. A., Active Site Metal Ion in UDP-3-O-((R)-3-Hydroxymyristoyl)-N-acetylglucosamine Deacetylase (LpxC) Switches between Fe(II) and Zn(II) Depending on Cellular Conditions. *Journal of Biological Chemistry* **2010,** *285* (44), 33788-33796.

129. Waltregny, D.; Glénisson, W.; Tran, S. L.; North, B. J.; Verdin, E.; Colige, A.; Castronovo, V., Histone deacetylase HDAC8 associates with smooth muscle alpha-actin and is essential for smooth muscle cell contractility. *The FASEB Journal* **2005**.

130. Waltregny, D.; de Leval, L.; Glénisson, W.; Ly Tran, S.; North, B. J.; Bellahcène, A.; Weidle, U.; Verdin, E.; Castronovo, V., Expression of Histone Deacetylase 8, a Class I Histone Deacetylase, Is Restricted to Cells Showing Smooth Muscle Differentiation in Normal Human Tissues. *The American Journal of Pathology* **2004,** *165* (2), 553-564.

131. Gao, J.; Siddoway, B.; Huang, Q.; Xia, H., Inactivation of CREB mediated gene transcription by HDAC8 bound protein phosphatase. *Biochemical and biophysical research communications* **2009,** *379* (1), 1-5.

132. Karolczak-Bayatti, M.; Sweeney, M.; Cheng, J.; Edey, L.; Robson, S. C.; Ulrich, S. M.; Treumann, A.; Taggart, M. J.; Europe-Finner, G. N., Acetylation of Heat Shock Protein 20 (Hsp20) Regulates Human Myometrial Activity. *Journal of Biological Chemistry* **2011,** *286* (39), 34346-34355.

133. Lee, H.; Sengupta, N.; Villagra, A.; Rezai-Zadeh, N.; Seto, E., Histone deacetylase 8 safeguards the human ever-shorter telomeres 1B (hEST1B) protein from ubiquitin-mediated degradation. *Mol Cell Biol* **2006,** *26* (14), 5259-69.

134. Joshi, P.; Greco, T. M.; Guise, A. J.; Luo, Y.; Yu, F.; Nesvizhskii, A. I.; Cristea, I. M., The functional interactome landscape of the human histone deacetylase family. *Molecular systems biology* **2013,** *9*, 672.

135. Deardorff, M. A.; Bando, M.; Nakato, R.; Watrin, E.; Itoh, T.; Minamino, M.; Saitoh, K.; Komata, M.; Katou, Y.; Clark, D.; Cole, K. E.; De Baere, E.; Decroos, C.; Di Donato, N.; Ernst, S.; Francey, L. J.; Gyftodimou, Y.; Hirashima, K.; Hullings, M.; Ishikawa, Y.; Jaulin, C.; Kaur, M.; Kiyono, T.; Lombardi, P. M.; Magnaghi-Jaulin, L.; Mortier, G. R.; Nozaki, N.; Petersen, M. B.; Seimiya, H.; Siu, V. M.; Suzuki, Y.; Takagaki, K.; Wilde, J. J.; Willems, P. J.; Prigent, C.; Gillessen-Kaesbach, G.; Christianson, D. W.; Kaiser, F. J.;

Jackson, L. G.; Hirota, T.; Krantz, I. D.; Shirahige, K., HDAC8 mutations in Cornelia de Lange syndrome affect the cohesin acetylation cycle. *Nature* **2012,** *489* (7415), 313-7.

136. Olson, D. E.; Udeshi, N. D.; Wolfson, N. A.; Pitcairn, C. A.; Sullivan, E. D.; Jaffe, J. D.; Svinkina, T.; Natoli, T.; Lu, X.; Paulk, J.; McCarren, P.; Wagner, F. F.; Barker, D.; Howe, E.; Lazzaro, F.; Gale, J. P.; Zhang, Y.-L.; Subramanian, A.; Fierke, C. A.; Carr, S. A.; Holson, E. B., An unbiased approach to identify endogenous substrates of "histone" deacetylase 8. *ACS chemical biology* **2014,** *9* (10), 2210-6.

137. Lopez, J. E.; Haynes, S. E.; Majmudar, J. D.; Martin, B. R.; Fierke, C. A., HDAC8 Substrates Identified by Genetically Encoded Active Site Photocrosslinking. *Journal of the American Chemical Society* **2017,** *139* (45), 16222-16227.

138. Olson, D. E.; Udeshi, N. D.; Wolfson, N. A.; Pitcairn, C. A.; Sullivan, E. D.; Jaffe, J. D.; Svinkina, T.; Natoli, T.; Lu, X.; Paulk, J.; McCarren, P.; Wagner, F. F.; Barker, D.; Howe, E.; Lazzaro, F.; Gale, J. P.; Zhang, Y. L.; Subramanian, A.; Fierke, C. A.; Carr, S. A.; Holson, E. B., An unbiased approach to identify endogenous substrates of "histone" deacetylase 8. *ACS chemical biology* **2014,** *9* (10), 2210-6.

139. Haberland, M.; Mokalled, M. H.; Montgomery, R. L.; Olson, E. N., Epigenetic control of skull morphogenesis by histone deacetylase 8. *Genes & Development* **2009,** *23* (14), 1625-1630.

140. Deardorff, M. A.; Porter, N. J.; Christianson, D. W., Structural aspects of HDAC8 mechanism and dysfunction in Cornelia de Lange syndrome spectrum disorders. *Protein science : a publication of the Protein Society* **2016,** *25* (11), 1965-1976.

141. Helgeson, M.; Keller-Ramey, J.; Knight Johnson, A.; Lee, J. A.; Magner, D. B.; Deml, B.; Deml, J.; Hu, Y. Y.; Li, Z.; Donato, K.; Das, S.; Laframboise, R.; Tremblay, S.; Krantz, I.; Noon, S.; Hoganson, G.; Burton, J.; Schaaf, C. P.; Del Gaudio, D., Molecular characterization of HDAC8 deletions in individuals with atypical Cornelia de Lange syndrome. *Journal of human genetics* **2018,** *63* (3), 349-356.

142. Kaiser, F. J.; Ansari, M.; Braunholz, D.; Concepcion Gil-Rodriguez, M.; Decroos, C.; Wilde, J. J.; Fincher, C. T.; Kaur, M.; Bando, M.; Amor, D. J.; Atwal, P. S.; Bahlo, M.; Bowman, C. M.; Bradley, J. J.; Brunner, H. G.; Clark, D.; Del Campo, M.; Di Donato, N.; Diakumis, P.; Dubbs, H.; Dyment, D. A.; Eckhold, J.; Ernst, S.; Ferreira, J. C.; Francey, L. J.; Gehlken, U.; Guillen-Navarro, E.; Gyftodimou, Y.; Hall, B. D.; Hennekam, R.; Hudgins, L.; Hullings, M.; Hunter, J. M.; Yntema, H.; Innes, A. M.; Kline, A. D.; Krumina, Z.; Lee, H.; Leppig, K.; Lynch, S. A.; Mallozzi, M. B.; Mannini, L.; McKee, S.; Mehta, S. G.; Micule, I.; Mohammed, S.; Moran, E.; Mortier, G. R.; Moser, J. A.; Noon, S. E.; Nozaki, N.; Nunes, L.; Pappas, J. G.; Penney, L. S.; Perez-Aytes, A.; Petersen, M. B.; Puisac, B.; Revencu, N.; Roeder, E.; Saitta, S.; Scheuerle, A. E.; Schindeler, K. L.; Siu, V. M.; Stark, Z.; Strom, S. P.; Thiese, H.; Vater, I.; Willems, P.; Williamson, K.; Wilson, L. C.; Hakonarson, H.; Quintero-Rivera, F.; Wierzba, J.; Musio, A.; Gillessen-Kaesbach, G.; Ramos, F. J.; Jackson, L. G.; Shirahige, K.; Pie, J.; Christianson, D. W.; Krantz, I. D.; Fitzpatrick, D. R.; Deardorff, M. A., Loss-of-function

HDAC8 mutations cause a phenotypic spectrum of Cornelia de Lange syndrome-like features, ocular hypertelorism, large fontanelle and X-linked inheritance. *Human molecular genetics* **2014,** *23* (11), 2888-900.

143. Oehme, I.; Deubzer, H. E.; Wegener, D.; Pickert, D.; Linke, J.-P.; Hero, B.; Kopp-Schneider, A.; Westermann, F.; Ulrich, S. M.; von Deimling, A.; Fischer, M.; Witt, O., Histone Deacetylase 8 in Neuroblastoma Tumorigenesis. *Clinical Cancer Research* **2009,** *15* (1), 91.

144. Chakrabarti, A.; Oehme, I.; Witt, O.; Oliveira, G.; Sippl, W.; Romier, C.; Pierce, R. J.; Jung, M., HDAC8: a multifaceted target for therapeutic interventions. *Trends in pharmacological sciences* **2015,** *36* (7), 481-92.

145. Nakagawa, M.; Oda, Y.; Eguchi, T.; Aishima, S.; Yao, T.; Hosoi, F.; Basaki, Y.; Ono, M.; Kuwano, M.; Tanaka, M.; Tsuneyoshi, M., Expression profile of class I histone deacetylases in human cancer tissues. *Oncol Rep* **2007,** *18* (4), 769-74.

146. Wu, J.; Du, C.; Lv, Z.; Ding, C.; Cheng, J.; Xie, H.; Zhou, L.; Zheng, S., The up-regulation of histone deacetylase 8 promotes proliferation and inhibits apoptosis in hepatocellular carcinoma. *Dig Dis Sci* **2013,** *58* (12), 3545-53.

147. Balasubramanian, S.; Ramos, J.; Luo, W.; Sirisawad, M.; Verner, E.; Buggy, J. J., A novel histone deacetylase 8 (HDAC8)-specific inhibitor PCI-34051 induces apoptosis in T-cell lymphomas. *Leukemia* **2008,** *22*, 1026.

148. Higuchi, T.; Nakayama, T.; Arao, T.; Nishio, K.; Yoshie, O., SOX4 is a direct target gene of FRA-2 and induces expression of HDAC8 in adult T-cell leukemia/lymphoma. *Blood* **2013,** *121* (18), 3640-9.

149. Durst, K. L.; Lutterbach, B.; Kummalue, T.; Friedman, A. D.; Hiebert, S. W., The inv(16) Fusion Protein Associates with Corepressors via a Smooth Muscle Myosin Heavy-Chain Domain. *Molecular and Cellular Biology* **2003,** *23* (2), 607.

150. Qi, J.; Singh, S.; Hua, W. K.; Cai, Q.; Chao, S. W.; Li, L.; Liu, H.; Ho, Y.; McDonald, T.; Lin, A.; Marcucci, G.; Bhatia, R.; Huang, W. J.; Chang, C. I.; Kuo, Y. H., HDAC8 Inhibition Specifically Targets Inv(16) Acute Myeloid Leukemic Stem Cells by Restoring p53 Acetylation. *Cell Stem Cell* **2015,** *17* (5), 597-610.

151. Huang, W.-J.; Wang, Y.-C.; Chao, S.-W.; Yang, C.-Y.; Chen, L.-C.; Lin, M.-H.; Hou, W.-C.; Chen, M.-Y.; Lee, T.-L.; Yang, P.; Chang, C.-I., Synthesis and Biological Evaluation of ortho-Aryl N-Hydroxycinnamides as Potent Histone Deacetylase (HDAC) 8 Isoform-Selective Inhibitors. *ChemMedChem* **2012,** *7* (10), 1815-1824.

152. Yan, W.; Liu, S.; Xu, E.; Zhang, J.; Zhang, Y.; Chen, X.; Chen, X., Histone deacetylase inhibitors suppress mutant p53 transcription via histone deacetylase 8. *Oncogene* **2012,** *32*, 599.

153. Bykov, V. J. N.; Eriksson, S. E.; Bianchi, J.; Wiman, K. G., Targeting mutant p53 for efficient cancer therapy. *Nature Reviews Cancer* **2017,** *18*, 89.

154. Hsieh, C.-L.; Ma, H.-P.; Su, C.-M.; Chang, Y.-J.; Hung, W.-Y.; Ho, Y.-S.; Huang, W.-J.; Lin, R.-K., Alterations in histone deacetylase 8 lead to cell migration and poor prognosis in breast cancer. *Life Sciences* **2016,** *151*, 7-14.

155. Park, S. Y.; Jun, J. A.; Jeong, K. J.; Heo, H. J.; Sohn, J. S.; Lee, H. Y.; Park, C. G.; Kang, J., Histone deacetylases 1, 6 and 8 are critical for invasion in breast cancer. *Oncol Rep* **2011,** *25* (6), 1677-81.

156. Janoueix-Lerosey, I.; Schleiermacher, G.; Delattre, O., Molecular pathogenesis of peripheral neuroblastic tumors. *Oncogene* **2010,** *29*, 1566.

157. Rettig, I.; Koeneke, E.; Trippel, F.; Mueller, W. C.; Burhenne, J.; Kopp-Schneider, A.; Fabian, J.; Schober, A.; Fernekorn, U.; von Deimling, A.; Deubzer, H. E.; Milde, T.; Witt, O.; Oehme, I., Selective inhibition of HDAC8 decreases neuroblastoma growth in vitro and in vivo and enhances retinoic acid-mediated differentiation. *Cell death & disease* **2015,** *6*, e1657.

158. Zhao, G.; Wang, G.; Bai, H.; Li, T.; Gong, F.; Yang, H.; Wen, J.; Wang, W., Targeted inhibition of HDAC8 increases the doxorubicin sensitivity of neuroblastoma cells via up regulation of miR-137. *European journal of pharmacology* **2017,** *802*, 20-26.

159. Prashad, N., miR-665 targets c-MYC and HDAC8 to inhibit murine neuroblastoma cell growth. *Oncotarget* **2018,** *9* (69), 33186-33201.

160. Oger, F.; Dubois, F.; Caby, S.; Noël, C.; Cornette, J.; Bertin, B.; Capron, M.; Pierce, R. J., The class I histone deacetylases of the platyhelminth parasite Schistosoma mansoni. *Biochemical and biophysical research communications* **2008,** *377* (4), 1079-1084.

161. Caby, S.; Pagliazzo, L.; Lancelot, J.; Saliou, J.-M.; Bertheaume, N.; Pierce, R. J.; Roger, E., Analysis of the interactome of Schistosoma mansoni histone deacetylase 8. *PLOS Neglected Tropical Diseases* **2017,** *11* (11), e0006089.

162. Kannan, S.; Melesina, J.; Hauser, A.-T.; Chakrabarti, A.; Heimburg, T.; Schmidtkunz, K.; Walter, A.; Marek, M.; Pierce, R. J.; Romier, C.; Jung, M.; Sippl, W., Discovery of Inhibitors of Schistosoma mansoni HDAC8 by Combining Homology Modeling, Virtual Screening, and in Vitro Validation. *Journal of Chemical Information and Modeling* **2014,** *54* (10), 3005-3019.

163. Simoben, C.; Robaa, D.; Chakrabarti, A.; Schmidtkunz, K.; Marek, M.; Lancelot, J.; Kannan, S.; Melesina, J.; Shaik, T.; Pierce, R.; Romier, C.; Jung, M.; Sippl, W., A Novel Class of Schistosoma mansoni Histone Deacetylase 8 (HDAC8) Inhibitors Identified by Structure-Based Virtual Screening and In Vitro Testing. *Molecules (Basel, Switzerland)* **2018,** *23* (3), 566.

164. Yamauchi, Y.; Boukari, H.; Banerjee, I.; Sbalzarini, I. F.; Horvath, P.; Helenius, A., Histone deacetylase 8 is required for centrosome cohesion and influenza A virus entry. *PLoS pathogens* **2011,** *7* (10), e1002316.

165. Hai, Y.; Christianson, D. W., Histone deacetylase 6 structure and molecular basis of catalysis and inhibition. *Nature chemical biology* **2016,** *12* (9), 741-7.

166. Voelter-Mahlknecht, S.; Mahlknecht, U., Cloning and structural characterization of the human histone deacetylase 6 gene. *Int J Mol Med* **2003,** *12* (1), 87-93.

167. Verdel, A.; Curtet, S.; Brocard, M. P.; Rousseaux, S.; Lemercier, C.; Yoshida, M.; Khochbin, S., Active maintenance of mHDA2/mHDAC6 histone-deacetylase in the cytoplasm. *Curr Biol* **2000,** *10* (12), 747-9.

168. Khochbin, S.; Verdel, A.; Lemercier, C.; Seigneurin-Berny, D., Functional significance of histone deacetylase diversity. *Curr Opin Genet Dev* **2001,** *11* (2), 162-6.

169. Simoes-Pires, C.; Zwick, V.; Nurisso, A.; Schenker, E.; Carrupt, P. A.; Cuendet, M., HDAC6 as a target for neurodegenerative diseases: what makes it different from the other HDACs? *Mol Neurodegener* **2013,** *8*, 7.

170. Hubbert, C.; Guardiola, A.; Shao, R.; Kawaguchi, Y.; Ito, A.; Nixon, A.; Yoshida, M.; Wang, X. F.; Yao, T. P., HDAC6 is a microtubule-associated deacetylase. *Nature* **2002,** *417* (6887), 455-8.

171. Janke, C.; Bulinski, J. C., Post-translational regulation of the microtubule cytoskeleton: mechanisms and functions. *Nature reviews. Molecular cell biology* **2011,** *12* (12), 773-86.

172. Li, L.; Yang, X. J., Tubulin acetylation: responsible enzymes, biological functions and human diseases. *Cellular and molecular life sciences : CMLS* **2015,** *72* (22), 4237-55.

173. Gao, Y. S.; Hubbert, C. C.; Lu, J.; Lee, Y. S.; Lee, J. Y.; Yao, T. P., Histone deacetylase 6 regulates growth factor-induced actin remodeling and endocytosis. *Mol Cell Biol* **2007,** *27* (24), 8637-47.

174. Gao, Y. S.; Hubbert, C. C.; Yao, T. P., The microtubule-associated histone deacetylase 6 (HDAC6) regulates epidermal growth factor receptor (EGFR) endocytic trafficking and degradation. *The Journal of biological chemistry* **2010,** *285* (15), 11219-26.

175. McClure, J. J.; Li, X.; Chou, C. J., Advances and Challenges of HDAC Inhibitors in Cancer Therapeutics. *Advances in cancer research* **2018,** *138*, 183-211.

176. Matsuyama, A.; Shimazu, T.; Sumida, Y.; Saito, A.; Yoshimatsu, Y.; Seigneurin-Berny, D.; Osada, H.; Komatsu, Y.; Nishino, N.; Khochbin, S.; Horinouchi, S.; Yoshida, M., In vivo destabilization of dynamic microtubules by HDAC6-mediated deacetylation. *The EMBO journal* **2002,** *21* (24), 6820-31.

177. Zhang, X.; Yuan, Z.; Zhang, Y.; Yong, S.; Salas-Burgos, A.; Koomen, J.; Olashaw, N.; Parsons, J. T.; Yang, X. J.; Dent, S. R.; Yao, T. P.; Lane, W. S.; Seto, E., HDAC6 modulates cell motility by altering the acetylation level of cortactin. *Mol Cell* **2007,** *27* (2), 197-213.

178. Zhang, Y.; Li, N.; Caron, C.; Matthias, G.; Hess, D.; Khochbin, S.; Matthias, P., HDAC-6 interacts with and deacetylates tubulin and microtubules in vivo. *The EMBO journal* **2003,** *22* (5), 1168-79.

179. Sadoul, K.; Khochbin, S., The growing landscape of tubulin acetylation: lysine 40 and many more. *The Biochemical journal* **2016,** *473* (13), 1859-68.

180. Aldana-Masangkay, G. I.; Sakamoto, K. M., The role of HDAC6 in cancer. *J Biomed Biotechnol* **2011,** *2011*, 875824.

181. Ciechanover, A., Proteolysis: from the lysosome to ubiquitin and the proteasome. *Nature reviews. Molecular cell biology* **2005,** *6* (1), 79-87.

182. Boyault, C.; Zhang, Y.; Fritah, S.; Caron, C.; Gilquin, B.; Kwon, S. H.; Garrido, C.; Yao, T. P.; Vourc'h, C.; Matthias, P.; Khochbin, S., HDAC6 controls major cell response pathways to cytotoxic accumulation of protein aggregates. *Genes Dev* **2007,** *21* (17), 2172-81.

183. Rodriguez-Gonzalez, A.; Lin, T.; Ikeda, A. K.; Simms-Waldrip, T.; Fu, C.; Sakamoto, K. M., Role of the aggresome pathway in cancer: targeting histone deacetylase 6-dependent protein degradation. *Cancer research* **2008,** *68* (8), 2557-60.

184. Kawaguchi, Y.; Kovacs, J. J.; McLaurin, A.; Vance, J. M.; Ito, A.; Yao, T. P., The deacetylase HDAC6 regulates aggresome formation and cell viability in response to misfolded protein stress. *Cell* **2003,** *115* (6), 727-38.

185. Reed, N. A.; Cai, D.; Blasius, T. L.; Jih, G. T.; Meyhofer, E.; Gaertig, J.; Verhey, K. J., Microtubule acetylation promotes kinesin-1 binding and transport. *Current biology : CB* **2006,** *16* (21), 2166-72.

186. Iwata, A.; Riley, B. E.; Johnston, J. A.; Kopito, R. R., HDAC6 and microtubules are required for autophagic degradation of aggregated huntingtin. *The Journal of biological chemistry* **2005,** *280* (48), 40282-92.

187. Bali, P.; Pranpat, M.; Bradner, J.; Balasis, M.; Fiskus, W.; Guo, F.; Rocha, K.; Kumaraswamy, S.; Boyapalle, S.; Atadja, P.; Seto, E.; Bhalla, K., Inhibition of histone deacetylase 6 acetylates and disrupts the chaperone function of heat shock protein 90: a novel basis for antileukemia activity of histone deacetylase inhibitors. *The Journal of biological chemistry* **2005,** *280* (29), 26729-34.

188. Murphy, P. J., Regulation of glucocorticoid receptor steroid binding and trafficking by the hsp90/hsp70-based chaperone machinery: implications for clinical intervention. *Leukemia* **2005,** *19* (5), 710-2.

189. Miyake, Y.; Keusch, J. J.; Wang, L.; Saito, M.; Hess, D.; Wang, X.; Melancon, B. J.; Helquist, P.; Gut, H.; Matthias, P., Structural insights into HDAC6 tubulin deacetylation and its selective inhibition. *Nature chemical biology* **2016,** *12* (9), 748-54.

190. Butler, K. V.; Kalin, J.; Brochier, C.; Vistoli, G.; Langley, B.; Kozikowski, A. P., Rational design and simple chemistry yield a superior, neuroprotective HDAC6 inhibitor, tubastatin A. *Journal of the American Chemical Society* **2010,** *132* (31), 10842-6.

191. Lopez, J. E.; Sullivan, E. D.; Fierke, C. A., Metal-dependent Deacetylases: Cancer and Epigenetic Regulators. *ACS chemical biology* **2016,** *11* (3), 706-16.

192. Vishwakarma, S.; Iyer, L. R.; Muley, M.; Singh, P. K.; Shastry, A.; Saxena, A.; Kulathingal, J.; Vijaykanth, G.; Raghul, J.; Rajesh, N.; Rathinasamy, S.; Kachhadia, V.; Kilambi, N.; Rajgopal, S.; Balasubramanian, G.; Narayanan, S., Tubastatin, a selective histone deacetylase 6 inhibitor shows anti-inflammatory and anti-rheumatic effects. *International immunopharmacology* **2013,** *16* (1), 72-8.

193. Seidel, C.; Schnekenburger, M.; Dicato, M.; Diederich, M., Histone deacetylase 6 in health and disease. *Epigenomics* **2015,** *7* (1), 103-18.

194. Zilberman, Y.; Ballestrem, C.; Carramusa, L.; Mazitschek, R.; Khochbin, S.; Bershadsky, A., Regulation of microtubule dynamics by inhibition of the tubulin deacetylase HDAC6. *J Cell Sci* **2009,** *122* (Pt 19), 3531-41.

195. Lee, Y. S.; Lim, K. H.; Guo, X.; Kawaguchi, Y.; Gao, Y.; Barrientos, T.; Ordentlich, P.; Wang, X. F.; Counter, C. M.; Yao, T. P., The cytoplasmic deacetylase HDAC6 is required for efficient oncogenic tumorigenesis. *Cancer research* **2008,** *68* (18), 7561-9.

196. Wu, J. Y.; Xiang, S.; Zhang, M.; Fang, B.; Huang, H.; Kwon, O. K.; Zhao, Y.; Yang, Z.; Bai, W.; Bepler, G.; Zhang, X. M., Histone deacetylase 6 (HDAC6) deacetylates extracellular signal-regulated kinase 1 (ERK1) and thereby stimulates ERK1 activity. *The Journal of biological chemistry* **2018,** *293* (6), 1976-1993.

197. Zhang, Z.; Yamashita, H.; Toyama, T.; Sugiura, H.; Omoto, Y.; Ando, Y.; Mita, K.; Hamaguchi, M.; Hayashi, S.; Iwase, H., HDAC6 expression is correlated with better survival in breast cancer. *Clin Cancer Res* **2004,** *10* (20), 6962-8.

198. Yoshida, N.; Omoto, Y.; Inoue, A.; Eguchi, H.; Kobayashi, Y.; Kurosumi, M.; Saji, S.; Suemasu, K.; Okazaki, T.; Nakachi, K.; Fujita, T.; Hayashi, S., Prediction of prognosis of estrogen receptor-positive breast cancer with combination of selected estrogen-regulated genes. *Cancer Sci* **2004,** *95* (6), 496-502.

199. Li, A.; Chen, P.; Leng, Y.; Kang, J., Histone deacetylase 6 regulates the immunosuppressive properties of cancer-associated fibroblasts in breast cancer through the STAT3-COX2-dependent pathway. *Oncogene* **2018**.

200. Li, C.; Cao, L.; Xu, C.; Liu, F.; Xiang, G.; Liu, X.; Jiao, J.; Niu, Y., The immunohistochemical expression and potential prognostic value of HDAC6 and AR in invasive breast cancer. *Hum Pathol* **2018,** *75*, 16-25.

201. Putcha, P.; Yu, J.; Rodriguez-Barrueco, R.; Saucedo-Cuevas, L.; Villagrasa, P.; Murga-Penas, E.; Quayle, S. N.; Yang, M.; Castro, V.; Llobet-Navas, D.; Birnbaum, D.; Finetti, P.; Woodward, W. A.; Bertucci, F.; Alpaugh, M. L.; Califano, A.; Silva, J., HDAC6 activity is a non-oncogene addiction hub for inflammatory breast cancers. *Breast Cancer Res* **2015,** *17* (1), 149.

202. Bazzaro, M.; Lin, Z.; Santillan, A.; Lee, M. K.; Wang, M. C.; Chan, K. C.; Bristow, R. E.; Mazitschek, R.; Bradner, J.; Roden, R. B., Ubiquitin proteasome system stress underlies synergistic killing of ovarian cancer cells by bortezomib and a novel HDAC6 inhibitor. *Clin Cancer Res* **2008,** *14* (22), 7340-7.

203. Haakenson, J.; Zhang, X., HDAC6 and ovarian cancer. *International journal of molecular sciences* **2013,** *14* (5), 9514-35.

204. Bitler, B. G.; Wu, S.; Park, P. H.; Hai, Y.; Aird, K. M.; Wang, Y.; Zhai, Y.; Kossenkov, A. V.; Vara-Ailor, A.; Rauscher, F. J., III; Zou, W.; Speicher, D. W.; Huntsman, D. G.; Conejo-Garcia, J. R.; Cho, K. R.; Christianson, D. W.; Zhang, R., ARID1A-mutated ovarian cancers depend on HDAC6 activity. *Nature cell biology* **2017,** *19* (8), 962-973.

205. Sakuma, T.; Uzawa, K.; Onda, T.; Shiiba, M.; Yokoe, H.; Shibahara, T.; Tanzawa, H., Aberrant expression of histone deacetylase 6 in oral squamous cell carcinoma. *Int J Oncol* **2006,** *29* (1), 117-24.

206. Marquard, L.; Poulsen, C. B.; Gjerdrum, L. M.; de Nully Brown, P.; Christensen, I. J.; Jensen, P. B.; Sehested, M.; Johansen, P.; Ralfkiaer, E., Histone deacetylase 1, 2, 6 and acetylated histone H4 in B- and T-cell lymphomas. *Histopathology* **2009,** *54* (6), 688-98.

207. Bradbury, C. A.; Khanim, F. L.; Hayden, R.; Bunce, C. M.; White, D. A.; Drayson, M. T.; Craddock, C.; Turner, B. M., Histone deacetylases in acute myeloid leukaemia show a distinctive pattern of expression that changes selectively in response to deacetylase inhibitors. *Leukemia* **2005,** *19* (10), 1751-9.

208. Hartl, F. U., Protein Misfolding Diseases. *Annu Rev Biochem* **2017,** *86*, 21-26.

209. Cook, C.; Gendron, T. F.; Scheffel, K.; Carlomagno, Y.; Dunmore, J.; DeTure, M.; Petrucelli, L., Loss of HDAC6, a novel CHIP substrate, alleviates abnormal tau accumulation. *Human molecular genetics* **2012,** *21* (13), 2936-45.

210. Selenica, M. L.; Benner, L.; Housley, S. B.; Manchec, B.; Lee, D. C.; Nash, K. R.; Kalin, J.; Bergman, J. A.; Kozikowski, A.; Gordon, M. N.; Morgan, D., Histone deacetylase 6 inhibition improves memory and reduces total tau levels in a mouse model of tau deposition. *Alzheimers Res Ther* **2014,** *6* (1), 12.

211. Kim, C.; Choi, H.; Jung, E. S.; Lee, W.; Oh, S.; Jeon, N. L.; Mook-Jung, I., HDAC6 inhibitor blocks amyloid beta-induced impairment of mitochondrial transport in hippocampal neurons. *PloS one* **2012,** *7* (8), e42983.

212. Khan, U.; Ghazanfar, H., T Lymphocytes and Autoimmunity. *International review of cell and molecular biology* **2018,** *341*, 125-168.

213. de Zoeten, E. F.; Wang, L.; Butler, K.; Beier, U. H.; Akimova, T.; Sai, H.; Bradner, J. E.; Mazitschek, R.; Kozikowski, A. P.; Matthias, P.; Hancock, W. W., Histone deacetylase 6 and heat shock protein 90 control the functions of Foxp3(+) T-regulatory cells. *Mol Cell Biol* **2011,** *31* (10), 2066-78.

CHAPTER II

Phosphorylation of Histone Deacetylase 8: Structural and Mechanistic Analysis of Phosphomimetic S39E Mutant[ab]

Abstract

Histone deacetylase (HDAC) enzymes that catalyze removal of acetyl-lysine post translational modifications are also frequently post-translationally modified. HDAC8 is phosphorylated within the deacetylase domain at conserved residue serine 39 which leads to decreased catalytic activity. HDAC8 phosphorylation at S39 is unique in its location and function and may represent a novel mode of deacetylation regulation. To better understand the impact of phosphorylation of HDAC8 on enzyme structure and function, we performed crystallographic, kinetic, and molecular dynamics studies of the S39E HDAC8 phosphomimetic mutant. This mutation decreases deacetylation of peptides taken from acetylated nuclear and cytoplasmic proteins. However, the magnitude of the effect depends on the peptide sequence and the identity of the active site metal ion (Zn(II) vs Fe(II)) with the value of k_{cat}/K_M for the mutant decreasing 9- to >200-fold compared to wild-type HDAC8. Furthermore, the dissociation rate constant of the active site metal ion increases by ~15-fold. S39E HDAC8 was crystallized in complex with the inhibitor Droxinostat revealing that phosphorylation of S39, as mimicked by the glutamate side chain, perturbs local structure through distortion of the L1 loop. Molecular dynamics simulations of both S39E and phosphorylated S39 HDAC8 demonstrate that the perturbation of the L1 loop most likely occurs because of the loss of the hydrogen bond between

[a] Manuscript in preparation for Katherine R. Welker Leng, Carol Ann Castañeda, Christophe Decroos, Barira Islam, Shozeb M. Haider, David W. Christianson, and Carol A. Fierke.

[b] Author contributions: The manuscript was written through contributions of all authors. All authors have given approval to the final version of the manuscript. Katherine Welker Leng and Carol Ann Castañeda performed in vitro HDAC8 experiments, and Katherine Welker Leng, Carol Ann Castañeda, and Carol A. Fierke analyzed the data and wrote corresponding text. Christophe Decroos and David W. Christianson (University of Pennsylvania) performed crystallography and related methods, analyzed structural data, and wrote text regarding crystal structure. Barira Islam and Shozeb Haider (University College London) performed molecular dynamics simulations, analyzed that data and wrote corresponding text.

D29 and S39. Furthermore, the S39 perturbation causes structural changes that propagate through the protein scaffolding to influence function in the active site. These data demonstrate that phosphorylation likely plays an important regulatory role for HDAC8 by affecting ligand binding, catalytic efficiency and substrate selectivity.

Introduction

Addition of post translational modifications (PTMs) is a well-known mechanism used by cells to reversibly regulate protein structure and function. The family of histone deacetylases (HDACs), enzymes responsible for the removal of acetylation PTMs on proteins, are frequently modified themselves by various PTMs, including phosphorylation. HDACs 1-9 are phosphorylated at one or more sites, and the PTM regulates their protein-protein interactions, protein complex formation, and subcellular localization.[1-2] Of these, only HDAC5, HDAC6, and HDAC8 have a phosphorylation site within the deacetylase domain of their protein structure, which is more likely to impact enzyme activity.[2]

The location of phosphorylation on HDAC8 within the deacetylase domain is unique among HDACs. HDAC8 is phosphorylated by protein kinase A at serine 39 (S39), a residue not conserved among the closely related class I HDACs (arginine in HDAC1 and HDAC2, alanine in HDAC3).[3-4] HDAC4, 5, 7, and 9 have a nearby serine based on sequence alignment, though the local sequence environment is different.[5] S39 is conserved in homologues from many species including *Mus musculus* (Mouse), *Bos taurus* (Bovine), *Xenopus laevis* (African clawed frog) and *Danio rerio* (Zebrafish),[6] suggesting that the residue is important for HDAC8 function. However, S39 is not conserved in the orthologue of *Schistosoma mansoni*. This blood fluke is the most common parasite infecting humans and is responsible for intestinal schistosomiasis, a neglected tropical disease inflicting over 200 million people whose main treatment option is widely used and at risk for development of resistance. Since *S. mansoni* HDAC8 is targeted for antiparasitic drug development, clarification of S39 phosphorylation structure and function could illuminate novel targeting approaches.[7-9] HDAC8 phosphorylation is also unique among HDACs in function. While phosphorylation has been suggested to activate the catalytic activity of HDAC1 and HDAC2,[3, 10-13] phosphorylation decreases HDAC8 activity.[4] Moreover, despite conflicting results, phosphorylation appears to play an important role in HDAC1 and HDAC2 complex formation.[3, 10-11] While it is unclear whether phosphorylation of HDAC8 impacts

complex formation in cells, HDAC8 activity *in vitro* is not dependent on complex formation as in the case of HDAC1 and HDAC2.

The purpose of HDAC8 S39 phosphorylation remains a mystery. However, S39 phosphorylation clearly impacts HDAC8 structure and function by means of several proposed mechanisms. First, HDAC8 phosphorylation appears to alter subcellular localization in certain cell types.[14] Unlike other class I isozymes, HDAC8 has been observed in both the nucleus and the cytoplasm.[14-16] In myometrial cells, unmodified HDAC8 is observed in the cytoplasmic, cytoskeletal, and nuclear fractions.[14] In contrast, phosphorylated HDAC8 co-localizes almost entirely with the cytoskeleton.[14] Intriguingly, phosphorylated HDAC8 levels are increased in the myometrial cells of pregnant women while overall HDAC8 expression remains unchanged.[14] Phosphorylation may be used as a way to direct all or a portion of HDAC8 to specific compartments within the cell, potentially dependent on cell status, type, or location. Phosphorylation-dependent mechanisms of translocation have been observed in other HDACs as well. Providing a precedent for this behavior, phosphorylation regulates class II HDACs movement between nucleus and cytosol.[17-22]

In addition to regulating subcellular localization, HDAC8 phosphorylation also impacts acetylation levels in cells. Although within the deacetylase domain, S39 is located over 20 Å from the catalytic metal ion.[23-29] Despite this distance, S39 phosphorylation leads to inhibition of catalytic activity by an unknown mechanism.[4] Increased acetylation was observed on histones isolated from PKA-activated HeLa cells expressing Flag-tagged HDAC8 and treated with the adenylyl cyclase PKA activator forskolin, compared with untreated, non-overexpressed, and S39A-HDAC8 expressed control cells, indicative of PKA-mediated HDAC8 inhibition.[4] Moreover, phosphorylated Flag-HDAC8, immunopurified from the PKA-activated cells, exhibited slower rates of deacetylation of core histones H3 and H4 compared to the non-phosphorylated HDAC8 control.[4]

One hypothesis suggests S39 phosphorylation impacts catalytic activity through altering protein-protein interactions. Phosphorylation increases HDAC8 association with Human Est1p-like protein B (hEST1B) and Hsp70 in co-immunoprecipitation experiments, demonstrating selectivity for binding phosphorylated HDAC8.[30] Alternatively, S39 phosphorylation may have a direct impact on the active site and surrounding areas by leading to structural changes. R37 (Figure II.1) is a highly conserved residue critical for catalytic activity that serves as the

gatekeeper to the internal channel of HDAC8 by regulating hydrogen bond interactions between conserved 'gate' residues G303 and G305.[31] Presumably, a conformational change of R37 due to nearby S39 phosphorylation could lead to a similar outcome. Moreover, as shown in crystal structures of HDAC8, S39 is located at the base of loop L1 (Figure II.1) and is poised to modulate interactions with binding partners, substrates, and/or inhibitors distal to the active site.[23-24, 28-29] The L1 and L2 loops flank the active site of HDAC8 and their high flexibility accommodate binding of different ligands, as shown by crystallographic and molecular dynamics studies.[23-24, 28-29, 32-33] Indeed, the L1 and L2 loops are critical for ligand recognition and binding in part through the interaction between K33 (L1 loop) and D101 (L2 loop),[32-33] and in comparison with other isozymes, such as HDAC1 whose loops are more rigid, likely govern binding selectivity.[34] Perturbing the size and charge of S39 would lead to distortions in the α2 helix, which could impact K33 positioning and possibly the K33-D101 interaction and thereby substrate binding affinity and selectivity.

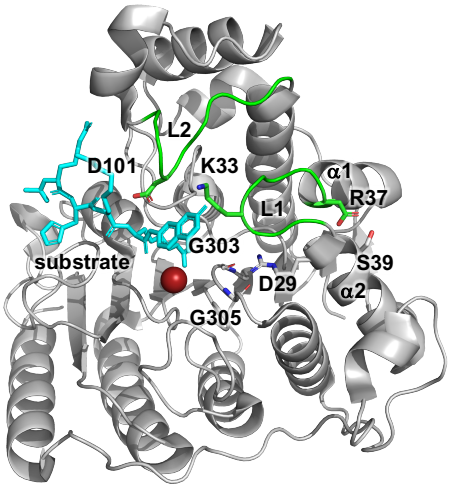

Figure II.1 Structure of HDAC8

Crystal structure of human, wild-type HDAC8 (grey, PDB ID 2V5W) bound to a peptide substrate derived from p53 (cyan)[26]. Loops L1 and L2 are shown in green and the active site zinc(II) ion is shown in red. Indicated are helices α1 and α2 and residues S39, R37, K33, D101, G303 and G305.

Since HDAC8 is involved in a variety of diseases, this isozyme is a target for drug development.[8] However, to date, no HDAC8-specific inhibitor has been approved for drug use. HDAC8 phosphorylation at S39 presents a unique mode of HDAC and specificially HDAC8

regulation, and therefore is an important subject for further investigation to identify and develop isozyme-specific drug targeting routes. Here we combine structural and biochemical data of the S39E phosphomimetic mutant to demonstrate that phosphorylation modulates conformational changes, which alter the reactivity and substrate selectivity of HDAC8.

Materials and Methods

Reagents

The HDAC inhibitor 4-(4-chloro-2-methylphenoxy)-*N*-hydroxybutanamide (Droxinostat) was obtained from Sigma Aldrich and was used without further purification. Tris(2-carboxyethyl)phosphine (TCEP) was purchased from GoldBio. All other reagents were purchased from Fisher unless otherwise specified.

Expression and purification of S39E HDAC8 for crystallization

The S39E mutation was introduced into the HDAC8-His_6-pET20b construct[24] using Quickchange site directed-mutagenesis kit protocols (Agilent Technologies, Inc.). Primers used for PCR mutagenesis are as follows: forward, 5'-GCT AAA ATC CCG AAA CGT GCA gag ATG GTG CAT TCT TTG ATT GAA G-3'; and reverse, 5'-C TTC AAT CAA AGA ATG CAC CAT ctc TGC ACG TTT CGG GAT TTT AGC-3'. Incorporation of the desired mutations was confirmed by DNA sequencing at the University of Pennsylvania Perelman School of Medicine. Recombinant S39E HDAC8 was expressed in BL21(DE3) *Escherichia coli* cells and purified according to a previously published procedure.[35]

Expression and purification of wild-type and S39E HDAC8 for assays

The S39E mutation was introduced into the pHD4 (HDAC8-TEV-His_6) plasmid[36] using custom primers (Integrated DNA Technologies) and Quickchange site directed-mutagenesis kit protocols (Agilent Technologies, Inc.). Primers used for PCR mutagenesis are as follows: forward, 5'-CCC GAA ACG TGC Aga GAT GGT GCA TTC TTT GAT TGA AGC ATA TG-3'; and reverse, 5'-CAT ATG CTT CAA TCA AAG AAT GCA CCA TCt cTG CAC GTT TCG GG-3'. Incorporation of desired mutations was confirmed by DNA sequencing performed by the University of Michigan DNA Sequencing Core, and the corresponding mass of the purified S39E HDAC8 was confirmed by Q-TOF HPLC-MS (Agilent) analysis. Wild-type (WT) and S39E HDAC8 were expressed in BL21 (DE3) *Escherichia coli* cells and purified according to

previously published procedures with modifications.[36-37] Briefly, BL21(DE3) cells were grown in 2x-YT media at 34°C. Once the OD_{600} reached at least 0.4, the temperature was decreased to 18°C for 45 min followed by zinc supplementation with 0.2 mM $ZnSO_4$, and expression induction with 0.5 mM isopropyl β-D-1-thiogalactopyranoside (IPTG). At 16 h post-induction, the cells were harvested by centrifugation at 6,238 x g for 15 min at 4°C.

The pelleted cells were resuspended in nickel buffer A (30 mM 4-(2-hydroxyethyl)-1-piperazineethanesulfonic acid (HEPES) pH 8, 150 mM NaCl, 1 mM imidazole, 1 mM TCEP, 5 mM KCl) supplemented with a cocktail of protease inhibitors and lysed using a microfluidizer (Microfluidics). Nucleic acids were precipitated using 0.1% PEI, pH 7.9, added dropwise with stirring on ice for 10-15 min. The lysate was cleared by centrifugation for 45 min at 26,900 x g and 4°C. The cleared lysate was loaded onto a 15-mL pre-charged HisPur Ni-NTA resin (Thermo Scientific) column, and HDAC8 was eluted using a 1-200 mM linear imidazole gradient. For His_{6x}-tag cleavage, the fractions from the nickel column containing HDAC8, as determined by SDS-PAGE, were pooled, combined with 0.5 mg 6His-TEV protease per 1 L culture, and dialyzed overnight at 4°C against 30 mM HEPES, pH 8, 150 mM NaCl, 1 mM TCEP, and 5 mM KCl. After overnight dialysis, HDAC8 was separated from the protease using a 3-mL Ni-NTA column, concentrated in 30K MWCO Amicon centrifuge filters at 1700 x g to <2 mL.

Apo enzyme was prepared by dialyzing the concentrated enzyme against 200-fold metal-chelation buffer (25 mM MOPS pH 7.5, 5 mM KCl, 1 mM EDTA, 1 mM TCEP) containing 1 mM ethylenediaminetetraacetic acid (EDTA) twice at 4°C with one incubation occurring overnight. To remove EDTA, the enzyme was dialyzed in the same way against 200-fold metal-free buffer, omitting the EDTA. Residual EDTA was removed using a PD-10 column (GE Healthcare) in metal-free assay buffer (25 mM HEPES, pH 8, 137 mM NaCl, and 3 mM KCl) plus 1 mM TCEP. Apo enzyme was verified to contain less than 10% metal contamination using inductively coupled plasma mass spectrometry (ICP-MS). Metal-free enzyme was aliquoted, flash frozen with liquid N_2, and stored at -80°C.

Fluor-de-Lys assay

The Fluor-de-Lys assay[38-39] (Enzo Life Sciences) was performed as described.[36] Metal-free HDAC8 was reconstituted for 1 h on ice with stoichiometric Zn(II) (Fluka Zinc Atomic Spectroscopy standard #96457) or Fe(II) (iron(II)chloride, Sigma). Reactions were performed at

30°C using the Fluor-de-Lys HDAC8 or Sirt1 p53-based commercial fluorophore-conjugated peptide substrate (Enzo Life Sciences). Enzyme was used to initiate reactions in HDAC8 assay buffer with substrate. Enzyme and substrate were equilibrated for at least 5 min at 30°C prior to initiation. For iron assays, solid iron(II)chloride (Sigma), solid ascorbic acid (Fluka), and HDAC8 assay buffer were equilibrated overnight in an anaerobic chamber (Coy Laboratory Products). The enzyme was equilibrated in the anaerobic chamber for 1 h prior to reconstitution, and substrate was equilibrated 1 h prior to the assay. Iron assays performed outside the anaerobic chamber were completed within 2 h, the effective working timespan for ascorbic acid to maintain Fe(II) (data not shown). Enzyme concentrations were 0.5 to 1 μM and substrate concentrations were 10 to 1000 μM. Time points were quenched using a combination of trypsin developer and trichostatin A (TSA) solution. After at least a 15 min incubation at room temperature, the fluorescence of product (ex. 340 nm, em. 450 nm) and substrate (ex. 340 nm, em. 380 nm) was measured using a PolarStar fluorescence plate reader. The ratio of product to substrate fluorescence was used to calculate HDAC8 activity using a standard curve derived from the completed reaction of HDAC8 with known amounts of substrate. k_{cat}/K_M values were generated by fitting the Michaelis-Menten equation (Equation II.1) to the v_0/[E] data at varying [S].

Equation II.1

$$\frac{v_0}{[E]} = \frac{k_{cat}}{K_M}\left(\frac{[S]}{\left(\frac{[S]}{K_M}+1\right)}\right)$$

Enzyme-coupled deacetylation assay

Non-fluorophore conjugated peptides were assayed by coupling deacetylation of acetyl-lysine residues to the formation of NADH as described.[40-41] Briefly, hydrolysis of acetyl-lysine forms acetate, which is converted to NADH via acetyl-CoA synthetase, citrate synthase, and malate dehydrogenase, and NADH is measured by fluorescence. Peptides (Peptide 2.0 or Synthetic Biomolecules) were N-terminally acetylated (N-terminal acetylation is not hydrolyzable by HDAC8) with C-terminal amides. The enzyme-coupled acetate-detection assay, referred to simply as the 'acetate assay', was performed as described.[40] As in the Fluor de Lys assay, metal-free HDAC8 was reconstituted for 1 h on ice with stoichiometric Zn(II) (Fluka Zinc Atomic Spectroscopy standard #96457). HDAC8 concentration ranged from 1-5 μM and substrate concentration varied from 10-1200 μM. Reaction time points (60 μL) were quenched into 5 μL 10% hydrochloric acid. Coupled enzyme solution reagents were purchased from Sigma, with the exception of acetyl-CoA synthetase, which was expressed and purified as

described.[40] Time points neutralized with 15 µL 6% sodium bicarbonate (60 µL) were loaded into wells of a black 96-well plate containing coupled enzyme solution (10 µL) and allowed to equilibrate protected from light. The fluorescence of the resulting NADH was measured (ex. = 340 nm, em. = 460 nm) and converted to product concentration using an acetate standard curve. An NADH standard curve was prepared to verify coupled solution activity. k_{cat}/K_M values were generated by fitting the Michaelis-Menten equation (Equation II.1) to the v_0/[E] data at varying [S].

Molecular dynamics (MD) simulations

The coordinates for the HDAC8-substrate complex for the simulations were taken from PDB ID: 2V5W.[26] The spatial positions of K^+ and Zn^{2+} ions were retained in the simulation from the original PDB. Three sets of simulations were completed: wild-type HDAC8, HDAC8 with phosphorylated S39 and HDAC8 with S39E mutation.

The modified phosphorylated protein simulation was made using the Forcefield PTM server (www.selene.princeton.edu/FFPTM). The AMBER forcefield parameters for post-translational modifications were taken from Khoury *et al*.[42-43] The S39E mutant structure was obtained from the crystal structure reported in this manuscript. Disordered loops were reconstructed using 2V5W structure as the template. The substrate was introduced in the HDAC8 enzyme after superimposition with 2V5W structure. A total of six simulations were carried out, with and without substrate.

The parameters for substrate were generated via the Antechamber module of the AMBER software using Generalized AMBER force field.[44-45] The charges were assigned to the substrate using the AM1-BCC method.[46] The systems were set up using xleap module of AMBER14.[47] K^+ ions were used for neutralization and TIP3P water molecules were used for solvation. AMBER-adapted Joung and Cheatham parameters specific for TIP3P waters and K^+ ions (radius 1.593 Å and well depth 0.4297054 kcal mol^{-1}) were used.[48] The system was solvated in a periodic box whose boundaries extended at least 10 Å from any solute atom. The periodic boundary conditions were defined by the PME algorithm and non-bonded cut-off was set to 10 Å.[49] All chemical bonds involving hydrogen atoms were restrained using SHAKE, allowing for stable simulations with a 2 fs time step.[50] Simulations were carried out using an NPT ensemble, using the Berendsen algorithm to control temperature and pressure.[51] Standard equilibration protocols were used for initial minimization of the structure.[52] The final MD simulations were carried out

for 400 ns using ACEMD and the frames were collected every 10 ps using a timestep of 4 fs.[53] Analyses of the trajectory were performed using the GROMACS 4.5 tools.[54-55] The programs ICM, VMD and PyMOL were used for visualization.[56-58]

Crystallization and data collection

Crystals of the S39E HDAC8-Droxinostat complex were grown in sitting drops at 21°C using the vapor diffusion method. A 500 nL drop containing 5.0 mg/mL S39E HDAC8, 50 mM Tris (pH 8.0), 150 mM KCl, 5% glycerol, 1 mM dithiothreitol, 2 mM Droxinostat, and 0.03 M glycylglycylglycine was added to a 500 nL drop of precipitant solution and equilibrated against a 100 μL reservoir of precipitant solution. The precipitant solution consisted of 100 mM BisTris (pH 6.5), 6% (w/v) PEG 8,000 (Hampton Research), and 4 mM TCEP.

Crystals appeared within 1 day. Crystals were flash-cooled in liquid nitrogen after transfer to a cryoprotectant solution consisting of precipitant solution supplemented with 25% glycerol. X-ray diffraction data were collected on beamline X29 at the National Synchrotron Light Source (NSLS, Brookhaven National Laboratory, New York). Data collection statistics are recorded in Table II.1. Data were indexed, integrated and scaled using HKL2000.[59]

Phasing, model building, and structure refinement

Crystals belonged to space group $P2_1$, with 2 molecules in the asymmetric unit. The crystal structure was solved by molecular replacement using PHENIX[60] with the atomic coordinates of the H143A HDAC8–tetrapeptide substrate complex (PDB accession code 3EWF)[24] less substrate, metal ions, and solvent molecules used as a search probe. The model was refined with iterative cycles of refinement in PHENIX[60] and manual model rebuilding in COOT.[61] Solvent molecules and inhibitors were added after initial rounds of refinement. Translation Libration Screw (TLS) refinement was performed in the late stages of refinement. TLS groups were automatically determined using PHENIX. Final refinement statistics are recorded in Table II.1.

Portions of the N-terminus, the C-terminus, and the L1 and L2 loops were characterized by missing or broken electron density. These segments appeared to be disordered and were excluded from the final model as follows: M1-S13 (monomers A and B), A32-I34 (monomer B), G86-D89 (monomer A) G86-E95 (monomer B), I378-H389 (monomer B), and E379-H389 (monomer A). Likewise, side chains of residues that were partially or completely disordered

were excluded from the model as follows: L14 (monomers A and B), K33 (monomer A), I34 (monomer A), K52 (monomer B), K58 (monomer B), K60 (monomers A and B), K81 (monomers A and B), Q84 (monomer A), E85 (monomer A), I94 (monomer A), E95 (monomer A), Y100 (monomer B), E106 (monomer B), K132 (monomers A and B), K221 (monomer B), E238 (monomer B), Q253 (monomers A and B), E358 (monomer B), K370 (monomer A), V377 (monomer A), and I378 (monomer A).

Occasional ambiguous electron density peaks were observed in the structure. These peaks were usually elongated and potentially correspond to disordered PEG fragments or other molecules present in the crystallization buffer. However, since these electron density peaks were not confidently interpretable, they were left unmodeled. Similarly, ambiguous electron density was observed around W141 in monomer A, possibly corresponding to alternative conformations. However, since such conformations were not confidently interpretable, the W141 side chain was modeled in only one primary conformation.

Results

Crystal structure of S39E HDAC8

Because the phosphorylated enzyme is difficult to obtain in the large quantities and purity needed for crystallization, we used the S39E-HDAC8 phosphomimetic mutant, which mimics phosphorylation at this site. The mutant was crystallized in an inhibitor-bound state. This is the first crystal structure of an HDAC isozyme complexed with Droxinostat, a selective HDAC3, HDAC6, and HDAC8 inhibitor with IC50s of 16.9 ± 5.0, 2.47 ± 1.09, and 1.46 ± 0.11 μM, respectively and >20 μM for HDACs 1, 2, 4, 5, 7, 9 and 10.[62] The structure of the S39E HDAC8-Droxinostat complex shows how phosphorylation of S39, as mimicked by the glutamate substitution, might influence inhibitor binding in the enzyme active site. Residue S39 is located in the α2 helix, approximately 20 Å away from the catalytic Zn^{2+} ion. The structure of the S39E HDAC8–Droxinostat complex is similar to that of the wild-type HDAC8–M344 complex (PDB accession code 1T67)[23] with a root mean square (r.m.s.) deviation of 0.49 Å for 356 Cα atoms and 0.47 Å for 350 Cα atoms, for monomers A and B, respectively. Although the S39E substitution does not cause any large-scale change in the HDAC8 structure (Figure II.2A), local structural changes are observed in the vicinity of E39 that propagate through to the active site via

structural changes in Loop L1. Presumably, these structural changes would be similarly triggered by phosphorylation of S39 in the wild-type enzyme.

In the wild-type HDAC8 structure, the hydroxyl group of S39 donates a hydrogen bond to the carboxylate group of D29, which is located in the adjacent α1 helix. In S39E HDAC8, the E39 side chain is oriented toward solvent and does not interact with any surrounding residues, including positively charged K36. Similarly, E39 does not perturb the nearby residue R37, the "gatekeeper" for the internal channel.[31] However, the S39E mutation induces a slight shift of D29 (0.6 Å for the Cα atom). The carboxylate side chain of D29 undergoes a conformational change away from E39, presumably to minimize electrostatic repulsion (Figure II.2A). A similar conformational change likely results from phosphorylation of S39 in wild-type HDAC8. The conformational change of D29 causes the L1 loop to reorganize. The L1 loop (L31-P35) connects helices α1 and α2 and is adjacent to the active site. Alternative conformations for the L1 and L2 loops are often observed in HDAC8 structures as they accommodate the binding of different ligands. Interestingly, the L1 loop in S39E HDAC8 appears to be more disordered than usually observed in HDAC8 complexes. This loop is characterized by higher thermal B factors, along with missing electron density for the side chains of K33 and I34 in monomer A, and weak electron density in monomer B that did not allow modeling of the A32-I34 segment.

This disorder appears to propagate through to the active site; the 4-chloro-2-methylphenoxyl capping group of the hydroxamate inhibitor Droxinostat is characterized by somewhat weaker electron density (Figure II.2B) and higher thermal B factors. The hydroxamate moiety of Droxinostat coordinates to the active site Zn^{2+} ion, forming a five-membered ring chelate, as typically observed in HDAC8-hydroxamate crystal structures.[23-26, 29, 35] The coordination distances to the Zn^{2+} ion are 2.0 Å and 2.2 Å for the hydroxamate hydroxyl and carbonyl groups, respectively. The Zn^{2+}-bound hydroxamate is also stabilized by hydrogen bond interactions with Y306, H142, and H143 (Figure II.2B). The capping group of Droxinostat does not make significant interactions with residues at the mouth of the active site. A contact is made between the chlorine atom of Droxinostat and the hydroxyl group of Y100 in the L2 loop (the Cl--O distance in monomer A is 3.2 Å; the side chain of Y100 is disordered in monomer B). However, Y100 is poorly oriented to consider this interaction as a hydrogen bond. The interaction may be a halogen bond.

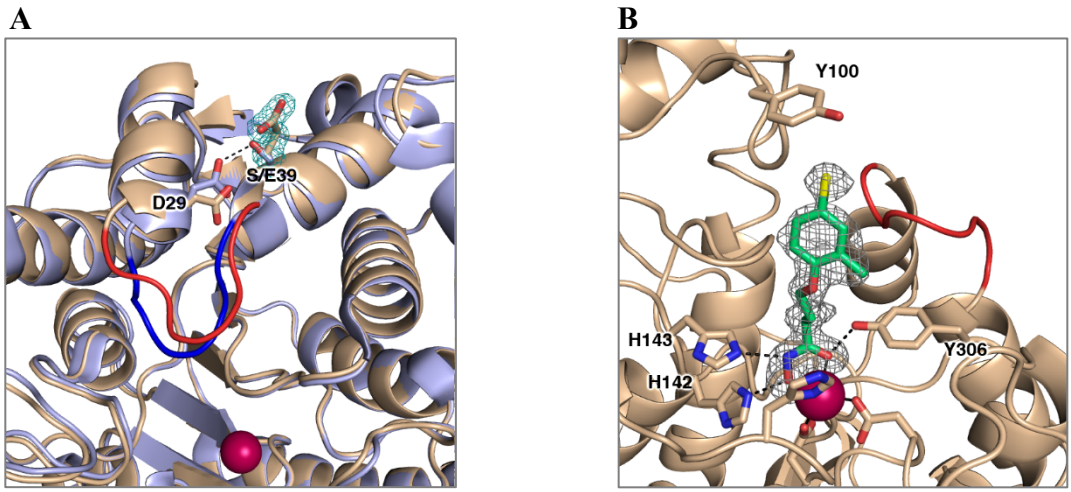

Figure II.2 Structural comparison of S39E and wild type HDAC8

A. Stereo view superimposition of the S39E HDAC8-Droxinostat complex (monomer A: C = wheat, N = blue, O = red, Zn^{2+} = magenta sphere) and the wild-type HDAC8-M344 complex (PDB 1T67, color-coded as above except C = light blue). In the wild-type structure, S39 donates a hydrogen bond (black dashed line) to D29. Upon substitution to a glutamate (simulated omit map contoured at 4.0σ showing the E39 side chain), this interaction is not conserved and causes local rearrangement. The L1 loop adopts a different conformation as highlighted in red and blue for the S39E HDAC8-Droxinostat complex and the wild-type HDAC8-M344 complex, respectively. B. Simulated annealing omit map of Droxinostat bound in the active site of S39E HDAC8 (monomer A, contoured at 3.0σ). Atomic color codes are as follows: C = wheat (protein, monomer A), or green (inhibitor), N = blue, O = red, Zn^{2+} = magenta sphere. Metal coordination and selected hydrogen bond interactions are shown as solid black or dashed black lines, respectively. As in A, the L1 loop of S39E HDAC8 is highlighted in red.

Table II.1 Data collection and refinement statistics for S39E-HDAC8-Droxinostat Complex

Unit cell	
Space group symmetry	$P2_1$
a, b, c (Å)	53.4, 84.4, 94.6
α, β, γ (deg)	90, 99.4, 90
Data collection	
Wavelength (Å)	1.075
Resolution limits (Å)	43.0-1.59
Total/unique reflections	819616/110604
R_{merge}[a,b]	0.080 (0.605)
I/σ(I)[a]	19.3 (4.7)
Redundancy[a]	7.4 (7.1)
Completeness (%)[a]	100 (100)
Refinement	
Reflections used in refinement/test set	110567/5539
R_{cryst}[c]	0.142
R_{free}[d]	0.160
Protein atoms[e]	5648
Water molecules[e]	777
Ligand molecules[e]	2
Zn^{2+} ions[e]	2
K^+ ions[e]	4
Glycerol molecules[e]	2
R.m.s. deviations from ideal geometry	
Bond lengths (Å)	0.010
Bond angles (°)	1.3
Dihedral angles (°)	12
Ramachandran plot (%)[f]	
allowed	91.1
additionally allowed	8.9
PDB accession code	5BWZ

[a] Values in parentheses refer to the highest shell of data.
[b] $R_{merge} = \sum | I_h - \langle I \rangle_h | / \sum I_h$, where $\langle I \rangle_h$ is the average intensity for reflection *h* calculated from replicate reflections.
[c] $R_{cryst} = \sum | |F_o| - |F_c| | / \sum |F_o|$ for reflections contained in the working set. $|F_o|$ and $|F_c|$ are the observed and calculated structure factor amplitudes, respectively.
[d] $R_{free} = \sum | |F_o| - |F_c| | / \sum |F_o|$ for reflections contained in the test set held aside during refinement.
[e] Per asymmetric unit. [f] Calculated with PROCHECK version 3.4.4
[f] Calculated with PROCHECK version 3.4.4.

***S39E decreases HDAC8 activity and changes substrate selectivity with peptides* in vitro**

While inhibition of HDAC8 activity by phosphorylation had been observed for core histone deacetylation in cell-based experiments,[4] detailed kinetic parameters for the phosphorylated enzyme or the phosphomimetic S39E mutant had not been determined. We hypothesized that perturbation of the L1 loop by S39 phosphorylation or mutation to glutamate could affect the substrate recognition by the enzyme. To investigate whether S39 alteration affects substrate selectivity or simply dampens activity globally towards all substrates, we measured the catalytic efficiency of Zn(II)-constituted S39E HDAC8 and wild-type HDAC8 toward deacetylation of a library of peptide substrates *in vitro*. Since the methylcoumarin fluorophore on the widely used Fluor-de-Lys peptide substrates enhances activity and substrate affinity with HDAC8, we selected additional un-labeled peptide substrates to test using the acetate assay, an assay that couples the formation of acetate to a fluorescent NADH readout.[40, 63] This selection of peptide substrates is taken from acetylated nuclear and cytoplasmic proteins that encompass a diverse range of cellular functions (Table II.2). Additionally, the list includes peptides from putative and novel HDAC8 substrates determined from computational modeling and cell-based proteomics screens including a peptide from SMC3, the best validated putative *in vivo* HDAC8 substrate to date.[64] [65-67] Consistent with previous reports, S39E HDAC8 activity was decreased compared to wild-type HDAC8 in all cases tested (Table II.2).

Notably, the deacetylase activity of S39E HDAC8 was reduced to differing extents, depending on the substrate (Table II.2, Figure II.4) with values ranging from a 9-fold to 220-fold decrease in activity for the S39E mutant compared to wild-type HDAC8. For the peptide corresponding to SMC3, the mutation nearly abolished activity. However, for the peptide corresponding to LARP1, the mutation caused a modest 9-fold reduction in activity compared to wild type (Figure II.3). Furthermore, while the wild-type catalytic efficiencies for the CAD and LARP1 peptides (660 ± 27 versus 653 ± 99 $M^{-1}s^{-1}$, respectively) were comparable, the S39E phosphomimetic displayed a 60-fold decrease in activity for the CAD peptide. Similarly, the value of k_{cat}/K_M for wild-type HDAC8 catalyzed deacetylation of the fluorogenic p53 HDAC8 peptide is comparable to the values for CAD and LARP1, yet S39E HDAC8 exhibited a 37-fold decreased catalytic efficiency for the labeled p53 HDAC8 peptide. These data indicate that the S39E mutation not only decreases activity but also has an impact on peptide substrate selectivity. These results suggest an alternate set of substrate recognition patterns triggered by S39

phosphorylation. Since the sequences for the CAD and LARP1 peptides are similar, we wondered whether swapping the C- and N-terminal sequences would impact selectivity. Unexpectedly, these sequence changes increased the reactivity of wild-type HDAC8 with both peptides by 4-5-fold while decreasing the reactivity with S39E HDAC8 by 4-7-fold. Therefore, the WT/S39E selectivity ratio increased significantly (Table II.2). This surprising result suggests alternate contacts between the peptide and the binding interface of the two enzymes caused by the shift in loop L1 due to changes in S39.

Table II.2 Kinetics of deacetylation of acetylated peptides catalyzed by S39E and wild-type HDAC8[a]

Substrate	Function	Sequence	WT: k_{cat}/K_M ($M^{-1}s^{-1}$)	S39E: k_{cat}/K_M ($M^{-1}s^{-1}$)	Ratio (WT/S39E)
H3K9	Chromatin	TKQTARK(ac)STGGKA	51 ± 3[b]	1.7 ± 0.2	30 ± 4
SMC3	Cell cycle	RVIGAKK(ac)DQY	58 ± 2	<0.5	>120
CSRP2BP	Acetyltransferase	STPVK(ac)FISR	160 ± 27[b]	11.5 ± 0.6	14 ± 2
LARP1	Translation	LGK(ac)FRR	653 ± 99	70 ± 10	9 ± 2
CAD Protein	Pyrimidine biosynthesis	LSK(ac)FLR	660 ± 27	11 ± 1	60 ± 6
MYH1 (CAD_LARP)	Muscle contraction	LSK(ac)FRR	2400 ± 100	10.6 ± 0.3	226 ± 11
LARP_CAD	Synthetic	LGK(ac)FLR	2900 ± 700	19 ± 4	153 ± 49
p53	Cell cycle	RHK(ac)K(ac)-AMC	950 ± 96	26 ± 3	37 ± 6
p53	Cell cycle	RHKK(ac)-AMC	1030 ± 200	8 ± 3	129 ± 54

[a] Values for k_{cat}/K_M were obtained by fitting the Michaelis-Menten equation (Equation II.1) to the dependence of the initial rates of deacetylation on the substrate concentration catalyzed by Zn(II)-constituted S39E and wild-type HDAC8. The p53 fluorogenic peptide substrates were measured using the Fluor de Lys assay (FdL) and all other peptides were measured using the acetate assay. Enzyme concentration was 1 μM and substrate concentration was varied from 10-1200 μM. Error was calculated from the linear fit of the initial rates (v_0).

[b] Values reported previously.[68] Control reactions were performed with 1 μM wild-type HDAC8 and 100 μM H3K9 and CSR2BP peptides parallel with the S39E reactions to verify that wild-type activity with peptide agreed with previously reported values.

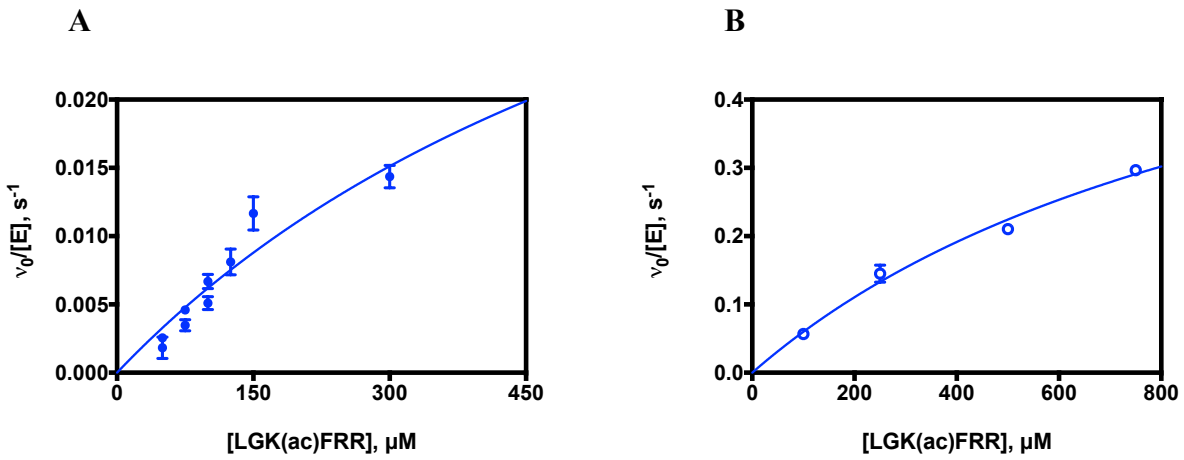

Figure II.3 Deacetylation of LARP1 peptide by S39E and wild-type HDAC8

Representative peptide assay data. Dependence of the initial rates of deacetylation of the LARP1 peptide (LGK(ac)FRR) on the substrate concentration catalyzed by Zn(II)-constituted (A) S39E (closed blue circles) and (B) wild-type HDAC8 (open blue circles) measured using the acetate assay[40]. Enzyme concentration was 1 µM and substrate concentration was 10-800 µM. The data are a combination of two experiments (Zn(II)-S39E), or one experiment (Zn(II)-WT), and the Michaelis-Menten equation (Equation II.1) was fit to the data using global regression analysis (GraphPad Prism).

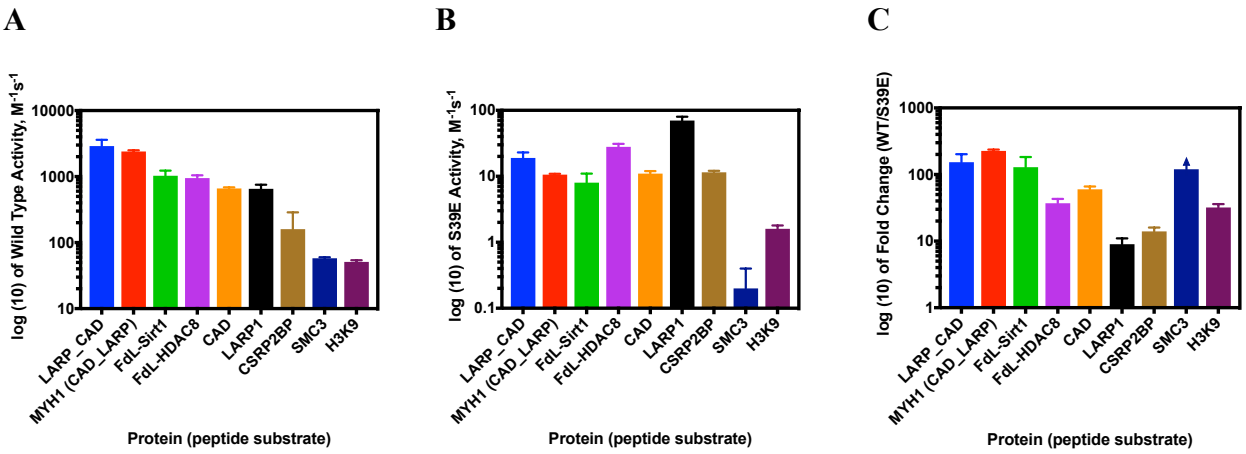

Figure II.4 Comparison of S39E and wild-type HDAC8 deacetylation of peptides

A. Catalytic efficiencies, k_{cat}/K_M, of wild-type HDAC8-catalyzed deacetyation of peptides listed in Table II.2 as measured by the Fluor de Lys assay (FdL-HDAC8 and FdL-Sirt1 peptides) and the acetate assay (remaining peptides). B. Catalytic efficiencies of S39E HDAC8 and C. fold change in catalytic efficiency of S39E HDAC8 compared to wild type for peptides. For all three graphs, peptides are ordered from most to least active with wild-type. Error bars are shown in same colors as columns. Substrate names on X-axis correspond to peptides listed in Table II.2.

S39E mutation increases metal dissociation rates and decreases metal-activation for iron(II) and zinc(II)

Additionally, we investigated the impact of phosphorylation on metal-selectivity. HDAC8 is activated by different metals, most notably iron(II) and the canonical catalytic ion zinc(II), and substrate selectivity changes based on the identity of the active site metal.[69] S39E HDAC8 activity was measured using the Fluor-de-Lys assay with Zn(II) and Fe(II) bound at the active site and the catalytic efficiencies were compared to those of Zn(II)- and Fe(II)-constituted wild-type HDAC8 (Table II.3, Figure II.5) Fe(II)- and Zn(II)-dependent catalytic efficiency (k_{cat}/K_M) was 6-fold and 34-fold lower, respectively, for the S39E mutant compared to wild type. Comparing the K_M and k_{cat} values for the Fe(II)-constituted enzymes revealed that the decrease in k_{cat}/K_M is due to both a 2-fold increase in K_M and a 3-fold reduction in k_{cat}. This suggests that the serine to glutamate mutation affects both substrate recognition and hydrolysis. As further evidence, the Zn(II) and Fe(II) metal dissociation rates were measured for the phosphomimetic and compared to those of wild type HDAC8 reported previously.[70] For both Zn(II) and Fe(II), the metal-dissociation rates of S39E increased approximately 15-fold compared to wild type (Figure II.6) providing further evidence of structural changes at the active site. Taken together, altering S39 enhances metal dissociation, decreases catalytic activity and alters substrate selectivity. These results indicate that HDAC8 phosphorylation may be an important modulator of HDAC8 activity.

Table II.3 Kinetics of Fe(II)- and Zn(II)-S39E and wild-type HDAC8[a]

HDAC8	k_{cat}/K_M ($M^{-1}s^{-1}$)	K_M (μM)	k_{cat} (s^{-1})	k_{cat}/K_M Ratio (WT/S39E)	k_{off} (min^{-1})	k_{off} Ratio (S39E/WT)
Fe(II)-S39E	440 ± 60	170 ± 30	0.077 ± 0.005	6 ± 2	0.48 ± 0.05	16 ± 3
Fe(II)-WT	2800 ± 700	90 ± 30	0.25 ± 0.02		0.030 ± 0.004[b]	
Zn(II)-S39E	28 ± 3	> 400[c]	> 0.05[c]	34 ± 5	0.57 ± 0.07	14 ± 2
Zn(II)-WT	950 ± 96	1200 ± 300	1.1 ± 0.3		0.040 ± 0.003[b]	

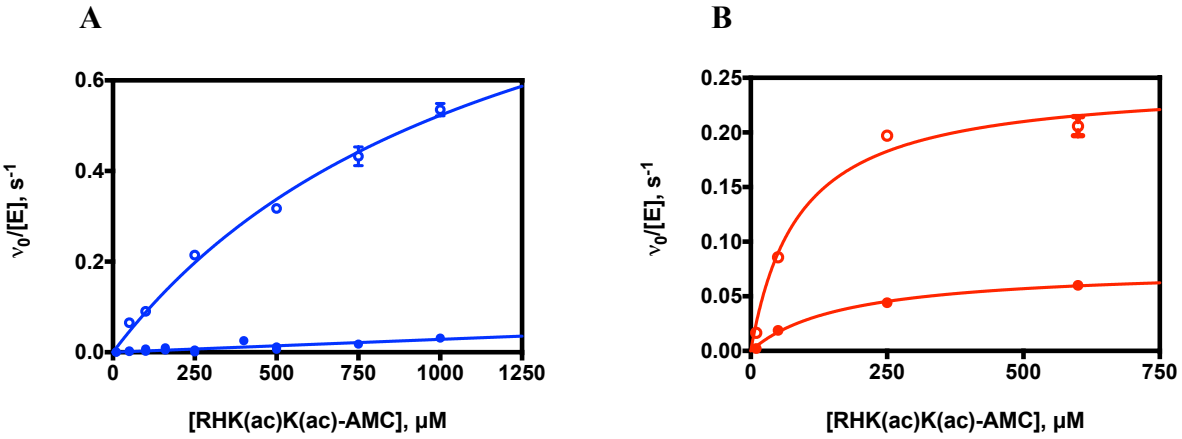

Figure II.5 Zinc(II)- and iron(II)-constituted S39E and wild-type HDAC8 catalyzed deacetylation of fluorescently-labeled Fluor de Lys HDAC8 test substrate

Dependence of the initial rates of deacetylation of the Fluor-de-Lys HDAC8 peptide substrate on substrate concentration catalyzed by A. Zn(II)-constituted S39E HDAC8 (closed blue circles) and Zn(II)-constituted WT HDAC8 (open blue circles) and B. Fe(II)-constituted S39E HDAC8 (closed red circles) and Fe(II)-constituted WT HDAC8 (open red circles). Enzyme concentration was 0.5-1 μM and substrate concentration was 10-1000 μM. The data are a combination of four experiments (Zn(II)-S39E), or one experiment (Zn(II)-WT, Fe(II)-S39E, Fe(II)-WT), and the Michaelis-Menten equation (Equation II.1) was fit to the data using global regression analysis (GraphPad Prism).

[a] Reactions consisting of 0.5 to 1 μM HDAC8 and 10 to 1000 μM substrate in 25 mM HEPES, pH 8.0, 137 mM NaCl, 3 mM KCl at 30°C.

[b] Little curvature was observed in the dependence of activity on substrate concentration so that K_M and k_{cat} are poorly defined by this data set. The necessity for excessively high enzyme and substrate concentrations preclude the accurate determination of these parameters.

[c] Values reported previously in Kim, et al. [70]

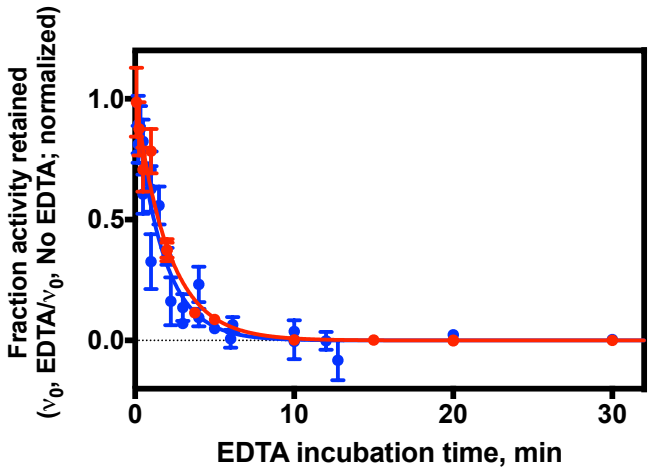

Figure II.6 Metal ion dissociation rates for zinc(II) and iron(II)-constituted S39E HDAC8

Initial rates for Zn(II)-constituted S39E HDAC8 (filled blue circles) and Fe(II)-constituted S39E HDAC8 (filled red circles) deacetylation activity as a function of time as measured using the Fluor-de-Lys assay after addition of 1 mM EDTA. The fraction activity is determined by dividing this activity by the activity of HDAC8 incubated in the absence of EDTA. The k_{off} values were calculated by fitting an exponential decay equation to data from replicates on different days using global regression analysis (GraphPad Prism).

Molecular dynamics simulations suggest phospho-HDAC8 structural changes

The crystal structure provides a snapshot of inhibitor-bound S39E HDAC8. To investigate the effects of phosphorylation on substrate-HDAC8 interactions, molecular dynamics simulations were performed, starting with an HDAC8-peptide substrate complex crystal structure (PDB ID: 2V5W).[26] We compared the substrate binding dynamics of phosphorylated HDAC8 (pS39-HDAC8, modeled), S39E HDAC8 (with substrate, modeled), and wild-type HDAC8. By simulating phosphorylation on the wild-type HDAC8 structure, we were able to predict the structure and dynamics of residues in the L1 loop that were not resolved in the S39E crystal structure and validate the S39E mutation as a mimic of phosphorylated HDAC8. While the mutant was crystalized in complex with an inhibitor, the simulations predict the structure of pS39-HDAC8 with and without peptide substrate bound. First, wild-type HDAC8 was modeled with and without the Fluor-de-Lys p53-based peptide substrate, to identify key residues in substrate binding. Relevant residue conformations surrounding S39 are highlighted in Figure II.7, with the most important being those of the substrate, Y306, and K33. Figure II.7 shows a comparison of wild-type, pS39- and S39E HDAC8 snapshots during substrate binding. The

simulations demonstrate that the pS39-HDAC8 structural behavior is comparable to that of the S39E-HDAC8 mutant, which validates use of the S39E-HDAC8 mutant for prediction of pS39-HDAC8 behavior *in vitro.* Importantly, the simulations also illustrate differences between wild-type and pS39/S39E-HDAC8 substrate binding conformations. Based on the simulations, modification of S39 leads to a disruption of the interaction between Y306 and K33, which perturbs substrate binding. In wild-type HDAC8, the interaction between S39-D29-K36 tethers the L1 loop and maintains the orientation of K36. This is distinct from the S39E-HDAC8 mutant dynamic simulation, in which there is no interaction between E39 and D29 (Figure II.8). The interaction between S39 and D29 is disrupted by the addition of negative charge at position 39. Instead, D29 interacts directly with K36 (Figure II.8). The strength of these interactions, and the disruption of interaction between residue 39 and D29 in the S39E mutant, is evident in the distance versus time plots in Figure II.8B. The K36-D29 interaction and altered Y306-K33 interaction preclude binding of substrate at the wild-type position. Instead, the peptide binds in a channel between K33 and Y306 where it is not optimally positioned for deacetylation by the active site metal-water nucleophile. These simulations provide insight into the basis for decreased pS39 and S39E HDAC8 activity and altered substrate selectivity, and although the D29-K36 contact is not noticeable in the S39E crystal structure, the altered orientation of D29 is consistent with the 0.6 Å shift for D29 that was observed in the crystal structure.

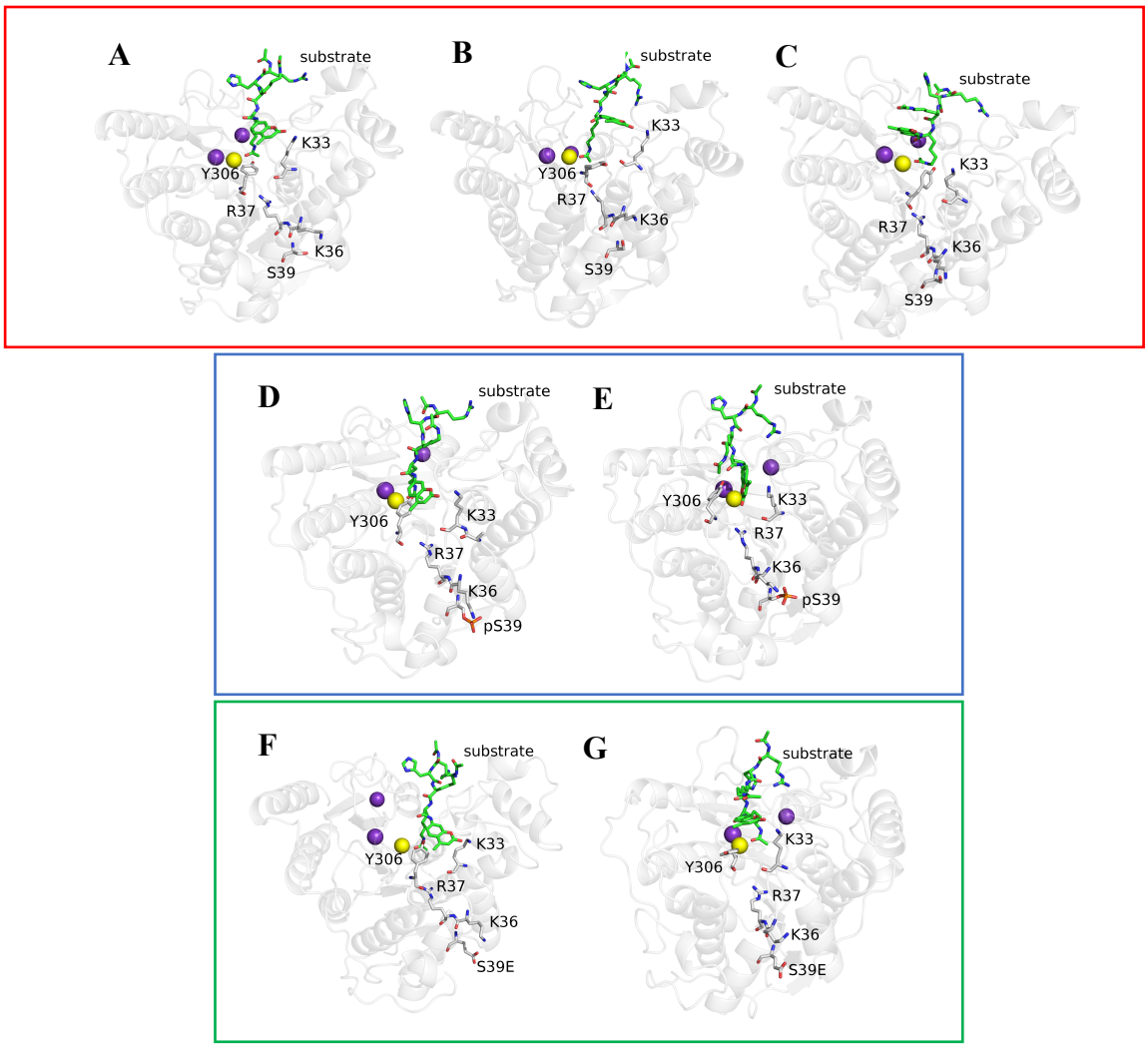

Figure II.7 Simulations of wild-type HDAC8 binding to substrate

Top panel (red box): The orientation of key residues in wild-type HDAC8 at A. the start, B. 51 ns, and C. 70 ns of the substrate binding simulation. S39 is solvent-exposed. Y306 bends at 90° toward K33, and the Hε of Y306 forms a hydrogen bond with the carbonyl of K33 (B). This opens the tunnel for substrate interaction with the active site, which is otherwise blocked by Y306. Yellow and purple spheres represent Zn^{2+} and K^{+} ions respectively. Center and bottom panels: Simulations of pS39 (blue box) and S39E (green box) bound to substrate. In the center panel (pS39 modeled on wild-type HDAC8), two snapshots (D. start and E. 400 ns) during the simulation demonstrate that the substrate is shifted in the active site between K33 and Y306 compared to wild-type HDAC8 (Figure II.7A-C). Y306 interacts with substrate but does not interact with K33. The bottom panel (S39E HDAC8 with modeled substrate) is a representation at F. the start and G. 400 ns of the simulation of key residues in S39E HDAC8 and demonstrates that the enzyme behaves similarly to pS39-HDAC8. The L1 loop is altered, Y306 and K33 do not interact (unlike in wild-type HDAC8 (Figure II.7B) where Y306 forms a hydrogen bond with the carbonyl oxygen of K33), and Y306 does not interact with substrate in this simulation. Substrate access to the active site is altered. Yellow and purple spheres represent Zn^{2+} and K^{+} ions respectively.

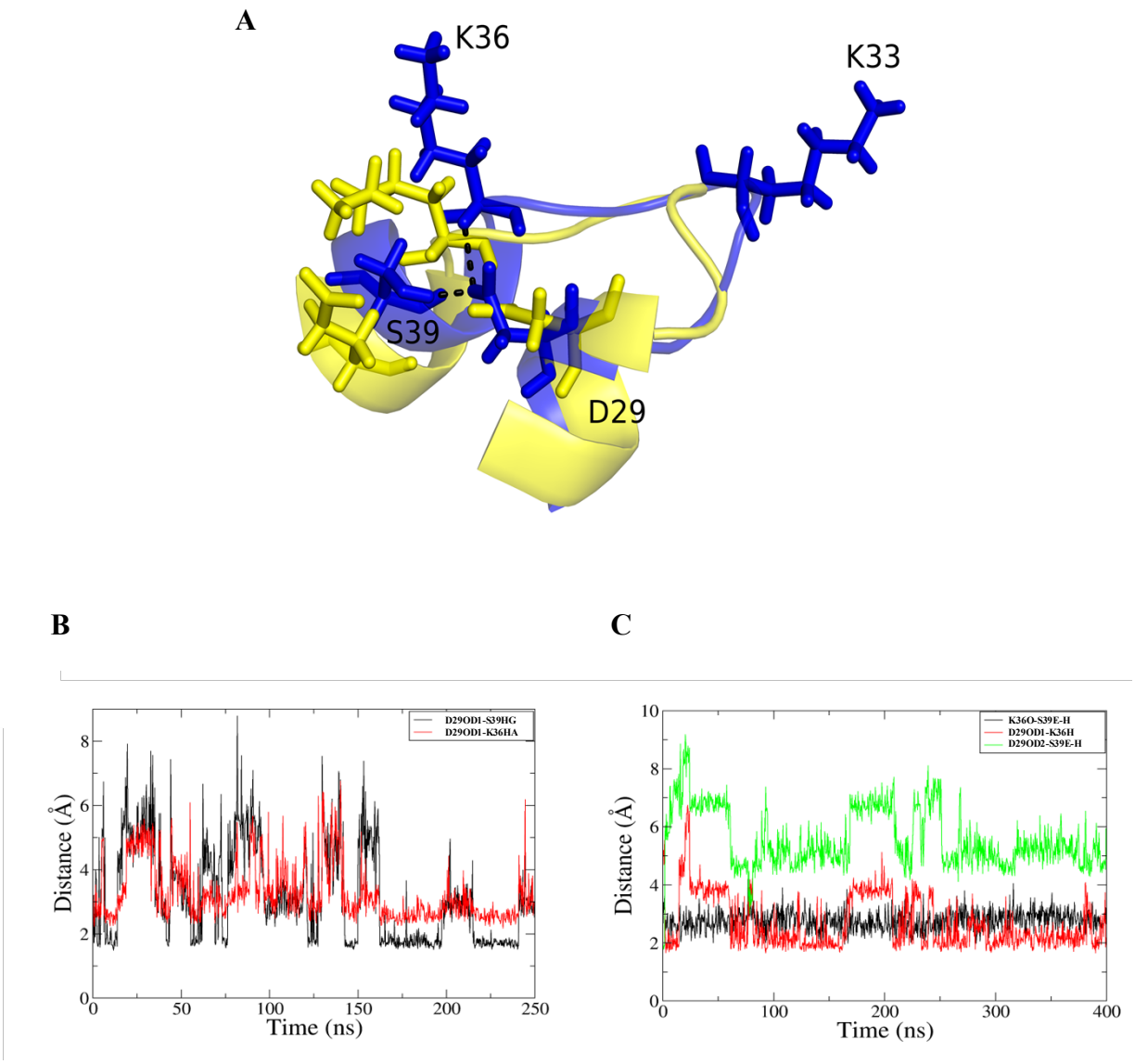

Figure II.8 Interaction between K36-D29-S39

A. The wild-type (blue) and mutant HDAC8 (yellow) is illustrated. The S39-D29 interaction tethers loop 1 and maintains the orientation of K33 in the wild-type protein. S39E can interact with K36 but not with D29 and therefore K33 orientation is not maintained in the mutant. B-C. Distance plot showing the interaction between D29, K36 and S39 in (B) wild-type and (C) S39E mutant HDAC8. In wild type, S39 can interact with D29 directly while in S39E, mutant residue S39E and D29 are beyond interacting distance (green).

Discussion

The mechanistic and functional roles of phosphorylation on HDAC8 are important facets of HDAC8 regulation that have not been well studied up to this point. To examine the effect of addition of a bulky negative charge at S39, S39E HDAC8 was used as a phosphomimetic. The validity of the mimic was bolstered by the fact that S39E HDAC8 and phospho-HDAC8 behave similarly in assays and in molecular simulations, while S39A HDAC8 behaves like the wild-type enzyme.[4] Previously, crystal structures of the S39D HDAC8 have been solved, and the structure of this mutant is reported to be essentially the same as the wild type.[26, 33] The S39E mutant, however, is a more appropriate mimic of phosphorylation[4] and the S39E-HDAC8-Droxinostat structure exhibits noticeable differences from the structure of the wild-type enzyme. The structure of the S39E HDAC8-Droxinostat complex reveals that the L1 loop undergoes a conformational change and the interaction between S39 and D29 is disrupted by the glutamate substitution. Loop L1 is important for HDAC8 substrate and inhibitor interactions, so this structural perturbation likely contributes to decreased catalytic efficiency.[33] It is important to note that a structure of wild-type HDAC8 complexed with Droxinostat has not been solved and comparing S39E HDAC8-Droxinostat directly to wild-type-HDAC8-Droxinostat would be useful to eliminate the possibility of structural changes induced by the identity of the inhibitor. However, structural comparisons indicate the capping group of the two inhibitors bound to the wild-type and S39E structures compared in this study is responsible for the selectivity seen with Droxinostat, and is thus less likely to affect active site orientation and structure, especially considering similar coordination of the hydroxamate moiety with the zinc(II) ion (Figure II.9).

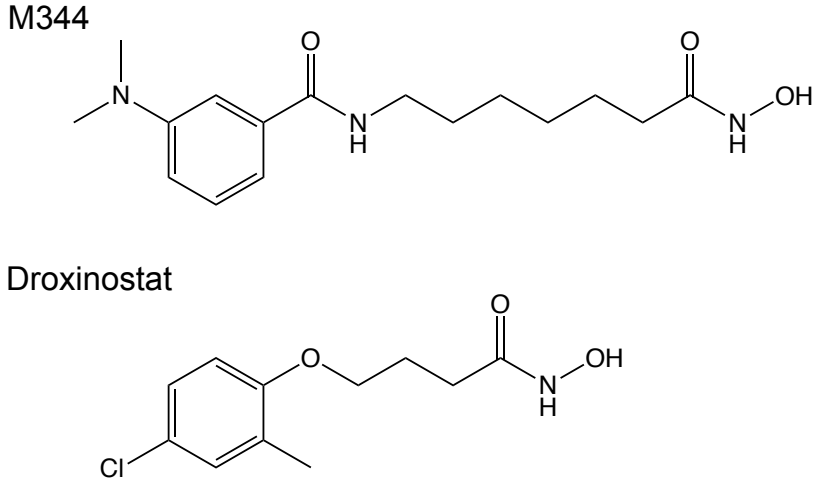

Figure II.9. Structures of HDAC inhibitors M344 and Droxinostat

Interestingly, contrary to previous hypotheses, the position of R37 is not altered in either the inhibitor-bound crystal structure or the phosphorylation simulation. As mentioned earlier, since R37 is in close proximity to S39E, conformational change of this important residue would not have been surprising.[31] Additionally, an electrostatic interaction between K36 and E39 had been anticipated but was not evident in the structure. Instead, the relevant structural changes observed were the perturbed interactions between Y306, substrate, and K33, the loss of a hydrogen bond between the hydroxyl of S39 and the carboxylate of D29 (which bridges the α1 and α2 helices), and the gain of an interaction between D29 and K36. Regarding the lost D29-S39 hydrogen bond, the inhibitor-bound structure shows that this change is correlated with a conformational change of the L1 loop. The pS39 HDAC8 simulation reveals that this lost interaction alters the position of the bound substrate. The substrate does not fully interact with the canonical substrate binding surface and instead is shifted into a channel between K33 and Y306. In this simulation, K36 interacts with D29 and the location of the side chain of the L1 loop residue, K33, is altered.

Substrate binding is typically oriented in part by Y306 and K33. However, in the absence of the hydrogen bond interaction between Y306 and the K33 backbone carbonyl, the substrate is shifted in the active site between these residues. This was the most significant difference observed in the simulations. The inhibitor-bound crystal structure does not show this altered Y306/K33 interaction and the inhibitor is positioned in the typical Zn(II)-bound orientation such that the carbonyl forms a hydrogen bond with Y306 (Figure II.2B). The fact that the crystal structure and the simulation provide somewhat different visualizations of ligand-bound S39E HDAC8 may be due to several factors. Mainly, the inhibitor is small and interacts primarily with the active site, limiting interactions with the HDAC8 peptide binding groove outside of the active site tunnel. Additionally, some residues (*e.g.* K33) cannot be directly compared to the simulated structure because they were not resolved in the crystal structure determination, suggesting significant mobility. Finally, while the crystal structure of S39E HDAC8 demonstrates structural difference and mimics phosphorylation, glutamate is not identical to phosphoserine and thus some differences between E39 and pS39 are expected.

S39E HDAC8 exhibits a 9- to 230-fold decrease in catalytic efficiency toward peptide substrates compared to wild type, consistent with previous data indicating phosphorylation decreases HDAC8 activity. However, the alteration in substrate selectivity by the

phosphomimetic mutant suggests that phosphorylation also regulates the targeting of specific cellular substrates for deacetylation by HDAC8. Phosphorylation could potentially lead to the alteration in acyl-group selectivity, as a number of the other HDACs have been observed to catalyze deacylation of other modified lysine residues including crotonyl-lysine, myristoyl-lysine, succinyl-lysine, and malonyl-lysine, among others.[71] However, this remains to be tested and no other reaction outside of deacetylation has been observed for HDAC8. The simulations and crystal structure suggest that the decrease in catalytic activity and change in substrate selectivity that accompanies perturbation of S39 arise from the consequent reordering of and/or disorder in the L1 loop flanking the active site cleft and changes to the ligand binding surface. Structural differences in this loop presumably influence its affinity for substrates and inhibitors binding to the active site. Assuming that the mutation does not change the kinetic mechanism of this enzyme, K_M is proposed to reflect the substrate binding affinity and k_{cat} reflects the rate of hydrolysis of the acetyl-lysine decreases.[36] Therefore, the increase in K_M observed for Fe(II)-constituted S39E HDAC8 compared to wild-type HDAC8 is consistent with the perturbation in the L1 loop affecting substrate affinity.[36] Furthermore, the decrease in k_{cat} indicates that the mutation also decreases catalysis of the hydrolytic step. This may be due to a direct effect on the reactivity of the metal-water nucleophile via structural changes propagated by the altered D29-S39 interaction, which could also explain the increase in the metal dissociation rates of Zn(II) and Fe(II) observed for S39E HDAC8. Additionally, as the substrate selectivity between the two metals was altered, the change in k_{cat} could also be linked to the alteration in the site of the bound peptide that leads to differential positioning of the acetyl-lysine amide bond relative to the nucleophilic metal-bound water molecule. However, the k_{cat} value was only accurately determined for the Fe(II)-constituted enzyme while the structure and simulations used Zn(II)-HDAC8, and activity data demonstrate that S39E HDAC8 and wild-type HDAC8 are activated to different extents depending on the identity of the catalytic metal ion.[36, 69]

Taken together, these data provide insight into the residue interactions (i.e. S39/D29) that lead to perturbation of the kinetic properties by S39 phosphorylation. Further study is needed to parse how the phosphorylation, substrate specificity, and metal-dependence of HDAC8 are interconnected. The role and regulation of phosphorylated HDAC8 in the cell is unclear, however, the peptide selectivity data suggest that phosphorylation both decreases catalytic activity and alters the cellular protein targets. Further examination of the cellular effect of

phosphorylation will provide insight into the regulation of deacetylation and inform drug discovery, as phosphorylation-dependent protein-protein interactions may present targeting approaches for small molecule therapeutics.

Funding Sources

We thank the National Institutes of Health for Grants 5-R01-GM-040602 (C.A.F.) and 5-R01-GM-49758 (D.W.C.), the University of Michigan Chemistry-Biology Interface (CBI) training program NIH grant 5T32GM008597 (C.A.C.), and Rackham Graduate School (C.A.C. and K.W.L.) for funding.

Accession Codes

The atomic coordinates and the crystallographic structure factors of S39E HDAC8 in complex with Droxinostat have been deposited in the Protein Data Bank (www.rcsb.org) with accession code 5BWZ.

Acknowledgements

We thank the NSLS for access to beamline X29 for X-ray crystallographic data collection. We thank Drs. Ted Huston and Lubomír Dostál for performing ICP-MS to verify solutions were free of metals. We thank Dr. Ningkun Wang and Oleta T. Johnson for collaboration on protein purification. We thank Noah A. Wolfson who helped with the substrate specificity assay using the NADH-coupled assay.

Abbreviations

HDAC, histone deacetylase; HEPES, 4-(2-hydroxyethyl)-1-piperazineethanesulfonic acid; IPTG, isopropyl β-D-1-thiogalactopyranoside; MD, molecular dynamics; PTM, post-translational modification; TCEP, tris(2-carboxyethyl)phosphine.

References

1. Brandl, A.; Heinzel, T.; Kramer, O. H., Histone deacetylases: salesmen and customers in the post-translational modification market. *Biology of the cell / under the auspices of the European Cell Biology Organization* **2009,** *101* (4), 193-205.

2. Eom, G. H.; Kook, H., Posttranslational modifications of histone deacetylases: Implications for cardiovascular diseases. *Pharmacology & Therapeutics* **2014,** *143* (2), 168-180.

3. Tsai, S. C.; Seto, E., Regulation of histone deacetylase 2 by protein kinase CK2. *The Journal of biological chemistry* **2002,** *277* (35), 31826-33.

4. Lee, H.; Rezai-Zadeh, N.; Seto, E., Negative Regulation of Histone Deacetylase 8 Activity by Cyclic AMP-Dependent Protein Kinase A. *Molecular and Cellular Biology* **2004,** *24* (2), 765-773.

5. Bottomley, M. J.; Lo Surdo, P.; Di Giovine, P.; Cirillo, A.; Scarpelli, R.; Ferrigno, F.; Jones, P.; Neddermann, P.; De Francesco, R.; Steinkuhler, C.; Gallinari, P.; Carfi, A., Structural and functional analysis of the human HDAC4 catalytic domain reveals a regulatory structural zinc-binding domain. *The Journal of biological chemistry* **2008,** *283* (39), 26694-704.

6. UniProt Consortium, T., UniProt: the universal protein knowledgebase. *Nucleic acids research* **2018,** *46* (5), 2699-2699.

7. Simoben, C.; Robaa, D.; Chakrabarti, A.; Schmidtkunz, K.; Marek, M.; Lancelot, J.; Kannan, S.; Melesina, J.; Shaik, T.; Pierce, R.; Romier, C.; Jung, M.; Sippl, W., A Novel Class of Schistosoma mansoni Histone Deacetylase 8 (HDAC8) Inhibitors Identified by Structure-Based Virtual Screening and In Vitro Testing. *Molecules (Basel, Switzerland)* **2018,** *23* (3), 566.

8. Chakrabarti, A.; Oehme, I.; Witt, O.; Oliveira, G.; Sippl, W.; Romier, C.; Pierce, R. J.; Jung, M., HDAC8: a multifaceted target for therapeutic interventions. *Trends in pharmacological sciences* **2015,** *36* (7), 481-92.

9. Kannan, S.; Melesina, J.; Hauser, A.-T.; Chakrabarti, A.; Heimburg, T.; Schmidtkunz, K.; Walter, A.; Marek, M.; Pierce, R. J.; Romier, C.; Jung, M.; Sippl, W., Discovery of Inhibitors of Schistosoma mansoni HDAC8 by Combining Homology Modeling, Virtual Screening, and in Vitro Validation. *Journal of Chemical Information and Modeling* **2014,** *54* (10), 3005-3019.

10. Galasinski, S. C.; Resing, K. A.; Goodrich, J. A.; Ahn, N. G., Phosphatase inhibition leads to histone deacetylases 1 and 2 phosphorylation and disruption of corepressor interactions. *The Journal of biological chemistry* **2002,** *277* (22), 19618-26.

11. Pflum, M. K.; Tong, J. K.; Lane, W. S.; Schreiber, S. L., Histone deacetylase 1 phosphorylation promotes enzymatic activity and complex formation. *The Journal of biological chemistry* **2001,** *276* (50), 47733-41.

12. Cai, R.; Kwon, P.; Yan-Neale, Y.; Sambuccetti, L.; Fischer, D.; Cohen, D., Mammalian histone deacetylase 1 protein is posttranslationally modified by phosphorylation. *Biochemical and biophysical research communications* **2001,** *283* (2), 445-53.

13. Eom, G. H.; Cho, Y. K.; Ko, J.-H.; Shin, S.; Choe, N.; Kim, Y.; Joung, H.; Kim, H.-S.; Nam, K.-I.; Kee, H. J.; Kook, H., Casein Kinase-2α1 Induces Hypertrophic Response by Phosphorylation of Histone Deacetylase 2 S394 and its Activation in the Heart. *Circulation* **2011,** *123* (21), 2392-2403.

14. Karolczak-Bayatti, M.; Sweeney, M.; Cheng, J.; Edey, L.; Robson, S. C.; Ulrich, S. M.; Treumann, A.; Taggart, M. J.; Europe-Finner, G. N., Acetylation of Heat Shock Protein 20 (Hsp20) Regulates Human Myometrial Activity. *Journal of Biological Chemistry* **2011,** *286* (39), 34346-34355.

15. Waltregny, D.; Glénisson, W.; Tran, S. L.; North, B. J.; Verdin, E.; Colige, A.; Castronovo, V., Histone deacetylase HDAC8 associates with smooth muscle alpha-actin and is essential for smooth muscle cell contractility. *The FASEB Journal* **2005**.

16. Waltregny, D.; de Leval, L.; Glénisson, W.; Ly Tran, S.; North, B. J.; Bellahcène, A.; Weidle, U.; Verdin, E.; Castronovo, V., Expression of Histone Deacetylase 8, a Class I Histone Deacetylase, Is Restricted to Cells Showing Smooth Muscle Differentiation in Normal Human Tissues. *The American Journal of Pathology* **2004,** *165* (2), 553-564.

17. Wang, A. H.; Kruhlak, M. J.; Wu, J.; Bertos, N. R.; Vezmar, M.; Posner, B. I.; Bazett-Jones, D. P.; Yang, X. J., Regulation of histone deacetylase 4 by binding of 14-3-3 proteins. *Mol Cell Biol* **2000,** *20* (18), 6904-12.

18. Grozinger, C. M.; Schreiber, S. L., Regulation of histone deacetylase 4 and 5 and transcriptional activity by 14-3-3-dependent cellular localization. *Proc Natl Acad Sci U S A* **2000,** *97* (14), 7835-40.

19. Li, X.; Song, S.; Liu, Y.; Ko, S. H.; Kao, H. Y., Phosphorylation of the histone deacetylase 7 modulates its stability and association with 14-3-3 proteins. *The Journal of biological chemistry* **2004,** *279* (33), 34201-8.

20. Kao, H. Y.; Verdel, A.; Tsai, C. C.; Simon, C.; Juguilon, H.; Khochbin, S., Mechanism for nucleocytoplasmic shuttling of histone deacetylase 7. *The Journal of biological chemistry* **2001,** *276* (50), 47496-507.

21. Ha, C. H.; Kim, J. Y.; Zhao, J.; Wang, W.; Jhun, B. S.; Wong, C.; Jin, Z. G., PKA phosphorylates histone deacetylase 5 and prevents its nuclear export, leading to the inhibition of gene transcription and cardiomyocyte hypertrophy. *Proc Natl Acad Sci U S A* **2010,** *107* (35), 15467-72.

22. Chang, C.-W. J.; Lee, L.; Yu, D.; Dao, K.; Bossuyt, J.; Bers, D. M., Acute β-Adrenergic Activation Triggers Nuclear Import of Histone Deacetylase 5 and Delays Gq-induced Transcriptional Activation. *Journal of Biological Chemistry* **2013,** *288* (1), 192-204.

23. Somoza, J. R.; Skene, R. J.; Katz, B. A.; Mol, C.; Ho, J. D.; Jennings, A. J.; Luong, C.; Arvai, A.; Buggy, J. J.; Chi, E.; Tang, J.; Sang, B. C.; Verner, E.; Wynands, R.; Leahy, E. M.; Dougan, D. R.; Snell, G.; Navre, M.; Knuth, M. W.; Swanson, R. V.; McRee, D. E.; Tari, L. W., Structural snapshots of human HDAC8 provide insights into the class I histone deacetylases. *Structure (London, England : 1993)* **2004,** *12* (7), 1325-34.

24. Dowling, D. P.; Gantt, S. L.; Gattis, S. G.; Fierke, C. A.; Christianson, D. W., Structural studies of human histone deacetylase 8 and its site-specific variants complexed with substrate and inhibitors. *Biochemistry* **2008,** *47* (51), 13554-63.

25. Dowling, D. P.; Gattis, S. G.; Fierke, C. A.; Christianson, D. W., Structures of metal-substituted human histone deacetylase 8 provide mechanistic inferences on biological function. *Biochemistry* **2010,** *49* (24), 5048-56.

26. Vannini, A.; Volpari, C.; Gallinari, P.; Jones, P.; Mattu, M.; Carfi, A.; De Francesco, R.; Steinkuhler, C.; Di Marco, S., Substrate binding to histone deacetylases as shown by the crystal structure of the HDAC8-substrate complex. *EMBO Rep* **2007,** *8* (9), 879-84.

27. Whitehead, L.; Dobler, M. R.; Radetich, B.; Zhu, Y.; Atadja, P. W.; Claiborne, T.; Grob, J. E.; McRiner, A.; Pancost, M. R.; Patnaik, A.; Shao, W.; Shultz, M.; Tichkule, R.; Tommasi, R. A.; Vash, B.; Wang, P.; Stams, T., Human HDAC isoform selectivity achieved via exploitation of the acetate release channel with structurally unique small molecule inhibitors. *Bioorg Med Chem* **2011,** *19* (15), 4626-34.

28. Cole, K. E.; Dowling, D. P.; Boone, M. A.; Phillips, A. J.; Christianson, D. W., Structural basis of the antiproliferative activity of largazole, a depsipeptide inhibitor of the histone deacetylases. *Journal of the American Chemical Society* **2011,** *133* (32), 12474-7.

29. Vannini, A.; Volpari, C.; Filocamo, G.; Casavola, E. C.; Brunetti, M.; Renzoni, D.; Chakravarty, P.; Paolini, C.; De Francesco, R.; Gallinari, P.; Steinkuhler, C.; Di Marco, S., Crystal structure of a eukaryotic zinc-dependent histone deacetylase, human HDAC8, complexed with a hydroxamic acid inhibitor. *Proc Natl Acad Sci U S A* **2004,** *101* (42), 15064-9.

30. Lee, H.; Sengupta, N.; Villagra, A.; Rezai-Zadeh, N.; Seto, E., Histone deacetylase 8 safeguards the human ever-shorter telomeres 1B (hEST1B) protein from ubiquitin-mediated degradation. *Mol Cell Biol* **2006,** *26* (14), 5259-69.

31. Haider, S.; Joseph, C. G.; Neidle, S.; Fierke, C. A.; Fuchter, M. J., On the function of the internal cavity of histone deacetylase protein 8: R37 is a crucial residue for catalysis. *Bioorganic & medicinal chemistry letters* **2011,** *21* (7), 2129-32.

32. Kunze, M. B.; Wright, D. W.; Werbeck, N. D.; Kirkpatrick, J.; Coveney, P. V.; Hansen, D. F., Loop interactions and dynamics tune the enzymatic activity of the human histone deacetylase 8. *Journal of the American Chemical Society* **2013,** *135* (47), 17862-8.

33. Decroos, C.; Clausen, D. J.; Haines, B. E.; Wiest, O.; Williams, R. M.; Christianson, D. W., Variable Active Site Loop Conformations Accommodate the Binding of Macrocyclic Largazole Analogues to HDAC8. **2015,** *54* (12), 2126-2135.

34. Weerasinghe, S. V. W.; Estiu, G.; Wiest, O.; Pflum, M. K. H., Residues in the 11 Å Channel of Histone Deacetylase 1 Promote Catalytic Activity: Implications for Designing Isoform-Selective Histone Deacetylase Inhibitors †. **2008,** *51* (18), 5542-5551.

35. Decroos, C.; Bowman, C. M.; Moser, J. A.; Christianson, K. E.; Deardorff, M. A.; Christianson, D. W., Compromised structure and function of HDAC8 mutants identified in Cornelia de Lange Syndrome spectrum disorders. *ACS chemical biology* **2014,** *9* (9), 2157-64.

36. Gantt, S. L.; Gattis, S. G.; Fierke, C. A., Catalytic activity and inhibition of human histone deacetylase 8 is dependent on the identity of the active site metal ion. *Biochemistry* **2006,** *45* (19), 6170-8.

37. Wolfson, N. A. Determining HDAC8 Substrate Specificity. Dissertation, University of Michigan, 2014.

38. Wegener, D.; Wirsching, F.; Riester, D.; Schwienhorst, A., A fluorogenic histone deacetylase assay well suited for high-throughput activity screening. *Chem Biol* **2003,** *10* (1), 61-8.

39. Wegener, D.; Hildmann, C.; Riester, D.; Schwienhorst, A., Improved fluorogenic histone deacetylase assay for high-throughput-screening applications. *Analytical biochemistry* **2003,** *321* (2), 202-8.

40. Wolfson, N. A.; Pitcairn, C. A.; Sullivan, E. D.; Joseph, C. G.; Fierke, C. A., An enzyme-coupled assay measuring acetate production for profiling histone deacetylase specificity. *Analytical biochemistry* **2014,** *456*, 61-9.

41. Baumann, M.; Stürmer, R.; Bornscheuer, U. T., A High-Throughput-Screening Method for the Identification of Active and Enantioselective Hydrolases. *Angewandte Chemie International Edition* **2001,** *40* (22), 4201-4204.

42. Khoury, G. A.; Thompson, J. P.; Smadbeck, J.; Kieslich, C. A.; Floudas, C. A., Forcefield_PTM: Charge and AMBER Forcefield Parameters for Frequently Occurring Post-Translational Modifications. *J Chem Theory Comput* **2013,** *9* (12), 5653-5674.

43. Khoury, G. A.; Smadbeck, J.; Tamamis, P.; Vandris, A. C.; Kieslich, C. A.; Floudas, C. A., Forcefield_NCAA: ab initio charge parameters to aid in the discovery and design of therapeutic proteins and peptides with unnatural amino acids and their application to complement inhibitors of the compstatin family. *ACS Synth Biol* **2014,** *3* (12), 855-69.

44. Wang, J.; Wang, W.; Kollman, P. A.; Case, D. A., Automatic atom type and bond type perception in molecular mechanical calculations. *J Mol Graph Model* **2006,** *25* (2), 247-60.

45. Wang, J.; Wolf, R. M.; Caldwell, J. W.; Kollman, P. A.; Case, D. A., Development and testing of a general amber force field. *J Comput Chem* **2004,** *25* (9), 1157-74.

46. Jakalian, A.; Jack, D. B.; Bayly, C. I., Fast, efficient generation of high-quality atomic charges. AM1-BCC model: II. Parameterization and validation. *J Comput Chem* **2002,** *23* (16), 1623-41.

47. Case, D. A.; Berryman, J. T.; Betz, R. M.; Cerutti, D. S.; Cheatham, T. E. I.; Goetz, A. W.; Homeyer, N.; Izadi, P.; Janowksi, P.; Kaus, J.; Kovalenko, A.; Lee, T. S.; LeGrand, S.; Li, P.; Luchko, T.; Luo, R.; Madej, B.; Merz, K. M.; Monard, G.; Needham, P.; Nguyen, H.; Nguyen, H. T.; Omelyan, I.; Onufriev, A.; Roe, D. R.; Roitberg, A.; Salomon-Ferrer, R.; Simmerling, C. L.; Swails, J.; Walker, R. C.; Wang, J.; Wolf, R. M.; Wu, X.; York; Darden, T. A.; Cheatham, T. E.; Simmerling, C. L.; Wang, J.; Duke, R. E.; Luo, R.; Walker, R. C.; Zhang, W.; Merz, K. M.; Roberts, B.; Hayik, S.; Roitberg, A.; Seabra, G.; Swails, J.; Walker, R. C.; Wang, J.; Wolf, R. M.; Xu, X.; York, D. M.; Kollman, P. A., AMBER 15. University of California, San Francisco: 2015.

48. Joung, I. S.; Cheatham, T. E., 3rd, Determination of alkali and halide monovalent ion parameters for use in explicitly solvated biomolecular simulations. *J Phys Chem B* **2008,** *112* (30), 9020-41.

49. Darden, T.; York, D.; Pedersen, L., Particle mesh Ewald: An N·log(N) method for Ewald sums in large systems. *J. Chem. Phys.* **1993,** *98* (12), 10089-10092.

50. Ryckaert, J.-P.; Ciccotti, G.; Berendsen, H. J. C., Numerical integration of the cartesian equations of motion of a system with constraints: molecular dynamics of n-alkanes. *J. Comput. Phys.* **1977,** *23* (3), 327-341.

51. Berendsen, H. J. C.; Postma, J. P. M.; van Gunsteren, W. F.; DiNola, A.; Haak, J. R., Molecular dynamics with coupling to an external bath. *J. Chem. Phys.* **1984,** *81* (8), 3684-3690.

52. Ohnmacht, S. A.; Marchetti, C.; Gunaratnam, M.; Besser, R. J.; Haider, S. M.; Di Vita, G.; Lowe, H. L.; Mellinas-Gomez, M.; Diocou, S.; Robson, M.; Šponer, J.; Islam, B.; Barbara Pedley, R.; Hartley, J. A.; Neidle, S., A G-quadruplex-binding compound showing anti-tumour activity in an in vivo model for pancreatic cancer. *Sci. Rep.* **2015,** *5*.

53. Harvey, M. J.; Giupponi, G.; Fabritiis, G. D., ACEMD: Accelerating Biomolecular Dynamics in the Microsecond Time Scale. *Journal of Chemical Theory and Computation* **2009,** *5* (6), 1632-1639.

54. Lindahl, E.; Hess, B.; van der Spoel, D., GROMACS 3.0: a package for molecular simulation and trajectory analysis. *J Mol Model* **2001,** *7* (8), 306-317.

55. Pronk, S.; Páll, S.; Schulz, R.; Larsson, P.; Bjelkmar, P.; Apostolov, R.; Shirts, M. R.; Smith, J. C.; Kasson, P. M.; van der Spoel, D.; Hess, B.; Lindahl, E., GROMACS 4.5: a high-throughput and highly parallel open source molecular simulation toolkit. *Bioinformatics* **2013,** *29* (7), 845-854.

56. Humphrey, W.; Dalke, A.; Schulten, K., VMD: Visual molecular dynamics. *J. Mol. Graphics* **1996,** *14* (1), 33-38.

57. DeLano, W. L. *The PyMOL Molecular Graphics System*, Schrodinger, LLC., 2008.

58. Fernandez-Recio, J.; Totrov, M.; Abagyan, R., ICM-DISCO docking by global energy optimization with fully flexible side-chains. *Proteins* **2003,** *52* (1), 113-7.

59. Otwinowski, Z.; Minor, W., Processing of X-ray diffraction data collected in oscillation mode. *Methods Enzymol.* **1997,** *276*, 307-326.

60. Adams, P. D.; Afonine, P. V.; Bunkoczi, G.; Chen, V. B.; Davis, I. W.; Echols, N.; Headd, J. J.; Hung, L. W.; Kapral, G. J.; Grosse-Kunstleve, R. W.; McCoy, A. J.; Moriarty, N. W.; Oeffner, R.; Read, R. J.; Richardson, D. C.; Richardson, J. S.; Terwilliger, T. C.; Zwart, P. H., PHENIX: a comprehensive Python-based system for macromolecular structure solution. *Acta Crystallogr D Biol Crystallogr* **2010,** *66* (Pt 2), 213-21.

61. Emsley, P.; Lohkamp, B.; Scott, W. G.; Cowtan, K., Features and development of Coot. *Acta Crystallogr D Biol Crystallogr* **2010,** *66* (Pt 4), 486-501.

62. Wood, T. E.; Dalili, S.; Simpson, C. D.; Sukhai, M. A.; Hurren, R.; Anyiwe, K.; Mao, X.; Suarez Saiz, F.; Gronda, M.; Eberhard, Y.; MacLean, N.; Ketela, T.; Reed, J. C.; Moffat, J.; Minden, M. D.; Batey, R. A.; Schimmer, A. D., Selective inhibition of histone deacetylases sensitizes malignant cells to death receptor ligands. *Mol Cancer Ther* **2010,** *9* (1), 246-56.

63. Gurard-Levin, Z. A.; Kim, J.; Mrksich, M., Combining mass spectrometry and peptide arrays to profile the specificities of histone deacetylases. *Chembiochem : a European journal of chemical biology* **2009,** *10* (13), 2159-61.

64. Wolfson, N. A.; Pitcairn, C. A.; Fierke, C. A., HDAC8 substrates: Histones and beyond. *Biopolymers* **2013,** *99* (2), 112-26.

65. Deardorff, M. A.; Bando, M.; Nakato, R.; Watrin, E.; Itoh, T.; Minamino, M.; Saitoh, K.; Komata, M.; Katou, Y.; Clark, D.; Cole, K. E.; De Baere, E.; Decroos, C.; Di Donato, N.;

Ernst, S.; Francey, L. J.; Gyftodimou, Y.; Hirashima, K.; Hullings, M.; Ishikawa, Y.; Jaulin, C.; Kaur, M.; Kiyono, T.; Lombardi, P. M.; Magnaghi-Jaulin, L.; Mortier, G. R.; Nozaki, N.; Petersen, M. B.; Seimiya, H.; Siu, V. M.; Suzuki, Y.; Takagaki, K.; Wilde, J. J.; Willems, P. J.; Prigent, C.; Gillessen-Kaesbach, G.; Christianson, D. W.; Kaiser, F. J.; Jackson, L. G.; Hirota, T.; Krantz, I. D.; Shirahige, K., HDAC8 mutations in Cornelia de Lange syndrome affect the cohesin acetylation cycle. *Nature* **2012,** *489* (7415), 313-7.

66. Alam, N.; Zimmerman, L.; Wolfson, N. A.; Joseph, C. G.; Fierke, C. A.; Schueler-Furman, O., Structure-Based Identification of HDAC8 Non-histone Substrates. *Structure (London, England : 1993)* **2016,** *24* (3), 458-68.

67. Olson, D. E.; Udeshi, N. D.; Wolfson, N. A.; Pitcairn, C. A.; Sullivan, E. D.; Jaffe, J. D.; Svinkina, T.; Natoli, T.; Lu, X.; Paulk, J.; McCarren, P.; Wagner, F. F.; Barker, D.; Howe, E.; Lazzaro, F.; Gale, J. P.; Zhang, Y. L.; Subramanian, A.; Fierke, C. A.; Carr, S. A.; Holson, E. B., An unbiased approach to identify endogenous substrates of "histone" deacetylase 8. *ACS chemical biology* **2014,** *9* (10), 2210-6.

68. Castaneda, C. A.; Wolfson, N. A.; Leng, K. R.; Kuo, Y. M.; Andrews, A. J.; Fierke, C. A., HDAC8 substrate selectivity is determined by long- and short-range interactions leading to enhanced reactivity for full-length histone substrates compared with peptides. *The Journal of biological chemistry* **2017,** *292* (52), 21568-21577.

69. Castaneda, C. A.; Lopez, J. E.; Joseph, C. G.; Scholle, M. D.; Mrksich, M.; Fierke, C. A., Active Site Metal Identity Alters Histone Deacetylase 8 Substrate Selectivity: A Potential Novel Regulatory Mechanism. *Biochemistry* **2017,** *56* (42), 5663-5670.

70. Kim, B.; Pithadia, A. S.; Fierke, C. A., Kinetics and thermodynamics of metal-binding to histone deacetylase 8. *Protein science : a publication of the Protein Society* **2015,** *24* (3), 354-65.

71. Olsen, C. A., An Update on Lysine Deacylases Targeting the Expanding “Acylome”. *ChemMedChem* **2014,** *9* (3), 434-437.

CHAPTER III

HDAC8 Substrate Selectivity is Determined by Long- & Short-Range Interactions Leading to Enhanced Reactivity for Full-Length Histone Substrates Compared to Peptides[ab]

Abstract

Histone deacetylases (HDACs) catalyze deacetylation of acetyl-lysine residues within proteins. To date, HDAC substrate specificity and selectivity have been largely estimated using peptide substrates. However, it is unclear whether peptide substrates accurately reflect the substrate selectivity of HDAC8 toward full-length proteins. Here, we compare HDAC8 substrate selectivity in the context of peptides, full-length proteins, and protein-nucleic acid complexes. We demonstrate that HDAC8 catalyzes deacetylation of tetrameric histone (H3/H4) substrates with catalytic efficiencies that are 40- to 300-fold higher than those for corresponding peptide substrates. Thus, we conclude that additional contacts with protein substrates enhance catalytic efficiency. However, the catalytic efficiency decreases for larger multi-protein complexes. These differences in HDAC8 substrate selectivity for peptides and full-length proteins suggest that HDAC8 substrate preference is based on a combination of short- and long-range interactions. In summary, this work presents detailed kinetics for HDAC8-catalyzed deacetylation of singly-acetylated, full-length protein substrates, revealing that HDAC8 substrate selectivity is determined by multiple factors. These insights provide a foundation for understanding recognition of full-length proteins by HDACs.

---

[a] Reproduction with permission from the American Society for Biochemistry and Molecular Biology of Castañeda, C. A., Wolfson, N. A., Leng, K. R., Kuo, Y., Andrews, A., Fierke, C. A. HDAC8 substrate selectivity is determined by long- and short-range interactions leading to enhanced reactivity for full-length histone substrates compared with peptides. *J. Biol. Chem.* **2017**, *292(52),* 21568-21577.

[b] Author contributions: NAW and CAF designed the study. NAW designed the assays and performed the peptide and tetramer assays. NAW, CAC, and KRL purified proteins and performed octamer assays. CAP and KRL assembled nucleosomes and performed nucleosome assays. NAW, CAC, CAF, and KRL analyzed the data. Y-MK performed and AJA designed the histone mass spectrometry analysis. NAW, CAC, KRL, and CAF prepared the manuscript. All authors reviewed and approved the final manuscript.

Background

The histone deacetylase (HDAC) family of enzymes comprises 18 proteins that catalyze the hydrolysis of the acetyl moiety from acetyl-lysine residues within substrate proteins.[1-2] Protein acetylation, catalyzed by lysine acetyltransferases (KATs), alters various properties of the modified protein (*e.g.* protein-protein interactions).[3] These alterations can in turn affect downstream cellular events.[4-5] As a result, regulation of acetylation by the respective activities of KATs and HDACs is important for effective cellular signaling and homeostasis; aberrant acetylation/deacetylation is implicated in pathologies ranging from neurological diseases[6-7] to cancers.[8-9] HDAC inhibitors have been approved by the FDA for the treatment of T-cell lymphomas and multiple myeloma.[10-12] Identifying the specific substrate set for each HDAC isozyme is important for understanding the role of HDACs in disease progression and therapeutic development.

To date, testing HDAC substrate specificity has remained a challenge, due in part to HDAC isozyme interchangeability and promiscuity, and the inherent difficulty in measuring the disappearance of signal from a previously modified substrate. To mitigate these difficulties, the HDAC field has sought to identify sequence motifs that define the substrate selectivity of each isozyme.[13-16] Most of these studies have used peptide substrates to determine HDAC recognition motifs. However, the use of peptides to mimic recognition of protein substrates has not been sufficiently validated. Gurard-Levin and colleagues proposed an exocite model, in which HDAC8 contains one or more substrate binding surfaces away from the active site, after observing HDAC8 sequence selectivity distal to the acetyl lysine in H4-based peptides longer than 20 amino acids.[15] However, outside of qualitative experiments,[17-18] there has been no kinetic characterization of HDAC-catalyzed deacetylation of protein substrates. HDAC8 is the best-characterized HDAC, with numerous crystal structures,[19-27] kinetic studies,[28-30] and peptide substrate specificity measurements,[13-16] providing an important background for the investigation of HDAC activity with protein substrates. While several putative HDAC8 substrates have been identified by cellular studies, including overexpression (*e.g.* ERRα),[31] genetic mutation (*e.g.* SMC3),[32-33] and proteomic studies (*e.g.* ARID1A),[34] the complete protein substrate set for HDAC8 is largely undefined.[31-32, 35-40]

Histones are putative substrates for HDAC8. In HEK293 cells, H3 and H4 acetylation levels decrease upon overexpression of HDAC8.[41] Moreover, treatment with the HDAC8-

specific SAHA-PIP derivative inhibitor Jδ increased acetylated H3 levels and expression of HDAC8-regulated transcription factors in mouse embryonic fibroblasts (MEF).[42] Furthermore, HDAC8 catalyzes deacetylation of core histones and H3-based peptides *in vitro*[43-44], however detailed kinetics have not previously been determined.

Recently, substrate specificity for the *S. cerevisiae* lysine acetyltransferase piccolo NuA4 has been measured using histone protein substrates, demonstrating acetylation of multiple lysine residues.[45] However, HDAC substrate specificity studies to date have utilized acetylated peptides,[13-15, 46-50] predicated on the assumption that HDAC8 uses similar interactions to recognize peptide and full-length protein substrates. To test the validity of this assumption, we determined the deacetylation kinetics of peptides corresponding to three biologically relevant acetylation sites on the putative HDAC8 substrate histone H3 (H3 K9, K14, and K56)[51-52] and compared the values to HDAC8-catalyzed deacetylation of full-length histone substrates.

To elucidate HDAC8 substrate specificity and recognition of protein substrates, we present the first detailed kinetic study of HDAC-catalyzed deacetylation of singly-acetylated, full-length protein substrates. Single acetyl-lysine side chains are inserted into H3 using non-natural amino acid incorporation.[53-54] We directly compare HDAC8 activity toward peptide substrates and toward protein substrates with the same local primary sequences. Furthermore, we analyze the effect of large histone complexes (histone core octamer and mononucleosome) on HDAC8-catalyzed deacetylation of acetylated H3. We demonstrate that deacetylation of acetylated full-length H3 tetramer and octamer complexes catalyzed by HDAC8 is significantly faster (> 8-fold) than that of acetylated peptides. However, the addition of DNA to form mononucleosomes decreases reactivity with HDAC8. These results demonstrate that HDAC8 specificity for H3 peptide tetramer substrates is not determined solely based on the six amino acids proximal to the acetyl-lysine; substrate specificity of HDAC8 is modulated by both long-range and short-range contacts for H3 substrates.

Results

Local sequence governs HDAC8 peptide specificity

We focused on the activity of HDAC8 with three acetylated lysine sites within histone H3, a histone known to be amenable to non-natural acetyl-lysine incorporation.[54] Two H3 acetylation sites (H3K9ac and H3K14ac) are located within proximity to each other on the N-

terminal tail and share an unfolded secondary structure. Because these sites differ only in amino acid sequence, the role of primary sequence in HDAC8 substrate specificity can be probed. A third site (H3K56ac), located on an α-helix within the globular structure of H3 (Figure III.1), allows the role of secondary structure in HDAC8 substrate recognition to be probed.

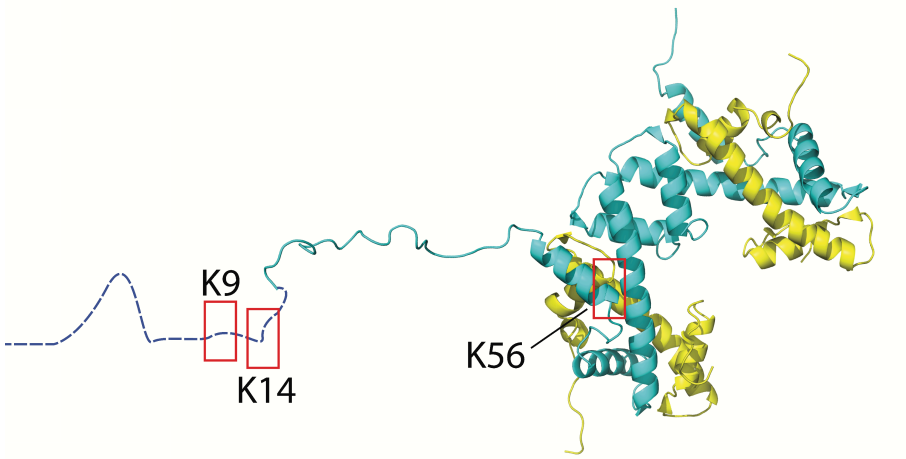

Figure III.1 Structure of histone H3/H4 tetramer with highlighted acetylation sites

Structure of histone H3/H4 tetramer[55] with boxes around the sites which were acetylated. H3 is shown in blue and H4 in yellow. H3 residues 1 to 20 are shown in an extended conformation as they have no discrete fold within the crystal structure. The structure was generated from PDB ID 1AOI using VMD.

The rates of HDAC8-catalyzed deacetylation of 7-mer peptides representing the 3 amino acids upstream and downstream of the H3K9ac, H3K14ac, and H3K56ac acetylation sites were measured under multiple turnover (MTO) conditions, using an assay coupling acetyl-lysine deacetylation to the formation of NADH[56] (Table III.1). The initial rates were linearly dependent on peptide concentration, indicating that the K_M values are higher than the peptide concentrations used in this assay (> 100 μM). The specificity constant (k_{cat}/K_M) is the best parameter to use for comparing the activity of HDAC8 toward multiple substrates.[57-59] HDAC8 has the highest catalytic efficiency for catalyzing hydrolysis of the H3K56ac peptide (k_{cat}/K_M = 78 ± 8.0 $M^{-1}s^{-1}$), followed by the H3K9ac (56 ± 6.0 $M^{-1}s^{-1}$) and H3K14ac (8.0 ± 0.70 $M^{-1}s^{-1}$) peptides (Table III.2).

To probe the importance of amino acids at further distances from the acetyl-lysine in determining substrate selectivity, longer peptides (13 and 17 amino acids) were assayed (Table III.2). Increasing the length of the peptides from 7 to 13 amino acids had little to no effect on catalytic efficiency (1- to 3-fold change) and did not affect the substrate selectivity trend of K56ac > K9ac > K14ac. A 17-amino acid peptide representing the H3K9ac site also showed less

than a three-fold increase in k_{cat}/K_M compared to the 7-amino acid peptide (56 ± 6.0 $M^{-1}s^{-1}$ vs. 120 ± 11 $M^{-1}s^{-1}$; (Table III.2). The modest differences in activity toward the longer peptides indicate that the primary sequence surrounding the acetylated lysine residue (+/- 3 of the acetyl-lysine) is the largest determinant of selectivity in peptide substrates, consistent with previously published data.[13-16]

Table III.1 Sequences of peptides used in this study[a]

Peptide	7-mer peptide sequence	13-mer peptide sequence	17-mer peptide sequence
H3K9ac	TARKacSTG	TKQTARKacSTGGKA	ARTKQTARKacSTGGKAPR
H3K14ac	TGGKacAPR	RKSTGGKacAPRKQL	
H3K56ac	RYQKacSTE	EIRRYQKacSTELLI	

HDAC8 catalyzes deacetylation of H3/H4 tetramers more efficiently than corresponding peptides

To investigate the importance of long-range HDAC8-substrate interactions in substrate recognition, we compared the rates of HDAC8-catalyzed deacetylation of peptide and the corresponding full-length protein. A major challenge in identifying HDAC substrates is determining the rates of deacetylation for individual acetyl-lysine sites, since HDAC substrates, such as histones, may have multiple acetylated lysine residues. We prepared proteins with single acetyl-lysine sites using the method of recombinant, non-natural amino acid incorporation developed by Jason Chin's group.[53-54] In each case, Q-TOF LC/MS of modified histone H3 demonstrated a mass change corresponding to an added acetylated lysine (data not shown). To stabilize H3, H3 was assembled into an H3/H4 tetramer. We measured HDAC8 activity toward the singly-acetylated H3 proteins acetylated at the H3K9, H3K14, and H3K56 sites under single turnover (STO) conditions (3-15 μM HDAC8 and 0.5 μM acetylated H3/H4 tetramer) and assayed deacetylation by MS analysis. STO experiments were used to minimize the amount of singly-acetylated H3/H4 tetramer needed. An exponential decay was fit to the reaction progress curves to determine the observed rate constants, k_{obs} (Figure III.2A). The observed rate of deacetylation of the H3K9ac/H4 tetramer was independent of the HDAC8 concentrations used in

[a] The amino acid sequences of the peptides assayed are listed above. Kac represents the acetyl-lysine residue. All peptides contain N-terminal acetyl and C-terminal carboxamide moieties.

these assays indicating that the enzyme concentration is above the $K_{1/2}$ for the reaction, even at the lowest concentration (3 μM). In contrast, the H3K14ac/H4 and H3K56ac/H4 tetramers show hyperbolic and nearly linear dependence, respectively, on the HDAC8 concentration. Assuming rapid equilibration of the HDAC8-H3/H4 complex, a hyperbolic fit to these data yields values of $k_{max}/K_{1/2}$ equal to >17,000 $M^{-1}s^{-1}$, 2,500 ± 70 $M^{-1}s^{-1}$, and 4,000 ± 600 $M^{-1}s^{-1}$ for the H3K9ac, H3K14ac, and H3K56ac tetramers, respectively (Figure III.2B-D and Table III.2). H3K9ac tetramer deacetylation is an order of magnitude faster than H3K56ac, followed by H3K14ac deacetylation. Each of these catalytic efficiencies is 40- to 300-fold faster than the corresponding peptide k_{cat}/K_M values.

The specificity constants indicate that substrate selectivity of HDAC8 for these H3 sites varies for the peptide (K56ac~K9ac>K14ac) and protein (K9ac>>K56ac>K14ac) substrates. The values of $k_{max}/K_{1/2}$ (measures binding through deacetylation) and k_{cat}/K_M (measures binding through dissociation) can be directly compared if product release is not rate limiting under multiple turnover conditions. Previous data suggest that the deacetylation step is likely the rate-limiting step (see discussion), also suggesting that $K_{1/2}$ and K_M reflect K_D.[28, 44] To validate our assumption in comparing the STO and MTO data, we assayed the 13-mer H3K9ac peptide under both STO and MTO conditions. MALDI-MS was used to measure HDAC8-catalyzed deacetylation of the peptide, due to the high enzyme concentration and sample size constraints in the enzyme-coupled peptide deacetylation assay. Using this method, the rate constant, $k_{max}/K_{1/2}$, is 153 $M^{-1}s^{-1}$ (data not shown). This rate constant is within three-fold of the value of the k_{cat}/K_M of 51 ± 3 $M^{-1}s^{-1}$ measured by the fluorescence-based peptide deacetylation assay. These data suggest that the STO measurements for the peptide substrates could be increased modestly compared to the MTO data but not enough to explain the increased reactivity of the protein substrates.

Comparison of the multiple turnover data for peptides and the single turnover data measured for full-length proteins demonstrates that interactions outside of short peptide sequences are important for directing HDAC8 substrate selectivity and enhancing catalytic efficiency. Further analysis demonstrates that the H3 peptides have K_M values higher than 100 μM (data not shown) while the H3K9ac/H4, H3K14ac/H4, and H3K56/H4 tetramers have $K_{1/2}$ values of < 1.5 μM, 19 ± 1 μM, and > 11 μM, respectively. Therefore, one factor leading to the increase in catalytic efficiency is a decrease in the value of $K_{1/2}$ in the STO reactions relative to

K_M for the peptides, suggesting enhanced binding affinity of the protein substrates. These differences suggest that long-range interactions enhance activity of HDAC8 toward full-length substrates.

The catalytic efficiency of HDAC8 towards its substrates is enhanced for all three H3Kac sites tested in the context of the tetramer compared to the corresponding peptides. However, relative HDAC8 activity for the tetramer sites compared to the peptides is different. The largest observed enhancement in catalytic efficiency is for the H3K9ac substrates (140- to 300-fold increase with the tetramer substrate), followed by H3K14ac (120- to 300-fold) and then H3K56ac (40- to 50-fold). In particular, the modest selectivity of HDAC8-catalyzed deacetylation of H3K56ac peptide compared to H3K9ac peptides is not maintained in the tetramer substrates, as would be expected if local sequence was the only determinant of substrate recognition.

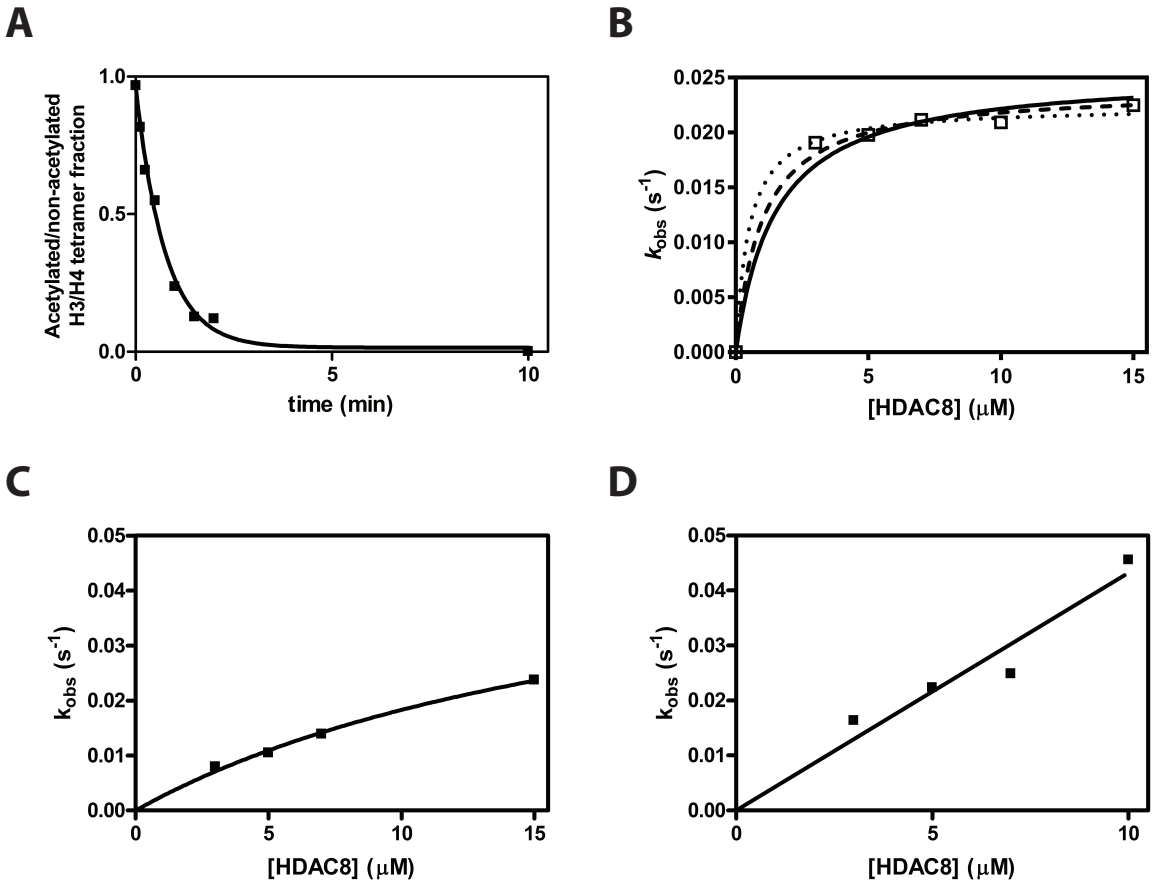

Figure III.2 Single turnover deacetylation of singly-acetylated H3/H4 tetramers

A. Sample data from a deacetylation reaction (7 μM HDAC8 and 0.5 μM H3K9ac/H4 tetramer (1 μM acetyl-lysine)) measured using mass spectrometry. The time-dependent decrease in acetylated protein is best described by a single exponential. B. Dependence of apparent deacetylation rate constant of H3K9ac/H4 on the concentration of HDAC8. The k_{obs} average of 0.021 ± 0.001 s^{-1} shows little dependence on the [HDAC8]. Three separate hyperbolic fits are shown that bracket potential $K_{1/2}$ values: $K_{1/2}$ = 0.5 μM (dotted line); $K_{1/2}$ = 1.0 μM (dashed line); $K_{1/2}$ = 1.5 μM (solid line). These fits demonstrate that the $K_{1/2}$ is < 1.5 μM and $k_{max}/K_{1/2}$ is > 17,000 $M^{-1}s^{-1}$. The data points are from multiple measurements in a single reaction at each HDAC8 concentration. C. Dependence of the deacetylation rate constant for H3K14ac/H4 on the concentration of HDAC8. The data points are from multiple measurements in a single reaction at each HDAC8 concentration. A hyperbolic fit indicates that the $k_{max}/K_{1/2}$ is 2,500 ± 70 $M^{-1}s^{-1}$ with an estimated value for k_{max} of 0.06 s^{-1}. D. Dependence of the deacetylation rate constant for H3K56ac/H4 on the concentration of HDAC8. The data points are from multiple measurements in a single reaction at each HDAC8 concentration. A linear fit indicates that the $k_{max}/K_{1/2}$ is 4,000 ± 600 $M^{-1}s^{-1}$.

Table III.2 Catalytic efficiencies for deacetylation of histone substrates by HDAC8[a]

Substrate	7-mer Peptide	13-mer peptide	17-mer Peptide	Tetramer	Octamer	Nucleosome
	k_{cat}/K_M (M^{-1} s^{-1})			$k_{max}/K_{1/2}$ (M^{-1} s^{-1})		
H3K9ac	56 ± 6	51 ± 3	120 ± 11	>17,000	3,700 ± 100	28 ± 3
H3K14ac	8.0 ± 0.7	21 ± 4	-	2,500 ± 70	1,000 ± 200	-
H3K56ac	78 ± 8	100 ± 10	-	4,000 ± 600	-	-

[a] HDAC8 activity was measured and catalytic efficiencies were determined as described in the Experimental Procedures and the legend of Figure III.2, Figure III.3, and Figure III.4

Octamer substrates less reactive than tetramers

To further examine full-length substrate selectivity, we measured the deacetylase activity of HDAC8 toward histone octamer complexes containing single acetylation sites. We compared the local sequence of the best and worst tetramer substrates, H3K9ac and H3K14ac, in the context of the complete histone octamer. Histone octamers were reconstituted with two copies of each core histone (H2A, H2B, singly-acetylated H3, and H4). The deacetylation rate catalyzed by HDAC8 was measured under single turnover conditions and analyzed as described for the tetramer. The resulting k_{obs} values for H3K9ac octamer are linearly dependent on the HDAC8 concentration (Figure III.3), yielding a $k_{max}/K_{1/2}$ value of 3,700 ± 100 $M^{-1}s^{-1}$. Deacetylation of the H3K14ac octamer has a hyperbolic dependence on HDAC8 concentration leading to a value of $k_{max}/K_{1/2}$ of 1,000 ± 200 $M^{-1}s^{-1}$. This catalytic efficiency is decreased three-fold compared to the H3K14ac/H4 tetramer and is 40-120 fold faster than the deacetylation of H3K14ac peptides. The catalytic efficiency for the H3K9ac octamer site is decreased four-fold compared to that of H3K9ac tetramer.

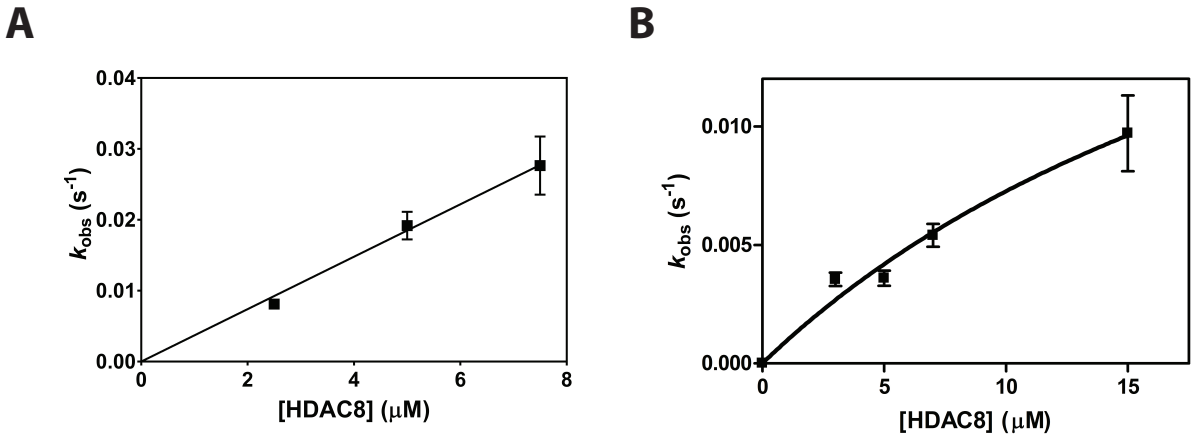

Figure III.3 Single turnover deacetylation of singly-acetylated H3 octamers

A. Dependence of the apparent deacetylation rate constant of H3K9ac octamer on the concentration of HDAC8. Data points are from multiple measurements in a single reaction at each HDAC8 concentration, and error bars on k_{obs} values represent errors calculated from the exponential fits. A linear fit of the data indicates that the $k_{max}/K_{1/2}$ is 3700 ± 100 $M^{-1}s^{-1}$. C. Dependence of the apparent deacetylation rate constant of H3K14ac octamer on the concentration of HDAC8. The data points are from multiple measurements in a single reaction at each HDAC8 concentration. A hyperbolic fit indicates that the $k_{max}/K_{1/2}$ is 1,000 ± 200 $M^{-1}s^{-1}$ with a k_{max} value of 0.03 ± 0.02 s^{-1}.

HDAC8-catalyzed deacetylation of acetylated nucleosome is slow

HDACs involved in transcriptional regulation are likely to encounter nucleic acid-bound substrate proteins. To test the selectivity of HDAC-catalyzed deacetylation for a substrate complex containing nucleic acids, we incorporated H3K9ac into recombinant mononucleosomes. Deacetylation of these complexes was assayed in the same manner as the tetramer and octamer substrates (Figure III.4). The addition of nucleic acids to the octamer to assemble nucleosomal substrates significantly decreased HDAC8 catalytic efficiency at the H3K9ac site, $k_{max}/K_{1/2}$ = 28 ± 3 $M^{-1}s^{-1}$. This is two-fold slower than the k_{cat}/K_M for the H3K9ac 7-mer peptide and 600-fold slower than deacetylation of this site in the H3/H4 tetramer. Adding the nucleosomal DNA to a Fluor-de-Lys peptide deacetylation assay resulted in an initial rate that is decreased only 25% compared to that of HDAC8 and peptide alone (data not shown); thus, the 130-fold decrease in HDAC8 activity observed between octamer and nucleosome substrates is not explained by DNA inhibition of the enzyme.

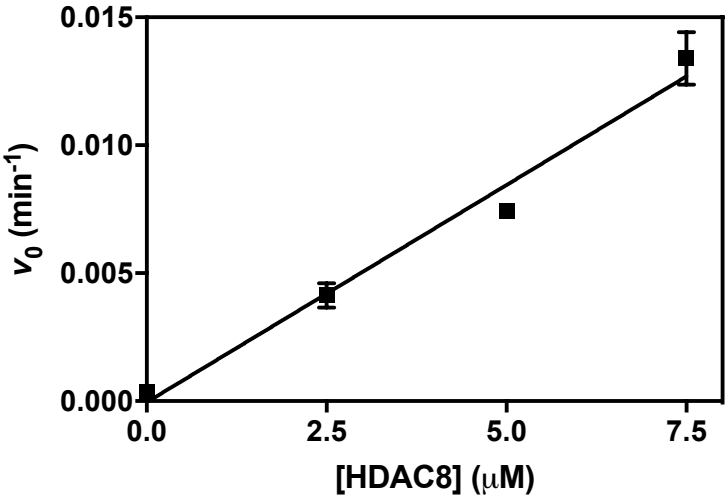

Figure III.4 Single turnover deacetylation of singly-acetylated H3 nucleosome

The initial rate of progress curves for deacetylation of H3K9ac nucleosome catalyzed by 0 – 7.5 μM HDAC8 were fit linearly and the rate constant calculated assuming 100% deacetylated product. The data points are from multiple measurements in a single reaction at each HDAC8 concentration, and error bars represent errors calculated from the initial rate fits. A linear fit of the data indicates that $k_{max}/K_{1/2}$ is 28 ± 3 $M^{-1}s^{-1}$.

Discussion

To understand the role of HDACs in cellular regulation, it is important to determine the substrate specificity and the molecular determinants of substrate recognition for each isozyme. Until now, HDAC recognition of protein substrates has largely been tackled by studying activity toward peptide substrates, which typically interact with less than an 8 x 20 $Å^2$ area of an approximately 2025 $Å^2$ binding surface.[22] Within this larger binding interface, there may be many more HDAC8-protein substrate contacts, including potential recognition hotspots and negative interaction sites. With a peptide, a single interaction of 0.5 - 2 kcal/mol can alter the catalytic efficiency by 50-fold.[56] With a protein substrate, the increased number of interaction sites could overcome the several kcal/mol interaction energy obtained from local contacts. Previously, distal HDAC8-substrate interactions have been observed using long peptide substrates; an upstream KRHR motif (based on histone H4) increases HDAC8-catalyzed deacetylation of an acetylated peptide.[15] To elucidate the role of long-range interactions on HDAC8 substrate recognition, we measured HDAC8-catalyzed deacetylation of substrates of increasing size and complexity, from peptide to full-length protein and protein-nucleic acid complex.

To analyze HDAC8-catalyzed deacetylation of peptide and protein substrates, we compared multiple turnover reactions (k_{cat}/K_M) of peptide substrates to single turnover ($k_{max}/K_{1/2}$) reactions of the protein substrates. This comparison of k_{cat}/K_M to $k_{max}/K_{1/2}$ was due mainly to the challenge of preparing sufficient quantities of singly-acetylated protein substrates to measure under MTO conditions. A variety of data suggest that the kinetic mechanism for deacetylation of most peptide substrates under MTO conditions is rapid equilibrium binding followed by a slow hydrolytic step. For example, our peptide assay demonstrated comparable deacetylation rate constants (within three-fold) under MTO and STO conditions. Additionally, HDAC8 catalyzes deacetylation of trifluoroacetate peptide substrates faster than non-fluorinated peptides (k_{cat}), indicating that product release is not the main rate-limiting step.[44] Furthermore, the k_{cat}/K_M values for peptides are significantly slower than diffusion control (10^2-10^3 $M^{-1}s^{-1}$ vs 10^7-10^8 $M^{-1}s^{-1}$) and the K_M values are large (> 100 μM), suggesting that a step other than substrate association, such as hydrolysis, is the rate-limiting step. Similarly, the values of $k_{max}/K_{1/2}$ are significantly lower than diffusion-controlled values suggesting that a step after association and at or before hydrolysis is the rate limiting step under STO conditions. Based on these data, we

assume that the apparent second order rate constants determined under MTO and STO conditions characterize the same hydrolytic step.

HDAC8 has remarkably enhanced catalytic efficiency for protein substrates in comparison to corresponding peptides. The varied HDAC8 catalytic efficiencies likely reflect the interactions between HDAC8 and substrate residues surrounding the acetyl-lysine, as previously demonstrated,[15] differences in accessibility of the acetyl-lysine to the active site, and distal interactions between HDAC8 and protein substrates. Previous analysis of activity toward acetylated peptide substrates has shown that HDAC8 prefers substrates with aromatic amino acids on the C-terminal side of the acetyl-lysine (+1 position).[13-14] Based on these empirical data, the mediocre catalytic efficiency of the histone H3-based peptides (10 to 10^2 $M^{-1}s^{-1}$) (Table III.2) was predictable due to the lack of aromatic residues. The interactions between the 7-mer peptides and HDAC8 occur within an approximately 10 Å radius of the active site. HDAC8-catalyzed hydrolysis of the acetylated H3/H4 tetramers, which still lack an aromatic residue in the +1 position, is 40 - 400 times faster than the corresponding peptides. Thus, HDAC8-tetramer interactions that are absent with the peptide substrates enhance HDAC8 substrate recognition. The increased catalytic efficiency for deacetylation of the acetylated H3/H4 tetramer compared to peptides corresponds to a Gibbs free energy increase of 2-4 kcal/mol, indicating a lower activation energy (Equation III.1) and demonstrating the importance of long-range interactions for HDAC8 substrate recognition.

Equation III.1 $$\Delta\Delta G^{\ddagger} = RTln\left(\frac{{k_{cat}}/{K_{M1}}}{{k_{cat}}/{K_{M2}}}\right)$$

The Mrksich group previously demonstrated that distal HDAC8-peptide interactions can enhance deacetylation and proposed an exosite model which involves binding at the active site and at a second location elsewhere on the HDAC8 surface.[15] Structures of peptides bound to HDAC8 are in an extended conformation.[19, 22, 30] Consistent with this, H3K9ac and H3K14ac sites are both located on the unstructured histone tail. The H3K9ac/H4 tetramer has both the highest value of $k_{max}/K_{1/2}$ and the largest increase in reactivity compared to the corresponding 9-mer peptide (300-fold), which could be attributed to one or a few strong interactions or several weak interactions. H3K14ac/H4 is the slowest of the singly-acetylated tetramers tested, but the fold difference between H3K14ac/H4 tetramer and 9-mer peptide (300-fold) is similar to that of H3K9ac/H4 tetramer. H3K9ac and H3K14ac are similarly positioned in the H3 tail, so the

surprising disparity in HDAC8 activity toward these sites suggests the important role of local sequence on HDAC8 selectivity, even within the context of a full-length protein. Moreover, H3K56ac is located on an α-helix which may significantly hinder interaction with HDAC8. Consistent with this, while H3K56ac/H4 tetramer demonstrates the second fastest reactivity, the fold difference compared to the 9-mer peptide is the smallest (50-fold). This could reflect either weak affinity with the α-helix structure or a requirement for unfolding of the helix.

The crystal structure of HDAC8 is useful in visualizing potential protein-protein interactions involved in full-length substrate recognition. In many crystal structures, HDAC8 forms a dimer at the substrate binding interface, as part of the fundamental crystal unit. This potential protein substrate binding interface is a flexible 45 x 45 $Å^2$ surface containing multiple interaction sites, including 10 van der Waals interactions and 6 hydrogen bonds between the HDAC8 dimers.[21, 23] The interactions observed between these two HDAC8 units provide a framework for exploring the differences in catalytic efficiency observed for peptide and full-length substrates. The 2-4 kcal/mol difference in Gibbs free energy between the peptide and tetramer deacetylation could be explained by the van der Waals interactions and/or hydrogen bonds that are observed in the dimeric crystal structures. The dimer also displays repulsive charge-charge interactions. The attractive and repulsive protein-protein interactions likely work in concert to determine HDAC8 substrate specificity. The HDAC8 substrate binding interface is mainly composed of flexible loops. Recent crystal structures have shown conformational changes in HDAC8 loops L1 and L2 upon binding of largazole analogs, as well as different L1 and L2 loop conformations between two monomers of the same crystal structure, demonstrating the adaptability and importance of these loops in HDAC8 inhibitor and substrate binding.[26] Catalytic efficiency is not enhanced by increasing the size and complexity of the protein substrate from a tetramer to the histone octamer. The H3K14ac histone octamer was deacetylated with a similar catalytic efficiency to the corresponding tetrameric substrate, suggesting that interactions with the tetramer are sufficient to explain HDAC8 substrate interactions in that case. In contrast, the H3K9ac octamer was deacetylated at least 4-fold slower than the tetrameric substrate. This is likely due to decreased accessibility of the acetyl-lysine to the HDAC8 active site, although other effects including protein-protein interactions and allosteric effects could be involved in the recognition of these proteins. This suggests that HDAC8 substrate recognition is highly dependent on the histone complex. A concern with assaying octamer under low salt

conditions (HDAC8 assay buffer and less than 240 mM NaCl) is that the octamer would disassemble into H3/H4 tetramer and H2A/H2B dimers. However, the sensitivity of HDAC8 toward NaCl precluded higher salt concentrations.[29] HDAC8 activity is salt and pH sensitive, and the selected assay buffer conditions were optimal for HDAC8 activity.[29] The observed kinetics for the tetramer and octamer substrates are significantly different and suggest that the octamers, once assembled, remain intact during our assays.

Addition of nucleic acid to form a nucleosome converted the most efficient protein substrate, the H3K9ac/H4 tetramer, to a substrate that is deacetylated by HDAC8 less efficiently than the corresponding peptide. The drastic decrease in $k_{max}/K_{1/2}$ for nucleosomal H3K9ac likely reflects decreased substrate accessibility to the acetyl-lysine on the H3 tail by the nucleosome. One possibility is that the positively charged histone H3 tail interacts with the negatively charged DNA in the nucleosome and is no longer accessible to HDAC8. These data are consistent with proteomic studies suggesting that histones are not physiological substrates for HDAC8.[34] However, the low reactivity observed for nucleosomal H3K9ac does not completely preclude deacetylation by HDAC8 under all conditions. The chromatin structure can be altered by transcription factors, DNA binding proteins, chromatin remodeling factors and other proteins, possibly complexed with HDAC, to alter the accessibility of acetylated lysines in the tail of H3. This work presents the first report of detailed kinetics for HDAC8-catalyzed deacetylation of singly-acetylated, full-length protein substrates and adds integral information to the field of HDAC substrate specificity. The direct comparison of peptides and protein substrates reveals that additional factors alter activity of HDAC8 with protein substrates, including both increased activity due to distal protein-protein interactions and decreased activity due to decreased accessibility of the acetyl-lysine side chain. HDAC8 catalyzes deacetylation of tetrameric protein substrates with catalytic efficiencies more than 40-fold greater than corresponding peptide substrates due to enhanced protein-protein interactions. However, further increasing the protein complex size decreases catalytic efficiency, likely due to decreased side chain accessibility. These differences in catalytic efficiency represent the effects of HDAC8-protein substrate interactions that are absent in HDAC8-peptide interactions. This work provides a foundation for the study of full-length protein substrate specificity of HDACs.

Experimental Procedures

Materials

Adenosine triphosphate (ATP), coenzyme A, nicotinamide adenine dinucleotide (NAD^+), L-malic acid, citrate synthase, malate dehydrogenase, and propionic anhydride were purchased from Sigma. Peptides were purchased from Peptide 2.0 Inc. Zinc(II) used to reconstitute HDAC8 was purchased as an ICP standard (GFS Chemicals) or atomic spectroscopy standard (Fluka) and the acetic acid standard was purchased from Ricca Chemical Company. Chelex 100 resin was purchased from Bio-Rad. Acetyl-lysine was purchased from Chem-Impex Chemical International Inc. Alpha-cyano-4-hydroxy-cinnamic acid (CHCA) MALDI matrix was purchased from Thermo Scientific. All other materials were purchased from Fisher or Sigma Aldrich and were of a purity >95 % unless otherwise noted.

HDAC8 expression and purification

HDAC8 was expressed and purified using the method described previously[28, 56] with the following modifications. BL21(DE3) *E. coli* cells transformed with the plasmid pHD4-HDAC8-TEV-His_6 were used to express HDAC8 in modified autoinduction-TB medium (12 g/L tryptone, 24 g/L yeast extract, 8.3g/L Tris-HCl, 4 g/L lactose, 1 g/L glucose, 1% (v/v) glycerol, pH 7.4) supplemented with 100 µg/mL ampicillin and 200 µM $ZnSO_4$. The cells were grown overnight at 30°C and harvested 20 - 24 hours post inoculation (9,000 x g, 10 min, 4°C). The cell pellet was resuspended either in low salt DEAE buffer (50 mM HEPES, 200 µM $ZnSO_4$, 1 mM TCEP, 50 mM NaCl, 5 mM KCl, 1 µg/mL *tert*-amyl methyl ether (TAME), 10 µg/mL phenylmethylsulfonyl fluoride (PMSF), pH 7.8) and lysed using a microfluidizer (Microfluidics). Nucleic acids were then precipitated by addition of 0.1% polyethylenimine (pH 7.9) followed by centrifugation (39,000 x g, 45 min, 4°C). HDAC8 was fractionated on a DEAE Sepharose column with a stepwise salt elution (50 mM HEPES, 200 µM $ZnSO_4$, 1 mM TCEP, 5 - 500 mM NaCl, 5 mM KCl, pH 7.8) and dialyzed against Buffer A (50 mM HEPES, 100 mM NaCl, 25 mM imidazole, pH 7.8). The eluate was dialyzed against 50 mM HEPES, 50 mM NaCl, 25 mM imidazole, pH 7.8 for 1 hour at 4°C then incubated with Ni(II)-charged chelating sepharose fast flow resin (GE) for 30 minutes, stirring on ice. HDAC8 was eluted from the metal affinity chromatography column by a stepwise (50 mM - 250 mM) imidazole gradient. HDAC8, together with at least 1 mg His-Tagged TEV(S219V) protease per 15 mg protein, was dialyzed overnight

against Buffer A without imidazole at 4˚C. Following the overnight TEV cleavage, HDAC8 was separated from TEV protease on a second Ni(II) column. The protein was further purified by size exclusion chromatography using a HiPrep 16/60 Sephacryl S200 HR column (GE) using size exclusion buffer (30 mM HEPES pH 8, 150 mM NaCl, 1 mM TCEP). HDAC8 was then dialyzed against metal-free chelation buffer (25 mM MOPS pH 7.5, 1 mM EDTA, 1 mM TCEP, 5 mM KCl) overnight, followed by metal-free buffer (25 mM MOPS pH 7.5, 1 mM TCEP, 5 mM KCl). Finally, residual EDTA was removed with a PD-10 column (GE) eluting with storage buffer (25 mM HEPES pH 8, 127 mM NaCl, 3 mM KCl, and 1 mM TCEP). HDAC8 was concentrated, aliquoted, and stored at -80°C. HDAC8 activity was confirmed using the Fluor de Lys assay as described previously.[28, 60-61]

Peptide deacetylation assay

HDAC8-catalyzed deacetylation of acetylated peptides was characterized using an enzyme-coupled assay, performed as previously described with a few modifications.[56] To prepare peptide stocks, lyophilized peptides were dissolved in water, 50% acetonitrile, or 10% DMSO, depending on their solubility. Peptide solutions were chelated by incubation with Chelex resin at 4°C for at least three hours. Peptide concentrations were measured using the fluorescamine assay or absorbance at 280 nm, as previously described.[56, 62] Peptides (0-100 μM) were incubated in HDAC8 assay buffer (50 mM HEPES, 137 mM NaCl, 3.7 mM KCl, pH 7.8) for 10 minutes at 30°C before initiating reactions with the addition of 0.5 μM Zn(II)-HDAC8. Acetate formation was coupled to NADH formation measured by an increase in fluorescence (ex = 340 nm, em = 460 nm).[56] Initial rates were fit to the linear portion of the product versus time curve.

Histone expression and purification

Recombinant His_6-tagged histone H3 variants containing a single acetyl-lysine were expressed and purified as previously described with a few modifications.[54] The acetyl-lysine was incorporated into expressed proteins at an amber codon site (TAG) using a tRNA-cognate tRNA synthetase pair encoded on the pAcKRS-3 plasmid.[54] Amber codons were substituted for the K9, K14, and K56 codons in the His_6-tagged *Xenopus* histone H3 in the PCDF PyLT-1 plasmid, a generous gift from Jason Chin[53-54] using QuikChange Site-Directed Mutagenesis (Agilent). BL21(DE3) cells were transformed with the mutant or wild type PCDF PyLT-1 and pAcKRS-3

plasmids for His_6-tagged H3 expression. Expression plasmids for preparation of recombinant H2A, H2B, and H4 *Xenopus* histones were generous gifts from Geeta Narlikar. BL21(DE3) cells were transformed with the respective H2A, H2B, and H4 plasmids and grown in LB or 2xYT supplemented with antibiotic (kanamycin and streptomycin for H3, or ampicillin for H2A, H2B, and H4) at 37°C until reaching an OD_{600} of 0.7. To express full-length histone H3 proteins with a single acetyl-lysine residue, 20 mM nicotinamide and 10 mM acetyl-lysine were added to the medium; 30 minutes later 0.5 mM Isopropyl β-D-1-thiogalactopyranoside (IPTG) was added to induce protein expression. For expression of the other histones, the cells were induced with 0.5 mM IPTG. The cultures were harvested 3 - 4 hours after induction (9,000 x g, 10-15 min, 4°C). The cell pellets were stored at -80°C.

Histones were purified using established protocols,[54-55, 63] with H3 Ni(II) column buffers modified to include 7 M urea and 1 mM TCEP. Tetramer, octamer, and nucleosome were assembled as previously described, and nucleosomes contained a 147-base pair DNA fragment containing the 601 octamer positioning sequence prepared as described.[54-55, 63-64] The 601 plasmid was a generous gift from Yali Dou. Tetramer and octamer were purified by size exclusion chromatography, selecting a single peak in each case. Tetramer assembly was tested using IM-MS (data not shown). Native PAGE was used to verify nucleosome consisted of DNA-bound histone protein. EDTA dialysis was used to remove any contaminating metal from histone protein complexes. Octamer and nucleosome were subsequently treated with Chelex resin for at least 1 hour at 4°C to ensure metal removal. Inductively coupled plasma mass spectrometry (ICP-MS) was used to verify less than 10% metal contamination. Nucleosome was stored in 20% glycerol, 20 mM HEPES pH 7.5 – 7.8, 1 mM TCEP.

Protein deacetylation assays

Apo-HDAC8 was reconstituted with stoichiometric Zn(II) for 1 hour on ice in HDAC8 assay buffer (50 mM HEPES, 137 mM NaCl, 3.7 mM KCl, pH 7.8) [28]. Histone complexes were incubated in HDAC8 assay buffer for 10 minutes at 30°C before initiating reactions by addition of 0 - 15 μM Zn(II)-HDAC8. The final concentration of NaCl in the assays with octamer was 137 or 239 mM NaCl. This salt concentration is lower than typical histone octamer storage buffer (2 M NaCl),[65] but allows for measurement of HDAC8 activity uninhibited by salt. Reactions were quenched by addition of 25% trichloroacetic acid at each time point, incubated for 30 minutes on ice, and centrifuged (16,000 x g, 10 min, 4°C), and then the pellets were

washed in cold acetone twice. Acetone-washed pellets were resuspended in 2 µL propionic anhydride and 6 µL ammonium hydroxide (NH_4OH) and incubated at 51°C for 1 hour. 30 µL of 50 mM NH_4HCO_3 was added to each tube, and the pH of each sample was adjusted to 7 – 9 using NH_4OH. Then 0.2 µg trypsin (Promega) was added for overnight digest at 37°C. The pH was then reduced for mass spectrometry (MS) by addition of 3.5 µL of 10% formic acid. Tryptic peptides were analyzed by MS/MS analysis in the lab of Andrew Andrews (Fox Chase Cancer Center) as previously described [45, 66]. Graphical analysis was done using Prism (GraphPad Software, Inc.). For each single turnover reaction, the k_{obs} was determined by fitting a single exponential decay (Equation III.2) to the fraction substrate over time determined from the MS/MS analysis. The $k_{max}/K_{1/2}$ values were determined by fitting hyperbola (Equation III.3E) or line (Equation III.4) to the dependence of k_{obs} on HDAC8 concentration, depending on the substrate.

Equation III.2
$$\frac{\text{Substrate}}{(\text{Substrate}+\text{Product})} = e^{-k_{obs} \times t}$$

Equation III.3
$$k_{obs} = \frac{k_{max}}{K_{1/2}}\left(\frac{[\text{HDAC8}]}{1+\frac{[\text{HDAC8}]}{K_{1/2}}}\right)$$

Equation III.4
$$k_{obs} = \frac{k_{max}}{K_{1/2}}\,[\text{HDAC8}]$$

MALDI-TOF-MS Deacetylation Assay

HDAC8-catalyzed deacetylation of the H3K9ac 13-mer peptide was measured under single turnover (STO, [E]>>[S]) and multiple turnover (MTO, [S]>>[E]) conditions using MALDI-TOF-MS. Apo-HDAC8 was reconstituted with stoichiometric zinc(II) for 1 hour on ice in HDAC8 assay buffer. The H3K9ac 13-mer peptide was incubated in HDAC8 assay buffer for 10 minutes at 30°C, and the deacetylation reaction was initiated with Zn(II)-HDAC8. MTO control reactions contained either 1 µM enzyme and 50 µM peptide or 150 µM enzyme and 750 µM peptide, and STO reactions contained 20 µM peptide and 0, 50, 100 and 150 µM enzyme (2.5, 5 and 7.5 ratio of [E]/substrate). At each time point, 2 µL of reaction were quenched with 2

μL of 10% HCl. Samples were stored at -80°C prior to MS analysis. The samples were prepared by mixing the quenched reactions 1:1 with alpha-cyano-4-hydroxy-cinnamic acid (CHCA) MALDI matrix followed by spotting on a Bruker MALDI-TOF-MS plate. Spectra were collected using a Bruker AutoFlex Speed MALDI-TOF mass spectrometer calibrated with a series of five peptide standards. Three random measurements from each spot were averaged, and the fraction of product formed was calculated from the area under the curve of the product and substrate peaks. The k_{cat}/K_M for the multiple turnover reaction was determined by fitting a line to the initial rate of the reaction progress curve. The $k_{max}/K_{1/2}$ for the single turnover reaction was determined by fitting a hyperbola to the dependence of k_{obs} on HDAC8 concentration (Equation 2). The values for k_{obs} at each HDAC8 concentration were determined by fitting a single exponential to the time dependence of product formation (Equation III.5).

Equation III.5 $$\frac{(\text{Product})}{(\text{Product} + \text{Substrate})} = 1\text{-}e^{-k_{obs} \times t}$$

Acknowledgements

We thank members of the Fierke laboratory for helpful discussions and comments on the manuscript. We thank Jeffrey E. López for collaborating on HDAC8 purification. We thank Jason Chin (Medical Research Council) for non-natural amino acid incorporation plasmids, Geeta Narlikar (University of California San Francisco) for histone expression plasmids, and Yali Dou (University of Michigan) for the nucleosome DNA plasmid. We thank John Leonard (Narlikar lab) and Felicia Gray (Dou lab) for histone purification and nucleosome assembly protocols, and we thank Ted Huston and Lubomír Dostál (University of Michigan) for performing ICP-MS to measure metal content. We thank Brandon Ruotolo and Yueyang Zhong for their determination of the histone tetramer stoichiometry.

This work was supported in part by a National Science Foundation predoctoral fellowship (N.A.W.), National Institutes of Health Grant 5-R01-GM-040602 (C.A.F.), the University of Michigan Chemistry-Biology Interface (CBI) training program NIH grant 5T32GM008597 (C.A.C.), Rackham Graduate School (C.A.C.) and the Cellular Biotechnology Training Program T32-GM008353 (N.A.W. and K.R.L.).

Conflict of interest

The authors declare that they have no conflicts of interest with the contents of this article.

Footnotes

The abbreviations used are: ARID1A, AT-rich interaction domain 1A; CHCA, alpha-cyano-4-hydroxy-cinnamic acid; ERRα, estrogen related receptor alpha; H3/H4, tetrameric histone H3/H4; HDAC, histone deacetylase; ICP-MS, inductively coupled plasma mass spectrometry; IPTG, isopropyl β-D-1-thiogalactopyranoside; KAT, acetyltransferase; MTO, multiple turnover; PIP, pyrrole-imidazole polyamide; SAHA, suberanilohydroxamic acid; SMC3, structural maintenance of chromosomes 3; STO, single turnover; TAME, Nα-p-Tosyl-L-arginine methyl ester; TCEP, tris(2-carboxyethyl)phosphine hydrochloride.

References

1. Khochbin, S.; Verdel, A.; Lemercier, C.; Seigneurin-Berny, D., Functional significance of histone deacetylase diversity. *Curr Opin Genet Dev* **2001,** *11* (2), 162-6.

2. Yang, X. J.; Seto, E., The Rpd3/Hda1 family of lysine deacetylases: from bacteria and yeast to mice and men. *Nature reviews. Molecular cell biology* **2008,** *9* (3), 206-18.

3. Glozak, M. A.; Sengupta, N.; Zhang, X. H.; Seto, E., Acetylation and deacetylation of non-histone proteins. *Gene* **2005,** *363*, 15-23.

4. Choudhary, C.; Kumar, C.; Gnad, F.; Nielsen, M. L.; Rehman, M.; Walther, T. C.; Olsen, J. V.; Mann, M., Lysine acetylation targets protein complexes and co-regulates major cellular functions. *Science* **2009,** *325* (5942), 834-40.

5. Zhao, S.; Xu, W.; Jiang, W.; Yu, W.; Lin, Y.; Zhang, T.; Yao, J.; Zhou, L.; Zeng, Y.; Li, H.; Li, Y.; Shi, J.; An, W.; Hancock, S. M.; He, F.; Qin, L.; Chin, J.; Yang, P.; Chen, X.; Lei, Q.; Xiong, Y.; Guan, K. L., Regulation of cellular metabolism by protein lysine acetylation. *Science* **2010,** *327* (5968), 1000-4.

6. Li, G.; Jiang, H.; Chang, M.; Xie, H.; Hu, L., HDAC6 alpha-tubulin deacetylase: a potential therapeutic target in neurodegenerative diseases. *Journal of the neurological sciences* **2011,** *304* (1-2), 1-8.

7. D'Mello, S. R., Histone deacetylases as targets for the treatment of human neurodegenerative diseases. *Drug News Perspect* **2009,** *22* (9), 513-24.

8. Glozak, M. A.; Seto, E., Histone deacetylases and cancer. *Oncogene* **2007,** *26* (37), 5420-32.

9. Marks, P.; Rifkind, R. A.; Richon, V. M.; Breslow, R.; Miller, T.; Kelly, W. K., Histone deacetylases and cancer: causes and therapies. *Nature reviews. Cancer* **2001,** *1* (3), 194-202.

10. Fenichel, M. P., FDA Approves New Agent for Multiple Myeloma. *Journal of the National Cancer Institute* **2015,** *107* (6).

11. Poole, R. M., Belinostat: first global approval. *Drugs* **2014,** *74* (13), 1543-54.

12. Mottamal, M.; Zheng, S.; Huang, T. L.; Wang, G., Histone deacetylase inhibitors in clinical studies as templates for new anticancer agents. *Molecules (Basel, Switzerland)* **2015,** *20* (3), 3898-941.

13. Gurard-Levin, Z. A.; Kilian, K. A.; Kim, J.; Bahr, K.; Mrksich, M., Peptide arrays identify isoform-selective substrates for profiling endogenous lysine deacetylase activity. *ACS chemical biology* **2010,** *5* (9), 863-73.

14. Gurard-Levin, Z. A.; Kim, J.; Mrksich, M., Combining mass spectrometry and peptide arrays to profile the specificities of histone deacetylases. *Chembiochem : a European journal of chemical biology* **2009,** *10* (13), 2159-61.

15. Gurard-Levin, Z. A.; Mrksich, M., The activity of HDAC8 depends on local and distal sequences of its peptide substrates. *Biochemistry* **2008,** *47* (23), 6242-50.

16. Riester, D.; Hildmann, C.; Grunewald, S.; Beckers, T.; Schwienhorst, A., Factors affecting the substrate specificity of histone deacetylases. *Biochemical and biophysical research communications* **2007,** *357* (2), 439-45.

17. Buggy, J. J.; Sideris, M. L.; Mak, P.; Lorimer, D. D.; McIntosh, B.; Clark, J. M., Cloning and characterization of a novel human histone deacetylase, HDAC8. *The Biochemical journal* **2000,** *350 Pt 1*, 199-205.

18. Hu, E.; Chen, Z.; Fredrickson, T.; Zhu, Y.; Kirkpatrick, R.; Zhang, G. F.; Johanson, K.; Sung, C. M.; Liu, R.; Winkler, J., Cloning and characterization of a novel human class I histone deacetylase that functions as a transcription repressor. *The Journal of biological chemistry* **2000,** *275* (20), 15254-64.

19. Dowling, D. P.; Gantt, S. L.; Gattis, S. G.; Fierke, C. A.; Christianson, D. W., Structural studies of human histone deacetylase 8 and its site-specific variants complexed with substrate and inhibitors. *Biochemistry* **2008,** *47* (51), 13554-63.

20. Dowling, D. P.; Gattis, S. G.; Fierke, C. A.; Christianson, D. W., Structures of metal-substituted human histone deacetylase 8 provide mechanistic inferences on biological function. *Biochemistry* **2010,** *49* (24), 5048-56.

21. Vannini, A.; Volpari, C.; Filocamo, G.; Casavola, E. C.; Brunetti, M.; Renzoni, D.; Chakravarty, P.; Paolini, C.; De Francesco, R.; Gallinari, P.; Steinkuhler, C.; Di Marco, S., Crystal structure of a eukaryotic zinc-dependent histone deacetylase, human HDAC8, complexed with a hydroxamic acid inhibitor. *Proc Natl Acad Sci U S A* **2004,** *101* (42), 15064-9.

22. Vannini, A.; Volpari, C.; Gallinari, P.; Jones, P.; Mattu, M.; Carfi, A.; De Francesco, R.; Steinkuhler, C.; Di Marco, S., Substrate binding to histone deacetylases as shown by the crystal structure of the HDAC8-substrate complex. *EMBO Rep* **2007,** *8* (9), 879-884.

23. Somoza, J. R.; Skene, R. J.; Katz, B. A.; Mol, C.; Ho, J. D.; Jennings, A. J.; Luong, C.; Arvai, A.; Buggy, J. J.; Chi, E.; Tang, J.; Sang, B. C.; Verner, E.; Wynands, R.; Leahy, E. M.; Dougan, D. R.; Snell, G.; Navre, M.; Knuth, M. W.; Swanson, R. V.; McRee, D. E.; Tari, L. W., Structural snapshots of human HDAC8 provide insights into the class I histone deacetylases. *Structure (London, England : 1993)* **2004,** *12* (7), 1325-34.

24. Marek, M.; Kannan, S.; Hauser, A. T.; Moraes Mourao, M.; Caby, S.; Cura, V.; Stolfa, D. A.; Schmidtkunz, K.; Lancelot, J.; Andrade, L.; Renaud, J. P.; Oliveira, G.; Sippl, W.; Jung, M.; Cavarelli, J.; Pierce, R. J.; Romier, C., Structural basis for the inhibition of histone deacetylase 8 (HDAC8), a key epigenetic player in the blood fluke Schistosoma mansoni. *PLoS pathogens* **2013,** *9* (9), e1003645.

25. Whitehead, L.; Dobler, M. R.; Radetich, B.; Zhu, Y.; Atadja, P. W.; Claiborne, T.; Grob, J. E.; McRiner, A.; Pancost, M. R.; Patnaik, A.; Shao, W.; Shultz, M.; Tichkule, R.; Tommasi, R. A.; Vash, B.; Wang, P.; Stams, T., Human HDAC isoform selectivity achieved via exploitation of the acetate release channel with structurally unique small molecule inhibitors. *Bioorg Med Chem* **2011,** *19* (15), 4626-34.

26. Decroos, C.; Clausen, D. J.; Haines, B. E.; Wiest, O.; Williams, R. M.; Christianson, D. W., Variable Active Site Loop Conformations Accommodate the Binding of Macrocyclic Largazole Analogues to HDAC8. *Biochemistry* **2015,** *54* (12), 2126-35.

27. Cole, K. E.; Dowling, D. P.; Boone, M. A.; Phillips, A. J.; Christianson, D. W., Structural basis of the antiproliferative activity of largazole, a depsipeptide inhibitor of the histone deacetylases. *Journal of the American Chemical Society* **2011,** *133* (32), 12474-7.

28. Gantt, S. L.; Gattis, S. G.; Fierke, C. A., Catalytic activity and inhibition of human histone deacetylase 8 is dependent on the identity of the active site metal ion. *Biochemistry* **2006,** *45* (19), 6170-8.

29. Gantt, S. L.; Joseph, C. G.; Fierke, C. A., Activation and inhibition of histone deacetylase 8 by monovalent cations. *The Journal of biological chemistry* **2010,** *285* (9), 6036-43.

30. Gantt, S. M. L.; Decroos, C.; Lee, M. S.; Gullett, L. E.; Bowman, C. M.; Christianson, D. W.; Fierke, C. A., General Base–General Acid Catalysis in Human Histone Deacetylase 8. *Biochemistry* **2016,** *55* (5), 820-832.

31. Wilson, B. J.; Tremblay, A. M.; Deblois, G.; Sylvain-Drolet, G.; Giguere, V., An acetylation switch modulates the transcriptional activity of estrogen-related receptor alpha. *Molecular endocrinology (Baltimore, Md.)* **2010,** *24* (7), 1349-58.

32. Deardorff, M. A.; Bando, M.; Nakato, R.; Watrin, E.; Itoh, T.; Minamino, M.; Saitoh, K.; Komata, M.; Katou, Y.; Clark, D.; Cole, K. E.; De Baere, E.; Decroos, C.; Di Donato, N.; Ernst, S.; Francey, L. J.; Gyftodimou, Y.; Hirashima, K.; Hullings, M.; Ishikawa, Y.; Jaulin, C.; Kaur, M.; Kiyono, T.; Lombardi, P. M.; Magnaghi-Jaulin, L.; Mortier, G. R.; Nozaki, N.; Petersen, M. B.; Seimiya, H.; Siu, V. M.; Suzuki, Y.; Takagaki, K.; Wilde, J. J.; Willems, P. J.; Prigent, C.; Gillessen-Kaesbach, G.; Christianson, D. W.; Kaiser, F. J.; Jackson, L. G.; Hirota, T.; Krantz, I. D.; Shirahige, K., HDAC8 mutations in Cornelia de Lange syndrome affect the cohesin acetylation cycle. *Nature* **2012,** *489* (7415), 313-7.

33. Kaiser, F. J.; Ansari, M.; Braunholz, D.; Concepcion Gil-Rodriguez, M.; Decroos, C.; Wilde, J. J.; Fincher, C. T.; Kaur, M.; Bando, M.; Amor, D. J.; Atwal, P. S.; Bahlo, M.; Bowman, C. M.; Bradley, J. J.; Brunner, H. G.; Clark, D.; Del Campo, M.; Di Donato, N.; Diakumis, P.; Dubbs, H.; Dyment, D. A.; Eckhold, J.; Ernst, S.; Ferreira, J. C.;

Francey, L. J.; Gehlken, U.; Guillen-Navarro, E.; Gyftodimou, Y.; Hall, B. D.; Hennekam, R.; Hudgins, L.; Hullings, M.; Hunter, J. M.; Yntema, H.; Innes, A. M.; Kline, A. D.; Krumina, Z.; Lee, H.; Leppig, K.; Lynch, S. A.; Mallozzi, M. B.; Mannini, L.; McKee, S.; Mehta, S. G.; Micule, I.; Mohammed, S.; Moran, E.; Mortier, G. R.; Moser, J. A.; Noon, S. E.; Nozaki, N.; Nunes, L.; Pappas, J. G.; Penney, L. S.; Perez-Aytes, A.; Petersen, M. B.; Puisac, B.; Revencu, N.; Roeder, E.; Saitta, S.; Scheuerle, A. E.; Schindeler, K. L.; Siu, V. M.; Stark, Z.; Strom, S. P.; Thiese, H.; Vater, I.; Willems, P.; Williamson, K.; Wilson, L. C.; Hakonarson, H.; Quintero-Rivera, F.; Wierzba, J.; Musio, A.; Gillessen-Kaesbach, G.; Ramos, F. J.; Jackson, L. G.; Shirahige, K.; Pie, J.; Christianson, D. W.; Krantz, I. D.; Fitzpatrick, D. R.; Deardorff, M. A., Loss-of-function HDAC8 mutations cause a phenotypic spectrum of Cornelia de Lange syndrome-like features, ocular hypertelorism, large fontanelle and X-linked inheritance. *Human molecular genetics* **2014,** *23* (11), 2888-900.

34. Olson, D. E.; Udeshi, N. D.; Wolfson, N. A.; Pitcairn, C. A.; Sullivan, E. D.; Jaffe, J. D.; Svinkina, T.; Natoli, T.; Lu, X.; Paulk, J.; McCarren, P.; Wagner, F. F.; Barker, D.; Howe, E.; Lazzaro, F.; Gale, J. P.; Zhang, Y.-L.; Subramanian, A.; Fierke, C. A.; Carr, S. A.; Holson, E. B., An unbiased approach to identify endogenous substrates of "histone" deacetylase 8. *ACS chemical biology* **2014,** *9* (10), 2210-6.

35. Durst, K. L.; Lutterbach, B.; Kummalue, T.; Friedman, A. D.; Hiebert, S. W., The inv(16) Fusion Protein Associates with Corepressors via a Smooth Muscle Myosin Heavy-Chain Domain. *Molecular and Cellular Biology* **2003,** *23* (2), 607-619.

36. Gao, J.; Siddoway, B.; Huang, Q.; Xia, H., Inactivation of CREB mediated gene transcription by HDAC8 bound protein phosphatase. *Biochemical and biophysical research communications* **2009,** *379* (1), 1-5.

37. Joshi, P.; Greco, T. M.; Guise, A. J.; Luo, Y.; Yu, F.; Nesvizhskii, A. I.; Cristea, I. M., The functional interactome landscape of the human histone deacetylase family. *Molecular systems biology* **2013,** *9*, 672.

38. Waltregny, D.; de Leval, L.; Glénisson, W.; Ly Tran, S.; North, B. J.; Bellahcène, A.; Weidle, U.; Verdin, E.; Castronovo, V., Expression of Histone Deacetylase 8, a Class I Histone Deacetylase, Is Restricted to Cells Showing Smooth Muscle Differentiation in Normal Human Tissues. *The American Journal of Pathology* **2004,** *165* (2), 553-564.

39. Waltregny, D.; Glénisson, W.; Tran, S. L.; North, B. J.; Verdin, E.; Colige, A.; Castronovo, V., Histone deacetylase HDAC8 associates with smooth muscle alpha-actin and is essential for smooth muscle cell contractility. *The FASEB Journal* **2005**.

40. Lee, H.; Sengupta, N.; Villagra, A.; Rezai-Zadeh, N.; Seto, E., Histone deacetylase 8 safeguards the human ever-shorter telomeres 1B (hEST1B) protein from ubiquitin-mediated degradation. *Mol Cell Biol* **2006,** *26* (14), 5259-69.

41. Van den Wyngaert, I.; de Vries, W.; Kremer, A.; Neefs, J.; Verhasselt, P.; Luyten, W. H.; Kass, S. U., Cloning and characterization of human histone deacetylase 8. *FEBS letters* **2000,** *478* (1-2), 77-83.

42. Saha, A.; Pandian, G. N.; Sato, S.; Taniguchi, J.; Hashiya, K.; Bando, T.; Sugiyama, H., Synthesis and biological evaluation of a targeted DNA-binding transcriptional activator with HDAC8 inhibitory activity. *Bioorganic & Medicinal Chemistry* **2013,** *21* (14), 4201-4209.

43. Lee, H.; Rezai-Zadeh, N.; Seto, E., Negative Regulation of Histone Deacetylase 8 Activity by Cyclic AMP-Dependent Protein Kinase A. *Molecular and Cellular Biology* **2004,** *24* (2), 765-773.

44. Smith, B. C.; Denu, J. M., Acetyl-lysine analog peptides as mechanistic probes of protein deacetylases. *The Journal of biological chemistry* **2007,** *282* (51), 37256-65.

45. Kuo, Y.-M.; Henry, Ryan A.; Tan, S.; Côté, J.; Andrews, Andrew J., Site specificity analysis of Piccolo NuA4-mediated acetylation for different histone complexes. *Biochemical Journal* **2015,** *472* (2), 239-248.

46. Wolfson, N. A.; Pitcairn, C. A.; Fierke, C. A., HDAC8 substrates: Histones and beyond. *Biopolymers* **2013,** *99* (2), 112-126.

47. Toro, T. B.; Watt, T. J., KDAC8 substrate specificity quantified by a biologically relevant, label-free deacetylation assay. *Protein Science* **2015,** *24* (12), 2020-2032.

48. Alam, N.; Zimmerman, L.; Wolfson, Noah A.; Joseph, Caleb G.; Fierke, Carol A.; Schueler-Furman, O., Structure-Based Identification of HDAC8 Non-histone Substrates. *Structure* **2016,** *24* (3), 458-468.

49. Dose, A.; Sindlinger, J.; Bierlmeier, J.; Bakirbas, A.; Schulze-Osthoff, K.; Einsele-Scholz, S.; Hartl, M.; Essmann, F.; Finkemeier, I.; Schwarzer, D., Interrogating Substrate Selectivity and Composition of Endogenous Histone Deacetylase Complexes with Chemical Probes. *Angewandte Chemie (International ed. in English)* **2016,** *55* (3), 1192-5.

50. Gober, I. N.; Waters, M. L., Supramolecular Affinity Labeling of Histone Peptides Containing Trimethyllysine and Its Application to Histone Deacetylase Assays. *Journal of the American Chemical Society* **2016,** *138* (30), 9452-9459.

51. Izzo, A.; Schneider, R., Chatting histone modifications in mammals. *Briefings in functional genomics* **2010,** *9* (5-6), 429-43.

52. Yuan, J.; Pu, M.; Zhang, Z.; Lou, Z., Histone H3-K56 acetylation is important for genomic stability in mammals. *Cell cycle (Georgetown, Tex.)* **2009,** *8* (11), 1747-1753.

53. Neumann, H.; Peak-Chew, S. Y.; Chin, J. W., Genetically encoding N(epsilon)-acetyllysine in recombinant proteins. *Nature chemical biology* **2008,** *4* (4), 232-4.

54. Neumann, H.; Hancock, S. M.; Buning, R.; Routh, A.; Chapman, L.; Somers, J.; Owen-Hughes, T.; van Noort, J.; Rhodes, D.; Chin, J. W., A method for genetically installing

site-specific acetylation in recombinant histones defines the effects of H3 K56 acetylation. *Mol Cell* **2009,** *36* (1), 153-63.

55. Luger, K.; Mader, A. W.; Richmond, R. K.; Sargent, D. F.; Richmond, T. J., Crystal structure of the nucleosome core particle at 2.8 A resolution. *Nature* **1997,** *389* (6648), 251-60.

56. Wolfson, N. A.; Pitcairn, C. A.; Sullivan, E. D.; Joseph, C. G.; Fierke, C. A., An enzyme-coupled assay measuring acetate production for profiling histone deacetylase specificity. *Analytical Biochemistry* **2014,** *456* (0), 61-69.

57. Eisenthal, R.; Danson, M. J.; Hough, D. W., Catalytic efficiency and kcat/KM: a useful comparator? *Trends in Biotechnology* **2007,** *25* (6), 247-249.

58. Northrop, D. B., On the Meaning of Km and V/K in Enzyme Kinetics. *Journal of Chemical Education* **1998,** *75* (9), 1153.

59. Hedstrom, L., Enzyme Specificity and Selectivity. In *eLS*, John Wiley & Sons, Ltd: 2001.

60. Wegener, D.; Hildmann, C.; Riester, D.; Schwienhorst, A., Improved fluorogenic histone deacetylase assay for high-throughput-screening applications. *Analytical biochemistry* **2003,** *321* (2), 202-8.

61. Wegener, D.; Wirsching, F.; Riester, D.; Schwienhorst, A., A fluorogenic histone deacetylase assay well suited for high-throughput activity screening. *Chem Biol* **2003,** *10* (1), 61-8.

62. Huang, X.; Hernick, M., A fluorescence-based assay for measuring N-acetyl-1-D-myo-inosityl-2-amino-2-deoxy-alpha-D-glucopyranoside deacetylase activity. *Analytical biochemistry* **2011,** *414* (2), 278-81.

63. Luger, K.; Rechsteiner, T. J.; Richmond, T. J., Preparation of nucleosome core particle from recombinant histones. *Methods Enzymol* **1999,** *304*, 3-19.

64. Dyer, P. N.; Edayathumangalam, R. S.; White, C. L.; Bao, Y.; Chakravarthy, S.; Muthurajan, U. M.; Luger, K., Reconstitution of nucleosome core particles from recombinant histones and DNA. *Methods Enzymol* **2004,** *375*, 23-44.

65. Shahian, T.; Narlikar, G., Analysis of Changes in Nucleosome Conformation Using Fluorescence Resonance Energy Transfer. In *Chromatin Remodeling*, Morse, R. H., Ed. Humana Press: 2012; Vol. 833, pp 337-349.

66. Kuo, Y. M.; Andrews, A. J., Quantitating the specificity and selectivity of Gcn5-mediated acetylation of histone H3. *PloS one* **2013,** *8* (2), e54896.

CHAPTER IV

Predicting HDAC6 Substrate Specificity and Selectivity[a]

Introduction

Histone deacetylases (HDACs) catalyze the hydrolysis of acetyl-lysine amino acids of certain proteins.[1] The acetyl-lysine post-translational modification (PTM) is an important regulatory feature that modulates vastly varied processes within all compartments of the cell.[2] This PTM is conserved from bacteria to humans and plays an integral role in modulating chromosomal architecture where acetylation of histone tails and interactions with transcription factors control the activation and silencing of specific genes.[3] In addition to histones and other transcriptional-related machinery within the nucleus, acetylation occurs on lysine residues in a wide variety of non-nuclear proteins.[4] Mass spectrometry-based proteomics has been used to identify thousands of acetylation sites in mammalian proteins, and the number continues to rise.[5] These acetylation events regulate proteins involved in most, if not all, cellular processes including cell-cycle regulation, cell signaling, metabolism, stress-response, cell integrity and mobility, and chromatin remodeling.[2, 6] Additionally, the regulatory functions of acetylation vary widely and include protein-protein interactions, protein-nucleic acid interactions, protein structure and stability, enzyme activity, and signaling.[6]

In the cytoplasm, well-known acetylation events include acetylation of α-tubulin at K40 that regulates cytoskeletal dynamics and acetylation of Hsp90 that modulates complex formation and stress response, among others.[7-8] Aberrant acetylation has been linked to devastating human diseases including cancer, neurodegeneration, and autoimmune disorders.[9] Many of these diseases are linked to deacetylation dysregulation where differential expression of HDACs correlate with poor disease prognoses.[9] The histone deacetylases, including the metal-dependent

[a] Protein purification and enzyme assays were performed by Katherine Welker Leng, study design and analysis was completed by Katherine Welker Leng and Carol A. Fierke, and computer-based modeling and analysis were carried out by Ora Schueler-Furman and Julia Varga (University of Jerusalem).

HDACs 1-11 and the NAD^+-dependent sirtuins SIRT1-7, are grouped into four classes based on homology, with class I HDACs, HDAC1, -2, -3, and -8, performing predominantly nuclear functions including transcriptional regulation and class II HDACs, HDAC4-7, and -9, performing predominantly cytoplasmic functions.[1] The other classes include class III HDACs, SIRT1-7, and class IV HDAC11.[1] The most notable of the class II HDACs is HDAC6, a particularly unique HDAC with regards to its structure and function.[10] Abnormal HDAC6 expression and/or activity has been implicated in cancer, neurodegeneration, and autoimmune disorders,[11-14] and recently the crystal structure of HDAC6 was solved spurring a greater emphasis on the discovery of HDAC6 small molecule modulators.[15-16] Between 2013-2017, over two-thirds of patents submitted for HDAC-specific small molecule inhibitors targeted HDAC6,[17] and several HDAC6-specific inhibitors are currently undergoing clinical trials, including the first clinically tested HDAC6-specific inhibitor ricolinostat.[18]

HDAC6 contains unique structural features including two tandem catalytic domains, a ubiquitin binding zinc-finger domain, and a dynein motor binding domain (Figure IV.1).[10, 16] The notable and well-conserved differences between HDAC6 and the other HDACs support significant and non-redundant functions for HDAC6 in the cell.[19] Indeed, HDAC6 plays important roles in the cytoplasm where it regulates cytoskeletal dynamics and stress-response through deacetylation of target substrates α-tubulin and Hsp90, among others.[20-22] Interestingly, global deletion of HDAC6 in mice is non-fatal and is the only HDAC global deletion to lack a pronounced phenotype,[23] suggesting that inhibition of this isozyme might have low cellular toxicity. Due to its association with numerous disease-types, developing HDAC6-specific inhibitors has been a priority yielding several clinical candidates and numerous others currently under investigation.[17-18, 24] Understanding HDAC6 function through its control of substrate acetylation levels and subsequent impact on the regulation of specific biological pathways is crucial for identifying where HDAC6 modulation would be most effective and developing targeted approaches to treating disease. Unfortunately, although there are thousands of acetylation events regulated by HDACs, relatively few HDAC-substrate pairs have been reported with significant confidence, and even fewer where their involvement in cellular processes is understood.[6]

Figure IV.1 Diagram of HDAC6 structural features

Human HDAC6 (blue) is composed of 1,215 amino acid residues organized into several key domains: N-terminal nuclear localization signal and C-terminal serine-glutamate tetradecapeptide repeat cytoplasmic retention domain (L and SE14, respectively in yellow), N- and C-terminal nuclear export signals (E in teal), catalytic domains 1 and 2 (CD1 and CD2 in orange), and finally the dynein motor binding domain and ubiquitin binding zinc finger domain (DM and BUZ, respectively in red).

Identifying HDAC substrates is challenging due to the complexity of biological processes, a poor understanding of the cellular dynamics regulating these reactions, differences between experimental methodology and model systems, overlapping action and redundancy of the activity of multiple isozymes, and the insufficiency and inconsistency in the tools currently available. Efforts to streamline HDAC substrate specificity characterization and identify HDAC substrates include using peptide and protein library screens and computational- and proteomics-based approaches.[25-29] One method pairs readily available tools and information with powerful computational technology. Using the crystal structure of HDAC8, a computational model was developed to predict HDAC8 activity.[25] Using a library of acetylated peptide substrates, an algorithm was developed for HDAC8 using Rosetta FlexPepBind that shows a significant correlation between a computational *activity score* and HDAC8 catalysis measured *in vitro*.[25] This powerful tool is able to rapidly score thousands of additional peptide sequences as HDAC substrates in a fraction of the time and cost required for traditional assay methods.[25] The correlation between activity and sequence observed in developing this model provides evidence that the sequence directly flanking the acetyl-lysine is significant in determining HDAC substrate selectivity[30].

Here we report the use of a similar approach to model HDAC6 substrate selectivity in efforts to identify novel and therapeutically significant HDAC6 substrates. This is the first computational model to predict HDAC6 activity and selectivity. Recombinantly purified HDAC6 exhibits significantly greater activity *in vitro* than recombinantly purified HDAC8, thus there was speculation as to the extent of substrate selectivity by HDAC6 activity. However, our data demonstrate that the increased reactivity results in a greater dynamic range of HDAC6

selectivity. HDAC6-catalyzed deacetylation of singly-acetylated peptides *in vitro* demonstrated up to 20,000-fold differences in reactivity, depending on the peptide sequence. While no simple sequence patterns were observed, the Rosetta FlexPepBind computational software using docked peptide substrates into the HDAC6 crystal structure led to a computational model able to identify good HDAC6 substrates. Test substrates demonstrating rapid turnover included peptides corresponding to putative HDAC6 substrate Hsp90 as well as novel substrates prelamin A, VDAC1, α-actinin, CRIP1, and MSH2. These results provide insight into the biological function of HDAC6, including its physiological substrates, and its participation in biological pathways and disease pathologies. This information will help predict how HDAC6 inhibition will impact disease pathology and identify which diseases are amenable to treatment with HDAC6 inhibitors.

Materials and Methods

Reagents

High flow amylose resin was purchased from New England Biolabs and Ni-NTA agarose was purchased from Qiagen. Adenosine triphosphate (ATP), coenzyme A (CoA), NAD^+, NADH, L-malic acid, malate dehydrogenase (MDH), citrate synthase (CS), and mouse monoclonal anti-polyhistidine-alkaline phosphatase antibody were purchased from Sigma. Rabbit monoclonal anti-HDAC6 antibody was purchased from Cell Signaling Technology. N-terminally acetylated and C-terminally carboxylated, singly-acetylated peptides were purchased from Peptide 2.0 or Synthetic Biomolecules at >85% purity. 3% (v/v) acetic acid standard was purchased from RICCA Chemical. All other materials were purchased from Fisher at >95% purity unless noted otherwise.

HDAC6 Expression and Purification

The plasmid and protocol for the expression and purification of zebrafish catalytic domain 2 (zCD2) was generously provided by David Christianson (University of Pennsylvania). The MBP-His6x-TEV-HDAC6 expression constructs were prepared previously by the Christianson lab by cloning the HDAC6 gene (gift from E. Verdin, University of California, San Francisco; Addgene plasmid #13823) into a modified pET28a(+) vector (gift from S. Gradia, University of California, Berkely; Addgene plasmid #29656) to encode HDAC6 with a Tev-protease cleavable N-terminal maltose binding protein/His_{6x} tag.[16] HDAC6 was expressed and purified as described with several alterations for expression optimization.[16] Briefly, commercial

competent BL21(DE3) *E. coli* cells (Novagen 69450-3) were transformed with plasmid according to the protocol and plated on LB-media agarose supplemented with 50 μg/mL kanamycin. Plates were incubated overnight at 37°C (16-18 hours), and one colony was added to an overnight LB/kanamycin starter culture and incubated with shaking at 37°C for 16-18 hours. This overnight starter culture was diluted (1:200) into 2x-YT media supplemented with 50 μg/mL kanamycin and incubated at 37°C with shaking until the cell density reached an OD_{600}=1. The cultures were then cooled to 18°C for one hour and supplemented with 500 μM isopropyl β-D-1-thiogalactopyranoside (IPTG) to induce expression and 100 μM $ZnSO_4$. The cultures were grown for an additional 16-18 hours with shaking at 18°C and harvested by centrifugation at 6,000 x g for 15 min at 4°C. Cell pellets were stored at -80°C. 1-mL pre- and post-induction samples were taken and tested for HDAC6 expression by polyhistidine and HDAC6 western blot analysis and activity measurements using the commercial Fluor de Lys assay (Enzo Life Sciences).

Cell pellets were resuspended in running buffer (50 mM HEPES, pH 7.5, 300 mM KCl, 10% (v/v) glycerol and 1 mM TCEP) supplemented with protease inhibitor tablets (Pierce) at 2 mL/g cell pellet. The cells were lysed by three passages through a chilled microfluidizer (Microfluidics) and centrifuged for 1 h at 26,000 x g at 4°C. Using an AKTA Pure FPLC (GE) running at 2 mL/min, the cleared lysate was loaded onto a 10-mL packed Ni-NTA column equilibrated with running buffer. The column was washed with 10 column volumes (CVs) of running buffer and 10 CVs of running buffer containing 30 mM imidazole, and the protein was eluted with 5 CVs elution buffer containing 500 mM imidazole. 8 mL fractions were collected and analyzed by SDS-PAGE and western blot, and fractions containing His-tagged HDAC6 were combined and loaded onto a 30-mL amylose column equilibrated with running buffer running at 1 mL/min. The column was washed with 2 CVs running buffer and the protein was eluted with 5 CVs of running buffer supplemented with 20 mM maltose. Fractions containing HDAC6 were combined with His_{6x}-Tev S219V protease (0.5 mg Tev protease/L culture) purified in-house[31] using a commercially purchased plasmid (Addgene plasmid pRK739) and dialyzed in 15-30 mL 20K molecular weight cut-off (MWCO) dialysis cassettes against 200-fold running buffer containing 20 mM imidazole overnight at 4°C. After dialysis, the sample was loaded onto a 10-mL Ni-NTA column running at 2 mL/min. The column was washed with 5 CVs of 50 mM imidazole running buffer to elute cleaved HDAC. Non-cleaved HDAC6 and His-tagged Tev-

protease were eluted with 20 CVs of a 50-500 mM linear imidazole gradient. Fractions containing cleaved HDAC6 were combined, concentrated to <2 mL, and loaded onto a 26/60 sephacryl S200 size exclusion chromatography (SEC) column (GE) equilibrated with SEC/storage buffer (50 mM HEPES, pH 7.5, 100 mM KCl, 5% glycerol, and 1 mM TCEP) running at 0.5 mL/min. Eluted peaks were tested for deacetylase activity, and active fractions were concentrated, aliquoted, flash frozen with liquid N_2, and stored at -80°C. A western blot analysis using an HDAC6 monoclonal antibody (Abcam 1:5,000) was performed to verify the identity of the protein.

ACS Expression and Purification

The expression plasmid was prepared previously. The chitin-tagged acetyl-CoA synthetase plasmid Acs/pTYB1 was a generous gift from Andrew Gulick (Hauptman-Woodward Institute). The pHD4-ACS-TEV-His_{6x} was prepared previously by inserting the ACS gene into a pET vector containing a His_{6x} tag to increase expression.[27, 32] The pHD4-ACS-TEV-His_{6x} construct was expressed and purified as previously described.[27]

Coupled Acetate Detection Assay

The coupled acetate detection assay or simply the *acetate assay* was performed as previously described with a few alterations.[27] Briefly, lyophilized peptides were re-suspended in water when possible or with up 25% dimethylsulfoxide (DMSO). Peptide concentration was determined, depending on the peptide sequence, by: measuring A_{280} using the extinction coefficients for tryptophan or tyrosine absorbance if the peptide contained a tryptophan or tyrosine, using the fluorescamine assay if the peptide contained a free lysine,[33] or performing the bicinchoninic (BCA) assay using bovine serum albumin (BSA) as a standard if the peptide had no aromatic or lysine residues. HDAC6 and singly-acetylated peptides (10-2000 μM) were pre-incubated in 1X HDAC6 assay buffer (50 mM HEPES, pH 8.0, 137 mM NaCl, 2.7 mM KCl, 1 mM $MgCl_2$) at 30°C for at least five minutes prior to initiation of the reaction by addition of 0.1-1 μM HDAC6. Reactions were allowed to proceed at 30°C, and 60 μL were removed at selected timepoints (<2 minutes for fast reactions and up to 90 minutes for slow reactions) and quenched into separate tubes containing 5 μL of 10% hydrochloric acid. Each timepoint was briefly centrifuged and incubated on ice until assay completion (no more than 90 minutes) prior to flash freezing with liquid nitrogen and storage at -80°C until work-up.

Coupled solution (50 mM HEPES, pH 8, 400 μM ATP, 10 μM NAD^+, 30 μM CoA, 0.07 U/μL CS, 0.04 U/μL MDH, 50 μM ACS, 100 mM NaCl, 3 mM KCl, 50 mM $MgCl_2$, and 2.5 mM L-malic acid) and standards (acetate and NADH equal to 0-10% of highest peptide concentration) were prepared the day of the work-up and the coupled solution was incubated at room temperature for at least 20 minutes. NADH standards and coupled solution were protected from light. Timepoints were quickly thawed and neutralized with 10 μL of freshly prepared and filtered 6% sodium bicarbonate. Neutralized samples were vortexed and spun down, and 60 μL of each sample and each standard were added to 10 μL coupled solution (or 1X assay buffer for NADH standards) in a black, flat-bottomed, half-area, non-binding, 96-well plate (Corning No. 3686). The NADH fluorescence (Ex=340 nm, Em=460 nm) of standards and samples was read on a fluorescence plate reader at 1-3-minute increments until the signal reached equilibrium (usually 30-60 min, depending on acetate concentration). The slopes of the acetate and NADH standard curves were compared to verify that the coupled mixture was working. When possible, a positive control reaction for enzyme activity was included. Using the acetate standard curve, the fluorescence of each timepoint was converted to μM product, and the slopes of the linear portion of the reaction (<10%) were plotted against substrate concentration. Using GraphPad Prism, the Michaelis-Menten equation (Equation IV.1) was fit to the resulting dependence of the initial velocity on substrate concentration to determine the kinetic parameters k_{cat}/K_M, k_{cat}, and K_M. Standard error was calculated directly from the output.

Equation IV.1

$$\frac{v_0}{[E]} = \frac{k_{cat}}{K_M}\left(\frac{[S]}{\left(\frac{[S]}{K_M}+1\right)}\right)$$

Modeling Peptide-Enzyme Complexes Using Rosetta FlexPepBind

The Rosetta FlexPepBind protocol used to model HDAC8 peptide-enzyme complexes and predict substrate specificity was followed as previously described, with modifications.[25, 34-35] Briefly, the human HDAC6 CD2 in complex with trichostatin A (TSA) (PDB ID 5EDU) and zebrafish HDAC6 H574A CD2 in complex with histone H4K6 tripeptide substrate (PDB ID 5EFN) crystal structures were used as the template ligand-receptor complexes to provide approximate starting models. Structural constraints (Table IV.1) were put in place to conserve key enzyme-substrate interactions such that the acetyl-lysine side-chain was locked into a favorable orientation, while allowing flexibility at the peptide-enzyme binding interface. These

constraints include the conserved His/Asp/Asp metal coordinating ligand contact to the acetyl-lysine and several other residue/side-chain interactions. Using the algorithm to generate 1000 models, the top scoring model, according to the most energetically favorable interface score (the total energy of the complex minus the energy of the individual partners when separated), was selected. The selected peptide sequences were then threaded into the peptide binding groove of the starting model using Rosetta fixed backbone design,[36] and the peptide orientation and binding conformation were optimized using Rosetta FlexPepDock.

The Rosetta default scoring function[37] was used to rank the peptides in order of relative binding ability/strength, and the correlation between different subsets of the total score versus the logarithm of peptide activity ($\log[k_{cat}/K_M]$) was determined. The model was then calibrated through adjusting the sampling protocol (*e.g.* refinement versus minimization) and analyzing the Rosetta score to determine the most correlative subset to provide a correlation *R* value (from -1 to 1 with 0 indicating no correlation and 1 or -1 indicating perfect correlation) less than -0.3 with a probability *p* value of below 0.05. To validate and/or further optimize the model, 6-mer peptide sequences selected from our in-house library were then scored using the computational model to distinguish between binders and non-binders (*i.e.* substrates and non-substrates) and provide reactivity predictions for a second test group. These calibration steps were repeated with HDAC6 activity data measured using the acetate assay to further optimize the model prior to screening the entire database of available acetylated sequences from PhosphoSitePlus.[38]

Table IV.1 Residue constraints for human HDAC6 CD2 complexed with TSA (5EDU)

Constraint type	**AA1**	**Position**	**AA2**
Zn coordinating	D	649	K-Ac
Zn coordinating	H	651	K-Ac
Zn coordinating	D	742	K-Ac
Lock side chain of K-Ac	H	610	K-Ac
Lock side chain of K-Ac	F	679	K-Ac
Lock side chain of K-Ac	F	620	K-Ac
Lock side chain of K-Ac	G	619	K-Ac
Enforce H-bond	S	568	K-Ac
cis-bind	K-Ac	-	res4 peptide
Lock side chain of K-Ac	H	611	K-Ac
Lock side chain	H	610	N (654)

Results

Optimization of HDAC6 Expression and Purification

After receiving plasmids from David Christianson for recombinant expression of HDAC6 for human (didomain, hCD12) and zebrafish (didomain and single catalytic domains 1 and 2, zCD12, zCD1, and zCD2, respectively), I optimized expression and purification. To increase the transformation efficiency, I used a commercial stock of competent BL(21)-DE3 cells (Novagen). To increase the yield of purified protein from the recombinant expressions, I modified the purification protocol by swapping the first nickel and amylose columns, streamlining the buffer system, and moving to an overnight cleavage of the His_{6x}-MBP tag catalyzed by Tev-protease in place of the less efficient on-column cleavage step in the original protocol. Total purified protein yield improved to 10 mg/L culture for zCD2.

As previously presented, HDAC6 contains two catalytic domains where domain 2 is considered the canonical domain with 23%-81% similarity between CD2 and the catalytic domain of the other Class II isozymes.[1] HDAC6 is most similar to the other class IIb enzyme, HDAC10, sharing 55% overall identity.[1] The CD2 domain has previously been shown to catalyze deacetylation of a small panel of fluorogenic and non-fluorogenic substrates with no obvious sequence selectivity.[16] In contrast, the CD1 domain shows selectivity for hydrolysis of C-terminal acetyl-lysine substrates.[16] Therefore, a systematic approach to identifying HDAC6 substrates is warranted and here we began by measuring and modeling the behavior of the canonical domain CD2.

The CD2 domains of HDAC6 are highly conserved in sequence and structure between zebrafish and human, with sequence identity of 59% and sequence similarity of 75%, particularly at the active site where only two side chains at the outer rim of the active site are not conserved (N530/N645 in zCD2 and D567/M682 in hCD2).[16] Comparisons of the crystal structures of hCD2 and zCD2 demonstrate structural similarity, with an r.m.s. deviation of 0.43 Å for 314 Cα (Figure IV.2).[16] These similarities demonstrate that zebrafish CD2 makes a valid surrogate for human CD2. Unfortunately, the human CD2 domain yields a protein that is ill-behaved *in vitro;* hCD2 is unstable in solution when cleaved from MBP and loses activity after a single freeze-thaw cycle. In contrast, Zebrafish CD2 (zCD2) is well-behaved and stable in the absence of the MBP tag and retains activity comparable to an enzyme containing both domains (CD12).[16] The high expression levels, robust activity, available crystal structures, and overall ease of use for the

zebrafish protein facilitates research towards a better understanding of human HDAC6 function. For these reasons, the zebrafish catalytic domain 2 was selected for *in vitro* testing and structure-based identification of HDAC6 substrates.

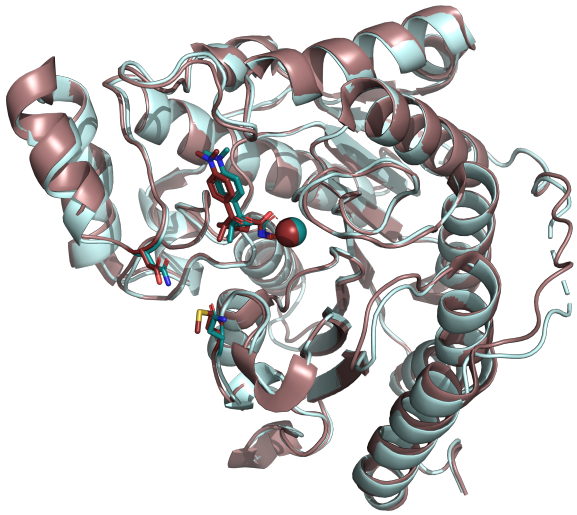

Figure IV.2 Catalytic domain 2 is conserved between humans and zebrafish

Overlay of zebrafish and human HDAC6 catalytic domain 2 (PDB IDs 5EEK and 5EDU, respectively) complexed with TSA**.** Human CD2 (raspberry) and zebrafish CD2 (light cyan) closely align indicating strong structural homology. Only two residue pairs differ between the two structures: hCD2 N530 and zCD2 D567 and hCD2 N645 and zCD2 M682. In hCD2, the Zn^{2+} ion, TSA, and residues D567 and M682 are shown in ruby. In zCD2, the Zn^{2+} ion, TSA, and residues N530 and N645 are shown in dark teal. Figure modeled as previously published.[16]

To test activity, zCD2-catalyzed deacetylation of four 6-mer, singly-acetylated peptides was measured using the acetate assay (Table IV.2) The four peptides selected correspond to acetyl-lysine residues in putative HDAC6 substrate Hsp90 and proteins involved in HDAC6-regulated processes including cytoskeletal dynamics (actinin 1 and 2) and stress response (endoplasmin). The sequences were selected from available peptides in our in-house library. Although the acetate assay had not been tested with HDAC6 previously, the assay was designed to function with any metal-dependent deacetylase. As expected, HDAC6 catalyzed deacetylation of all four peptides. Unexpectedly, HDAC6 showed a 90-fold variation in activity even with this small selection of peptides. These results demonstrated that HDAC6 activity depends on the peptide sequence and validated the search for a substrate model based on the sequences immediately flanking the acetyl-lysine. The fastest peptide tested, corresponding to a well-established HDAC6 substrate, Hsp90, was re-tested with varying substrate concentrations to

determine the steady state kinetic parameters: $k_{cat}/K_M = 85{,}000 \pm 35{,}000\ M^{-1}s^{-1}$, $k_{cat} = 1.8 \pm 0.6\ s^{-1}$, and $K_M = 21 \pm 9\ \mu M$ (Figure IV.3, Table IV.3). The k_{cat}/K_M for the peptide is higher than the $k_{cat}/K_{M,\ app}$ since the peptide concentration selected for the initial test (50 µM) is above the K_M for this peptide.

Table IV.2 Approximate Activity for zCD2-Catalyzed Deacetylation of Four Peptides

Protein	Kac	Function (Localization)	Peptide Sequence	$k_{cat}/K_{M,\ app}$, $M^{-1}s^{-1}$ [a]
HSP90A	K436	stress response (Cy)	YKKacFYE	19,000 ± 3,000
ACTN1	K195	alpha actinin, actin binding (Pm, Cs)	YGKacLRK	9,500 ± 700
HSP90B1	K682	endoplasmin, stress response (Er)	SQKacKTF	390 ± 190
ACTN2	K181	alpha actinin, actin binding (Cs)	SWKacDGL	210 ± 90

[a]Activity was measured at a single concentration of substrate (50 µM) and the value of $k_{cat}/K_{M,\ app}$ was determined from $v_0/[E][S]$. Abbreviations: Cy = cytoplasm; Pm = plasma membrane; Cs = cytoskeleton; Er = endoplasmic reticulum.

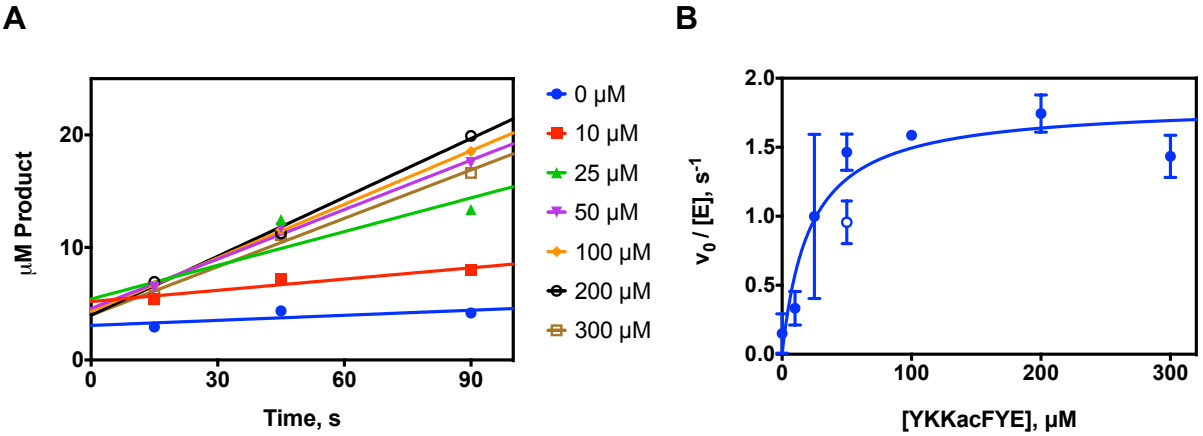

Figure IV.3 Dependence of HDAC6-catalyzed deacetylation on the concentration of Hsp90 K436ac Peptide

HDAC6 zCD2-catalyzed deacetylation of the Hsp90 peptide YKKacFYE was measured using the acetate assay with [HDAC6]=100 nM and [Peptide] ranging from 0-300 µM. The initial velocity, v_0, was determined from the first 10% of the reaction at each peptide concentration (up to 90 seconds) (A), and the steady-state kinetic parameters k_{cat}/K_M, k_{cat}, and K_M were determined by fitting the Michaelis-Menten equation (Equation IV.1) to the dependence of the initial velocity on the substrate concentration (B). Open blue circle denotes value for $v_0/[E]$ from the initial test. Analysis was performed, and standard errors were determined, using GraphPad Prism.

Peptide Screen Demonstrates Up to 20,000-fold Changes in Activity Depending on Sequence

To obtain further insight into the selectivity of HDAC6 CD2, the peptide reactivity for additional sequences was measured using the acetate assay. zCD2-catalyzed deacetylation of a library of 28 peptides was assayed at one concentration per peptide with two timepoints per reaction. The resulting values for $k_{cat}/K_{M,\ apparent}$ (assuming that the selected peptide concentrations are below the K_M) follow a similar trend as the initial four test peptides and demonstrate that some peptides are excellent HDAC6 substrates ($>10^3\ M^{-1}s^{-1}$) while other peptides are poor substrates ($<100\ M^{-1}s^{-1}$) (Table IV.3). The peptides were selected from an in-house peptide library used for HDAC8 substrate specificity determination and included peptides from a diverse set of proteins. The peptides were chosen from a library containing over 250 peptides, and the selection was based principally on amount of peptide available, solubility, and varied sequence and subsequently on diverse corresponding protein function (localization, cellular role, etc.) with special attention to proteins with known functions, proteins involved in HDAC6-related pathways (*e.g.* stress response, cytoskeletal dynamics) and proteins with clinical significance (*e.g.* LMNA, MSH2, PTEN). All peptides correspond to known acetyl-lysine modifications in the human proteome.

Table IV.3 Initial Peptide Screen and Model Training Set[a]

Protein	K(ac)	Function (Localization)[b]	Peptide Sequence	$k_{cat}/K_{M,\ app}$ $M^{-1}s^{-1}$
CRIP1	K22	zinc finger, zinc transport (Cy,Nu,Cn)	SLGKacDWHR	6500
LMNA	K450	nuclear assembly, dynamics (Nm)	EGKacFVR	5200
VDAC1	K61	membrane channel (Pm, Mi)	ETKacYRW	3200
ACTN1	K195	alpha actinin, actin binding (Pm, Cs)	YGKacLRK	3000
ACLY	K540	acetyl-CoA synthesis (Cy, Pm, Nu)	DHKQKacFYWGHK	3000
TRIM28	K770	nuclear co-repressor (Nu)	RMFKacQFNK	2700
MSH2	K635	DNA mismatch repair (Nu)	RIILKacASRH	2600
MCM6	K599	helicase (Nu)	EQYKacHLR	2600
SFPQ	K314	splicing factor (Nu)	EFKacRLF	2200
RDH16	K221	oxidoreductase, lipid metabolism (Er)	ERFLKacSFLE	2000
PTEN	K125	phosphatase, tumor suppressor (Nu, Cy)	HCKacAGK	1800
HNRL2	K570	transcriptional regulation (Nu)	DWKacKRL	1500
UPF1	K386	helicase, mRNA catabolism (Nu)	RYKGDLAPLWKacGIGHVIKVPD	1400
ITGB1	K134	receptor, cell signaling/adhesion (Pm)	TLKacFKR	1100
NPEPPS	K48	aminopeptidase (Nu,Cy)	PEKacKRP	1100
HS71	K146	chaperone, stress response (Nu, Cs)	EFKacRKH	910
HSPA1L	K321	chaperone, stress response (Nu, Cy)	VEKacALR	830
HSP90B1	K682	chaperone, stress response (Er)	SQKacKTF	820
QARS	K628	ligase, tRNA aminoacylation (Cy)	EPEPGFKacRLAWGQ	820
H4K16	K16	histone H4, chromatin (Nu)	KGGAKacRHR	490
RL3	K393	ribosomal protein, translation (Nu, Cy)	PLKacKDR	450
LMNA	K260	nuclear assembly, dynamics (Nm)	QYKacKEL	380
S10A8	K84	metal binding, immunity (Pm, Ec, Cy)	AHKacKSH	370
PARP1	K505	ribosyltransferase, DNA repair (Nu)	LSKacKSK	360
PTEN	K128	phosphatase, tumor suppressor (Nu, Cy)	AGKacGRT	260
PTEN	K6	phosphatase, tumor suppressor (Nu, Cy)	IIKacEIVSR	100
DPP3	K294	aminopeptidase (Cy)	AHKacRGS	80
AKR1C2	K246	oxidoreductase, lipid metabolism (Cy)	LAKacKHK	12

[a] Values for $k_{cat}/K_{M,\ app}$ were determined from a reaction of 100 nM HDAC6 and 100 μM peptide. Two timepoints were taken (15 and 600 seconds) per reaction. The values may be an underestimate of the value of k_{cat}/K_M if the peptide concentration is above the K_M value. Abbreviations: Cs=Cytoskeleton, Cy=Cytosol, Cn=Centrosome, Pm=Plasma membrane, Mi=Mitochondria, Nu=Nucleus, Nm=Nuclear Membrane, ER=endoplasmic reticulum, Ec-extracellular region).

[b] Function and localization information was taken from the UniProt protein database and the human atlas project.[39-40]

This initial screen provides a qualitative analysis of the catalytic activity of HDAC6 with these peptides, demonstrating selectivity for 6 amino acid peptide substrates of >400-fold. However, the values for $k_{cat}/K_{M,app}$ may underestimate the actual value for two reasons. First, since only two time points were taken in these assays, the reactions may have progressed beyond the initial 10% by the 10 min timepoint. Second, the peptide concentration (100 μM) used in the screen, may have been above the K_M and thus invalidated the approximation used in the calculation of $k_{cat}/K_{M,\,app}$. Both of these inaccuracies should have the largest effect for the best substrates. Therefore, the initial rate at multiple substrate concentrations was tested to calculate the steady-state kinetic parameters k_{cat}/K_M, k_{cat}, and K_M for several of the most reactive peptides including cysteine-rich protein 1 (CRIP1) Kac22, prelamin A (LMNA) Kac450, voltage-dependent anion-selective channel protein 1 (VDAC1) Kac61, α-actinin (ACTN1) Kac195, transcription intermediary factor 1-β (TRIM28) Kac770 , and DNA mismatch repair protein Msh2 (MSH2) Kac635, as well as one of the least reactive peptides dipeptidyl-peptidase 3 (DPP3) Kac294 as was done with Hsp90 K436ac (Table IV.4, Figure IV.4).

The results showed that, indeed, the $k_{cat}/K_{M,\,app}$ values from the initial screen underestimated the values for peptides at the upper range of activity, but the peptides on the lower range of activity were more accurately estimated (Figure IV.4, Table IV.4). These more accurate values demonstrated HDAC6 selectivity for 6 amino acid acetylated peptides of nearly 20,000-fold using the AKR1C2 peptide as the lower limit. Surprisingly, for the most reactive peptides, the k_{cat}/K_M values approach the estimated 10^6-10^8 $M^{-1}s^{-1}$ diffusion-controlled limits for catalytic turnover.[41] The selectivity ratios and k_{cat}/K_M values are significantly larger than previously reported for domain 2 of zebrafish HDAC6.[16]

Table IV.4 Training set steady-state kinetic parameters for HDAC6-catalyzed deacetylation of short peptides

Protein	K(ac)	Peptide Sequence	$k_{cat}/K_{M,}$ $M^{-1}s^{-1}$	$K_{M,}$ μM	$k_{cat,}$ s^{-1}
LMNA	K450	EGKacFVR	220,000 ± 35,000	19 ± 4	4.2 ± 0.7
HSP90A	K436	YKKacFYE	85,000 ± 29,000	21 ± 9	1.8 ± 0.6
VDAC1	K61	ETKacYRW	42,000 ± 9,500	160 ± 110	6.8 ± 1.5
ACTN1	K195	YGKacLRK	31,000 ± 3,500	200 ± 80	6.0 ± 0.7
CRIP1	K22	SLGKacDWHR	31,000 ± 4,900	320 ± 150	9.9 ± 1.5
TRIM28	K770	RMFKacQFNK	21,000 ± 1,300	>100	>2
MSH2	K635	RIILKacASRH	19,000 ± 3,000	210 ± 120	4.1 ± 0.6
DPP3	K294	AHKacRGS	115 ± 7	>200	>0.02

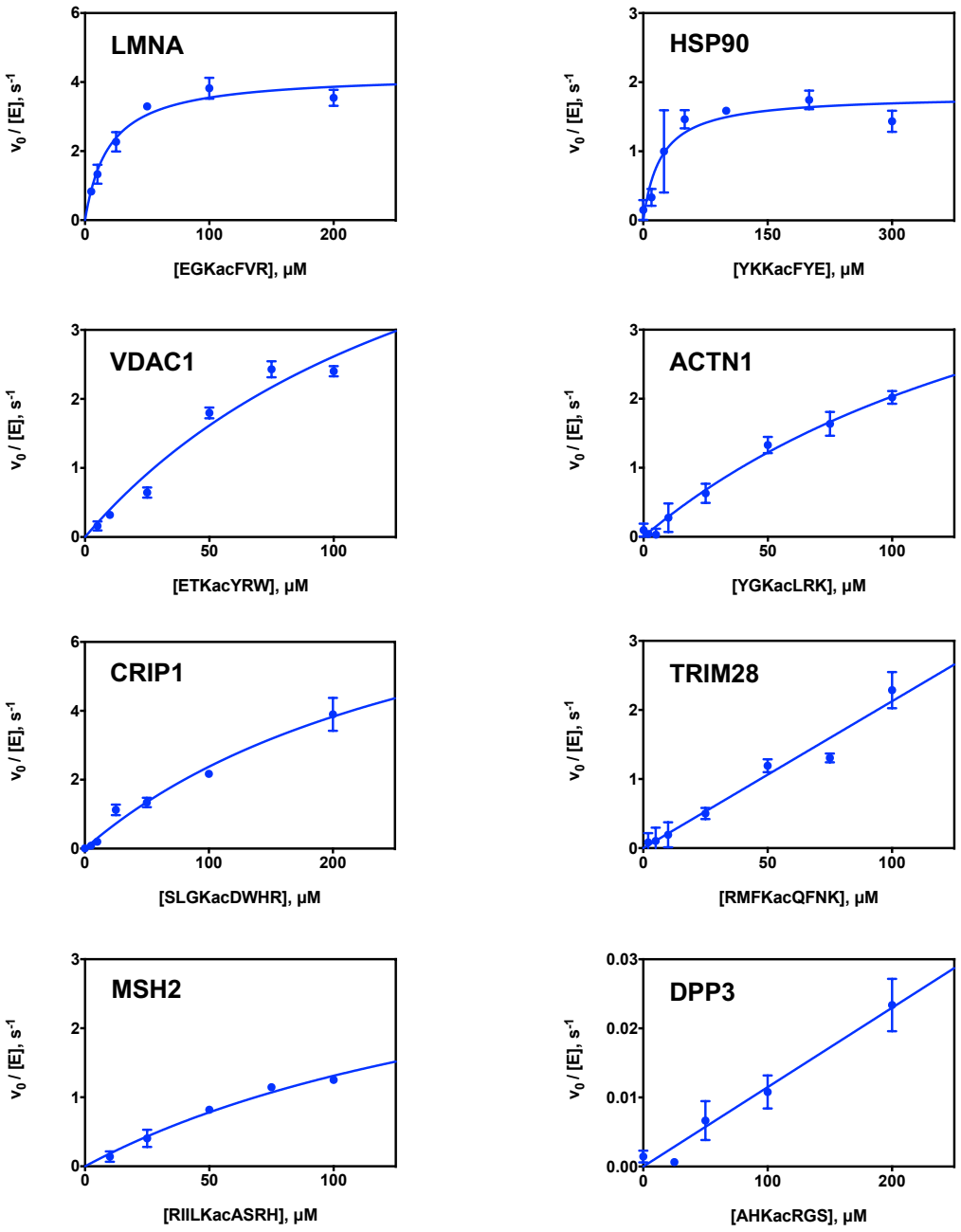

Figure IV.4 Dependence of HDAC6-Catalyzed Deacetylation on Peptides Concentration

HDAC6 zCD2 activity with short peptides, including LMNA peptide EGKacFVR, HSP90 peptide YKKacFYE, VDAC1 peptide ETKacYRW, ACTN peptide YGKacLRK, CRIP1 peptide SLGKacDWHR, TRIM28 peptide RMFKacQFNK, MSH2 peptide RIILKacASRH, and DPP3 peptide AHKacRGS was measured using the acetate assay. [HDAC6]=100 nM. [Peptide]=0-200 μM. The initial velocity, v_0, was determined from product formation for the first 10% of each reaction, and the steady-state kinetic parameters k_{cat}/K_M, k_{cat}, and K_M were determined by fitting the Michaelis-Menten equation (Equation IV.1) to the dependence of v_0 on the substrate concentration. Fitting and standard errors were determined using GraphPad Prism.

Development of Structure-Based Protocol for HDAC6 Using Initial Peptide Screen as Training Set

Using the first set of peptides and kinetic parameters (Table IV.3 and Table IV.4), an initial model of HDAC6 substrate binding was developed using the Rosetta framework and FlepPepDock and FlexPepBind protocols described previously.[25, 34-35] The milestones for model development include: 1) developing a model of HDAC6 binding capable of distinguishing between 6-mer peptide binders and non-binders (i.e. substrates and non-substrates), 2) optimizing the model to rank peptides in order of relative binding strength, and 3) screening acetylome databases to identify putative HDAC6 structures. This research encompasses efforts towards achieving the 1st milestone.

To create an initial receptor-ligand template structure, two HDAC6 structures were modeled using Rosetta FlexPepDock. The two crystal structures implemented were zebrafish HDAC6 CD2 bound to a 3-mer H3K6ac peptide (PDB ID 5EFN) and human HDAC6 CD2 bound to TSA (PDB ID 5EDU). Human and zebrafish structures were used to compare and identify differences, if any, between models. In order to maintain the acetyl side-chain in a favorable binding orientation for catalysis yet allow for flexibility within the flanking peptide sequence, key residues were identified and constrained such that the substrate was locked into the active site. This way, the protocol had access to only relevant conformations with enough flexibility to sample numerous possible structures. The residues selected for constraint include the conserved catalytic Zn(II) ligands D649, H651, and D742 for the human CD2-TSA structure (Table IV.1) and D612, H614, and D705 for the zebrafish CD2-H4Kac6 peptide structure to tether the acetyl-group to the Zn(II) binding site and to several residues with hydrogen-bond interactions along the peptide backbone of the acetyl-lysine.

With these constraints in place, the Rosetta protocol FlexPepDock was adapted to HDAC6 by modeling the binding of HDAC6 to the peptide sequence corresponding to the best substrate prelamin A, EGKacFVR. An output of 1,000 structures of HDAC6-peptide binding were produced and of these, the most energetically favorable structures were further analyzed, and the best structure was selected as the template to model multiple peptide interactions. In order to test and optimize the starting structure, additional peptide sequences were threaded into the peptide binding groove using the Rosetta protocol FlexPepBind and scored. Peptide binding of multiple peptides was optimized using FlexPepDock, and the correlation between score and

the logarithm of catalytic efficiency (log[k_{cat}/K_M]) was determined. Multiple subsets of the Rosetta default scoring function (total score) were analyzed to identify the best correlating parameter. Further changes were made to the protocol to optimize binding and correlation. These include increasing the amount of sampling (or the number of structural permutations analyzed by the program) and performing additional peptide minimization and structural refinement operations. For both zebrafish and human models, the interface score, the subset of the total score encompassing the sum of the interactions across the interface, yielded the best correlation. Correlation *R* values, which range from -1 to 1 with 0 indicating no correlation and 1 or -1 indicating perfect correlation, and probability *p* values were determined using GraphPad prism analysis. For the zebrafish and human models, the best correlation between the logarithm of catalytic efficiency (k_{cat}/K_M) and corresponding interface score for the training set of peptides listed in Table IV.3 were -0.59 and -0.74, respectively. Due to better correlation for the human structure, this model was selected to test additional sequences and identify a set of peptides for validation. The protocol was run for an additional 60 peptide sequences selected from our in-house peptide library of >250 peptides, and 8 peptides were chosen for validation.

Optimization of Structure-Based Protocol for HDAC6

In order to test the algorithm developed based on the data from the initial training set (Table IV.3, Table IV.4), a validation set of peptides was tested (Figure IV.5, Table IV.5) including peptides corresponding to TCOF1, PCBP1, KIF5B, CDK1, MATR3, LARP1, EIF3B, and GOT1. Six of the peptides were scored as good binders, while two of the peptides were scored as poor binders. HDAC6 zCD2 deacetylated all 8 peptides tested with catalytic efficiencies ranging from 16,000-44,000 $M^{-1}s^{-1}$. The k_{cat}/K_M values for TCOF1, PCBP1, KIF5B, and CDK1 peptides were reliably measured (Figure IV.5, Table IV.5). However, for the other 4 peptides, MATR3, LARP1, EIF3B, and GOT1, the values for k_{cat}/K_M were difficult to calculate reliably due to either inhibition at high peptide concentrations or K_M values below the detection level of the assay (<10 μM). For the peptides with inhibitory activity, an estimate of k_{cat}/K_M was calculated from the substrate concentration at the highest initial velocity. For LARP1, due to a low K_M, (HDAC6 was already saturated at [LARP1] = 10 μM), an estimated value for catalytic efficiency was determined from the initial velocity at the lowest peptide concentration measured. However, in order for accurate representation of catalytic activity, the assay would have to be optimized in order to evaluate <1 μM acetate, which is currently prohibited due to background

interference. The same estimation was performed for EIF5B, as HDAC6 was saturated at the lowest peptide concentration measured (50 μM). Moreover, peptide concentration will have to be carefully analyzed in order to verify stock concentration, as the concentration of certain peptides may not be accurately represented using measurements by BCA. This, however, has yet to be determined. Despite all of this, the resulting correlation for the peptides that were scored as good binders with interface scores > -26.5 was very good with R = -0.85 and p = 0.03. However, the two peptides that were scored as poor binders, PCBP1 and KIF5B, have values of k_{cat}/K_M and K_M comparable to the good binders (Table IV.5) and inclusion of these data made the correlation insignificant with R = -0.57 and p = 0.1 (Figure IV.6A). Due to these two false negatives, the model was further calibrated to distinguish between HDAC6 substrates and non-substrates. With this modified model, the resulting correlation for all data (Table IV.6) was R = -0.62 and p<0.0001(Table IV.6, Figure IV.6B).

Table IV.5 Validation peptide set kinetic parameters for HDAC6 structure-based model[a]

Protein	Kac	Function (Localization)[b]	Peptide Sequence	k_{cat}/K_M, $M^{-1}s^{-1}$	K_M, μM	I-S
TCOF1	K296	RNA pol I regulation (Nu)	SEKacILQ	44,000 ± 12,000	33 ± 11	-26.77
PCBP1	K23	iron chaperone (Nu)	HGKacEVG	39,000 ± 15,000	85 ± 51	-23.93
KIF5B	K346	kinesin, transport (Cs)	YEKacEKE	27,000 ± 4,600	66 ± 14	-24.08
CDK1	K33	kinase, cell cycle (Cs, Nu)	AMKacKIR	16,000 ± 1,600	60 ± 11	-26.76
MATR3[c]	K473	transcription (Nu)	SQKacYKR	99,000	20	-29.75
LARP1[de]	K1017	translation (Nu, Cy, Er)	LGKacFRR	97,000	ND	-29.01
EIF3B[de]	K364	translation (Nu, Cy)	GEKacFKQ	28,800 ± 500	ND	-27.91
GOT1[d]	K154	aminotransferase (Cy)	GFKacDIR	27,000 ± 1,000	ND	-27.07

[a] Values for k_{cat}/K_M and K_M are from Figure IV.5. Abbreviations: Nu=nucleus, Cs=Cytoskeleton, I-S = interface score.
[b] Function and localization information was taken from the UniProt protein database and the human atlas project.[39-40]
[c] Values for k_{cat}/K_M, and K_M were determined from 2 points at concentrations above the K_M (Figure IV.5).from lowest concentration of peptide measured/largest initial velocity
[d] Values for $k_{cat}/K_{M,app}$ were determined from lowest concentration of peptide measured (Figure IV.5).
[e] Enzyme was saturated at lowest peptide concentration measured (Figure IV.5).

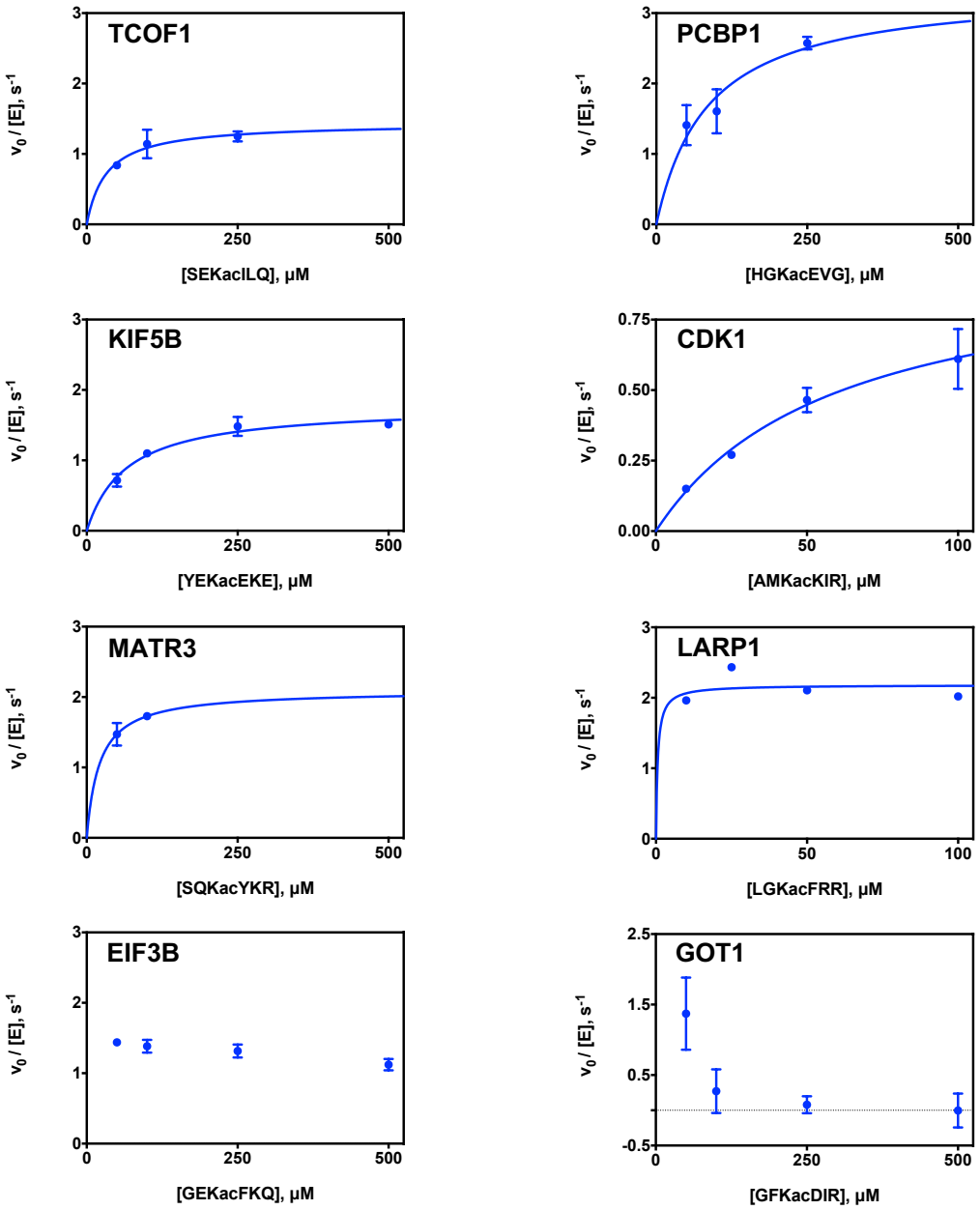

Figure IV.5 Validation set of peptides concentration dependence of HDAC6 deacetylation

HDAC6 zCD2 activity with peptides SEKacILQ (TCOF1), HGKacEVG (PCBP1), YEKacEKE (KIF5B), AMKacKIR (CDK1), SQKacYKR (MATR3), LGKacFRR (LARP1), GEKacFKQ (EIF3B), and GFKacDIR (GOT1) was measured using the acetate assay. For CDK1 and LARP1, [HDAC6]=500 nM and [Peptide]=0-100 µM. For all other peptides, [HDAC6]=100 nM and [Peptide]=0-500 µM. The initial velocity, v_0, was determined from the first 10% of the reaction at each peptide concentration, and the kinetic parameters k_{cat}/K_M, k_{cat}, and K_M were determined by fitting the Michaelis-Menten equation (Equation IV.1) to the initial velocity dependence on substrate concentration. Analysis was performed using GraphPad Prism and standard errors were determined from software calculations.

Table IV.6 Peptide kinetic parameters and interface scores for current structure-based binding model used to determine correlation[a]

Protein	K(ac)	Peptide Sequence	k_{cat}/K_M, $M^{-1}s^{-1}$	Interface Score	Conclusion
LMNA	K450	EGKacFVR	220000	-29.704	G
MATR3	K473	SQKacYKR	99000	-31.07	G
LARP1	K1017	LGKacFRR	97000	-31.28	G
HSP90	K436	YKKacFYE	85000	-29.784	G
TCOF1	K296	SEKacILQ	44000	-30.69	G
VDAC1	K61	ETKacYRW	42000	-29.54	G
PCBP1	K23	HGKacEVG	39000	-27.59	G
CRIP1	K22	SLGKacDWHR	31000	-27.941	G
ACTN1	K195	YGKacLRK	31000	-29.478	G
EIF3B	K364	GEKacFKQ	28800	-30.15	G
KIF5B	K346	YEKacEKE	27000	-27.22	G
GOT1	K154	GFKacDIR	27000	-29.78	G
TRIM28	K770	RMFKacQFNK	21000	-28.147	G
MSH2	K635	RIILKacASRH	19000	-28.035	G
CDK1	K33	AMKacKIR	16000	-28.26	G
ACLY	K540	DHKQKacFYWGHK	3000	-29.533	M
MCM6	K599	EQYKacHLR	2600	-31.064	M
SFPQ	K314	EFKacRLF	2200	-29.781	M
RDH16	K221	ERFLKacSFLE	2000	-29.147	M
PTEN	K125	HCKacAGK	1800	-30.109	M
HNRL2	K570	DWKacKRL	1500	-28.088	M
UPF1	K386	RYKGDLAPLWKacGIGHVIKVPD	1400	-28.248	M
ITGB1	K134	TLKacFKR	1100	-28.299	M
NPEPPS	K48	PEKacKRP	1100	-24.401	M
HS71	K146	EFKacRKH	910	-26.041	M
HSPA1L	K321	VEKacALR	830	-28.811	M
HSP90B1	K682	SQKacKTF	820	-25.666	M
QARS	K628	EPEPGFKacRLAWGQ	820	-29.62	M
H4K16	K16	KGGAKacRHR	490	-27	P
RL3	K393	PLKacKDR	450	-24.443	P
LMNA	K260	QYKacKEL	380	-25.99	P
S10A8	K84	AHKacKSH	370	-24.893	P
PARP1	K505	LSKacKSK	360	-25.614	P
PTEN	K128	AGKacGRT	260	-26.325	P
ACTN2	K181	SWKacDGL	210	-27.073	P
DPP3	K294	AHKacRGS	115	-25.531	P
PTEN	K6	IIKacEIVSR	100	-28.61	P
AKR1C2	K246	LAKacKHK	12	-26.46	P

[a] Compiled values for best k_{cat}/K_M measured for short peptides with HDAC6 zCD2. Interface scores are for current computational binding model and graphed in Figure IV.6. Abbreviations: K(ac) = acetyl-lysine, G = good substrate/binder (>16,000 $M^{-1}s^{-1}$), M = moderate substrate/binder (500—16,000 $M^{-1}s^{-1}$), P = poor substrate/binder (<500 $M^{-1}s^{-1}$).

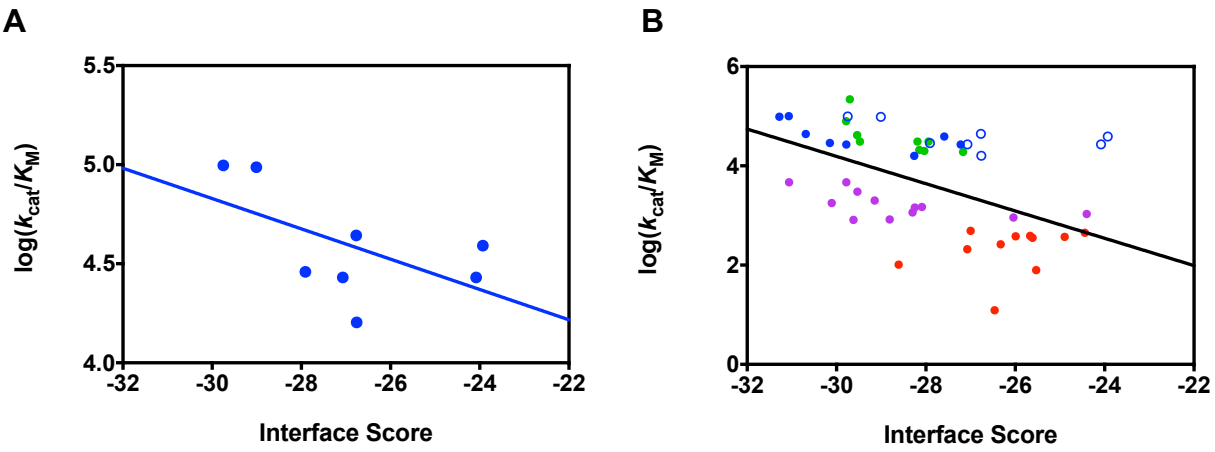

Figure IV.6 Correlation between modeled binding and HDAC6 activity for peptides

The correlation between the interface score and the logarithm of catalytic activity (log[k_{cat}/K_M]) for the validation set (A) and the training and validation sets with the optimized model (B) (Table IV.6). The line indicates a linear fit, and the correlation *R* and *p* values (from -1 to 1 with 0 indicating no correlation and 1 or -1 indicating perfect correlation) were calculated to be -0.57 and 0.1375 for the validation set (A) and -0.62 and <0.0001 for all data with the optimized model, respectively. Blue open circles = validation set (Table IV.5, Figure IV.5) and previous model interface scores, blue closed circles = validation set with new model interface scores, green closed circles = training set good substrates/binders (>16,000 $M^{-1}s^{-1}$), purple closed circles = training set moderate substrate/binder (500—16,000 $M^{-1}s^{-1}$), and red closed circles = training set poor substrate/binder (<500 $M^{-1}s^{-1}$) (Table IV.6).

Discussion

Histone deacetylase 6 is an important regulator of cellular processes including cytoskeletal dynamics and stress response.[13] Furthermore, aberrant HDAC6 activity has been linked to various types of human disease making HDAC6 an attractive target for drug discovery.[11, 13-14] Although HDAC6 has been studied extensively over the last decade, few specific substrates have been identified. Given that there are only 18 human deacetylases and thousands of acetylation events observed in humans, it is unlikely that the current shortlist of HDAC6 substrates, with the majority of reports relating to Hsp90, α-tubulin, and cortactin, is complete.[42] However, identifying which acetyl-lysines are HDAC6 substrates is a significant challenge. In order to provide a tool to virtually screen large numbers of potential substrates, we are developing a computational, structure-based model using the Rosetta FlexPepBind platform, optimized specifically to HDAC6. Previously, a similar model was developed for the class I deacetylase HDAC8, and after optimization, this algorithm successfully predicted HDAC8 peptide substrates.[25]

Our results demonstrate a wide range of HDAC6 catalytic activities, varying from 10-10^6 $M^{-1}s^{-1}$. Compared to HDAC8, HDAC6 displays more robust catalysis *in vitro*, deacetylating peptide substrates over 20 times more efficiently than the best HDAC8 *in vitro* substrate,[25] with larger values for k_{cat} and smaller values for K_M, suggesting both tighter binding and faster chemistry/product dissociation. Unfortunately, a comparison of the sequences of the slowest and fastest HDAC6 peptides reveals no obvious trend in sequence preference, as is the case for other HDACs. For example, although peptide screens identified favorable residues for HDAC2, HDAC3, and HDAC8, such as an arginine residue at the -1 position and an aromatic residue at the +1 position to the acetyl-lysine, this information is not sufficient to identify HDAC substrates.[29]

Our current model successfully predicts good peptide substrates for HDAC6, however further optimization is needed for the model to accurately predict which peptides are poor HDAC6 substrates and thus allow discrimination between good and bad binders/substrates. Part of the difficulty associated with predicting poor substrates is the high HDAC6 activity observed thus far and the relatively few examples of poor peptide substrates. Additionally, the distinction between a *good* substrate and a *bad* substrate is relative. Since HDAC6 catalyzes deacetylation of multiple substrates *in vivo*, under cellular conditions, selectivity should be dependent on both

the value of k_{cat}/K_M and the substrate concentration as reflected by the ratios of $(k_{cat}/K_M)[S_i]$. Expanding the study to include more peptides predicted to be poor binders will be critical for identifying additional sequences exhibiting low reactivity with HDAC6 and therefore improving model calibration.

The high *in vitro* activity observed for HDAC6 may also indicate that the deacetylase domain 2 has lower substrate selectivity than the previously modeled HDAC8. However, the initial data (Table IV.2, Table IV.3, and Table IV.4) showing large variations in reactivity argue against a lack of substrate selectivity. Furthermore, the divergent structure and localization of HDAC6 compared to other HDACs argue against complete redundancy, although substrate overlap is common and structural accommodations including flexible surface architecture, such the dynamic loops flanking the active site of HDAC8, allow for accommodation of multiple substrates.[1, 43]

A caveat to the use of such a model is that it only analyzes the interface between the peptide substrate with the assumption that substrate selectivity can be deduced from local sequence interactions and does not take into account contribution of contacts apart from those directly adjacent to the active site. Distal contacts between enzyme and substrate may play a more prominent role in substrate selectivity, and the overall structure of the substrate and the location of the acetyl-lysine residue within structured or unstructured regions of the protein must be considered. Furthermore, our model is limited to catalytic domain 2, and CD1 and other HDAC6 domains likely play a part in substrate recognition. However, recent data comparing HDAC8 with peptide and protein substrates (Chapter III), does provide a precedent for substrate selectivity dependence on local sequence, even with short 6-mer segments as used in this study. This has not yet been tested with HDAC6, but a similar study could be adapted to test HDAC6 activity with peptide and protein substrates, and as HDAC6 is proposed to catalyze deacetylation of numerous cytoplasmic substrates, these proteins may be more amenable to *in vitro* study than other nuclear or membrane-bound proteins or protein complexes. Other regulatory functions including post-translational modifications, protein-protein interactions, cellular localization, and environmental conditions are likely to impact HDAC6 substrate selectivity and may play a significant role in regulating HDAC6 substrate selectivity and activity.

The fastest peptide substrate measured for HDAC6 corresponds to prelamin A (LMNA) K450ac with a $k_{cat}/K_M = 220{,}000\ M^{-1}s^{-1}$. Prelamin A is the precursor to lamin A, a predominant

structural component of the nuclear lamina responsible for supporting numerous nuclear functions.[44] Prelamin A is highly post-translationally modified by prenylation, phosphorylation, and acetylation, which assist in prelamin maturation and function, and many of these PTMs have been linked to disease. For example, a prelamin A variant K39E, prevents acetylation at that site, which leads to altered ventricular dilation and systolic function resulting in congestive heart failure, arrhythmia, and increased risk of premature death.[45] Moreover, lamin A has been shown to interact with other HDACs, including Sirt1, HDAC1/2, and HDAC3.[46] Although lamin A is nuclear and HDAC6 is considered predominantly cytoplasmic, HDAC6 is able to shuttle into the nucleus and has been implicated in non-cytoplasmic processes, and direct interactions with prelamin A, and other nuclear proteins, cannot be ruled out.[47] This is the first evidence for HDAC6 involvement in nuclear lamina regulation, and prelamin A may represent a novel HDAC6 substrate suggesting HDAC6 inhibition could be a therapeutic avenue in slowing the progress of LMNA-related diseases.

The peptide corresponding to K437ac of matrin 3 (MATR3), another internal nuclear matrix protein, was one of the fastest HDAC6 substrates. Matrin 3 associates with lamin A and is implicated in similar muscular impairment diseases, including amyotrophic lateral sclerosis (ALS), a fatal disorder caused by degeneration of motor neurons.[48] HDAC6i has been shown to ameliorate transport defects in ALS motor neurons, presumably through increased alpha-tubulin acetylation.[49] The potential interactions between HDAC6 and these nuclear matrix proteins warrants a closer investigation, as HDAC6-catalyzed deacetylation of these and other nuclear proteins may be important in disease progression.

Hsp90 (HSP90), kinesin (KIF5B), and CDK1 were three substrates with evidence of HDAC6 interactions in the literature. HDAC6 immunoprecipitates with Hsp90 in mouse fibroblasts, and HDAC6 genetic knockout and inhibition with tubacin and tubastatin lead to Hsp90 hyperacetylation and support a model for HDAC6-mediated Hsp90 activation whereby deacetylation of Hsp90 results in Hsp90 repressive complex disassociation and increased chaperone activity.[50] Our data support HDAC6-catalyzed deacetylation of Hsp90. Kinesin, like dynein, is a molecular motor responsible for intercellular trafficking along microtubules, and HDAC6 promotes kinesin association with microtubules, thus facilitating cargo transport.[51] While this is thought to be due to HDAC6 α-tubulin deacetylation and/or an activity-independent mechanism, our data suggest a direct role for HDAC6 in kinesin acetylation regulation and

function. Another putative substrate, cyclin-dependent kinase 1 (CDK1), has previously been reported in association with HDAC6 and both have implications in breast cancer.[52-53] Our data suggests CDK1 K33ac may be an HDAC6 substrate thus connecting HDAC6 with CDK1-regulation and by association with CDK1-directed diseases. Testing other known acetyl-lysine sites within these substrates may provide additional evidence for HDAC6 function with these proteins and processes.

Measuring HDAC6-catalyed deacetylation of additional peptides will be necessary to expand our knowledge of HDAC6 substrates and further develop the computational model. Key residues to test include peptides corresponding to putative substrates α-tubulin K40ac, cortactin, as well as additional Kac residues from Hsp90 such as K294ac, a residue important for chaperone function and hyperacetylated upon HDACi treatment.[54] Testing of an additional set of peptides predicted to be poor HDAC6 substrates using the current structure-based model will also be necessary to further calibrate the model. These peptides include additional TCOF1 (treacle protein) residues K146ac, K379ac, and K1414ac and proteins EIF5 (eukaryotic translation initiation factor 5) residue K28ac, COPA (coatomer subunit alpha) residue K74ac, RL4 (60S ribosomal protein L4) residue K162ac, and UBA1 (ubiquitin-like modifier-activating enzyme 1) residue K1024ac.

Taken together, the data described above provide evidence that HDAC6 recognizes sequence-specific determinants in substrates adjacent to the acetyl-lysine reside that contribute to the substrate selectivity of this enzyme. After further optimization of the model, we plan to use this algorithm to screen the PhosphoSitePlus database[38] of known human protein acetyl-lysines to identify additional putative HDAC6 substrates. Cross referencing identified substrates with known HDAC6 interactions and HDAC6-regulated processes will help identify important connections between HDAC6 substrates and cell homeostasis. Use of orthogonal *in vitro* and *in vivo* approaches, similar to studies previously described, will be important for further validating this computational model, determining the impact of substrate structure on HDAC6 selectivity, and comparing *in vitro* activity to cellular function. Screening tools, such as this HDAC6 structure-based identification model, will facilitate progress in defining the function and dysfunction of HDAC6, and deacetylases in general, in biological processes.

References

1. Seto, E.; Yoshida, M., Erasers of histone acetylation: the histone deacetylase enzymes. *Cold Spring Harbor perspectives in biology* **2014,** *6* (4), a018713-a018713.

2. Choudhary, C.; Weinert, B. T.; Nishida, Y.; Verdin, E.; Mann, M., The growing landscape of lysine acetylation links metabolism and cell signalling. *Nature reviews. Molecular cell biology* **2014,** *15* (8), 536-50.

3. Drazic, A.; Myklebust, L. M.; Ree, R.; Arnesen, T., The world of protein acetylation. *Biochimica et Biophysica Acta (BBA) - Proteins and Proteomics* **2016,** *1864* (10), 1372-1401.

4. Glozak, M. A.; Sengupta, N.; Zhang, X.; Seto, E., Acetylation and deacetylation of non-histone proteins. *Gene* **2005,** *363*, 15-23.

5. Choudhary, C.; Kumar, C.; Gnad, F.; Nielsen, M. L.; Rehman, M.; Walther, T. C.; Olsen, J. V.; Mann, M., Lysine acetylation targets protein complexes and co-regulates major cellular functions. *Science* **2009,** *325* (5942), 834-40.

6. Narita, T.; Weinert, B. T.; Choudhary, C., Functions and mechanisms of non-histone protein acetylation. *Nature Reviews Molecular Cell Biology* **2019,** *20* (3), 156-174.

7. Sadoul, K.; Khochbin, S., The growing landscape of tubulin acetylation: lysine 40 and many more. *The Biochemical journal* **2016,** *473* (13), 1859-68.

8. Mollapour, M.; Neckers, L., Post-translational modifications of Hsp90 and their contributions to chaperone regulation. *Biochimica et Biophysica Acta (BBA) - Molecular Cell Research* **2012,** *1823* (3), 648-655.

9. Falkenberg, K. J.; Johnstone, R. W., Histone deacetylases and their inhibitors in cancer, neurological diseases and immune disorders. *Nature reviews. Drug discovery* **2014,** *13* (9), 673-91.

10. Grozinger, C. M.; Hassig, C. A.; Schreiber, S. L., Three proteins define a class of human histone deacetylases related to yeast Hda1p. *Proc Natl Acad Sci U S A* **1999,** *96* (9), 4868-73.

11. Aldana-Masangkay, G. I.; Sakamoto, K. M., The role of HDAC6 in cancer. *J Biomed Biotechnol* **2011,** *2011*, 875824.

12. Beier, U. H.; Akimova, T.; Liu, Y.; Wang, L.; Hancock, W. W., Histone/protein deacetylases control Foxp3 expression and the heat shock response of T-regulatory cells. *Curr Opin Immunol* **2011,** *23* (5), 670-8.

13. Seidel, C.; Schnekenburger, M.; Dicato, M.; Diederich, M., Histone deacetylase 6 in health and disease. *Epigenomics* **2015,** *7* (1), 103-18.

14. Simoes-Pires, C.; Zwick, V.; Nurisso, A.; Schenker, E.; Carrupt, P. A.; Cuendet, M., HDAC6 as a target for neurodegenerative diseases: what makes it different from the other HDACs? *Mol Neurodegener* **2013,** *8*, 7.

15. Miyake, Y.; Keusch, J. J.; Wang, L.; Saito, M.; Hess, D.; Wang, X.; Melancon, B. J.; Helquist, P.; Gut, H.; Matthias, P., Structural insights into HDAC6 tubulin deacetylation and its selective inhibition. *Nature chemical biology* **2016,** *12* (9), 748-54.

16. Hai, Y.; Christianson, D. W., Histone deacetylase 6 structure and molecular basis of catalysis and inhibition. *Nature chemical biology* **2016,** *12* (9), 741-7.

17. Faria Freitas, M.; Cuendet, M.; Bertrand, P., HDAC inhibitors: a 2013-2017 patent survey. *Expert opinion on therapeutic patents* **2018**, 1-17.

18. Yee, A. J.; Bensinger, W.; Voorhees, P. M.; Berdeja, J. G.; Richardson, P. G.; Supko, J.; Tamang, D.; Jones, S. S.; Wheeler, C.; Markelewicz, R. J.; Raje, N. S., Ricolinostat (ACY-1215), the First Selective HDAC6 Inhibitor, in Combonation with Lenalidomide and Dexamethasone in Patients with Relapsed and Relapsed-and-Refractory Multiple Myeloma: Phase 1b Results (ACE-MM-101 Study). *Blood* **2015,** *126* (23), 3055.

19. Gregoretti, I. V.; Lee, Y. M.; Goodson, H. V., Molecular evolution of the histone deacetylase family: functional implications of phylogenetic analysis. *J Mol Biol* **2004,** *338* (1), 17-31.

20. Bali, P.; Pranpat, M.; Bradner, J.; Balasis, M.; Fiskus, W.; Guo, F.; Rocha, K.; Kumaraswamy, S.; Boyapalle, S.; Atadja, P.; Seto, E.; Bhalla, K., Inhibition of histone deacetylase 6 acetylates and disrupts the chaperone function of heat shock protein 90: a novel basis for antileukemia activity of histone deacetylase inhibitors. *The Journal of biological chemistry* **2005,** *280* (29), 26729-34.

21. Boyault, C.; Sadoul, K.; Pabion, M.; Khochbin, S., HDAC6, at the crossroads between cytoskeleton and cell signaling by acetylation and ubiquitination. *Oncogene* **2007,** *26* (37), 5468-76.

22. Hubbert, C.; Guardiola, A.; Shao, R.; Kawaguchi, Y.; Ito, A.; Nixon, A.; Yoshida, M.; Wang, X. F.; Yao, T. P., HDAC6 is a microtubule-associated deacetylase. *Nature* **2002,** *417* (6887), 455-8.

23. Zhang, Y.; Kwon, S.; Yamaguchi, T.; Cubizolles, F.; Rousseaux, S.; Kneissel, M.; Cao, C.; Li, N.; Cheng, H.-L.; Chua, K.; Lombard, D.; Mizeracki, A.; Matthias, G.; Alt, F. W.; Khochbin, S.; Matthias, P., Mice lacking histone deacetylase 6 have hyperacetylated

tubulin but are viable and develop normally. *Molecular and cellular biology* **2008,** *28* (5), 1688-1701.

24. Wang, X. X.; Wan, R. Z.; Liu, Z. P., Recent advances in the discovery of potent and selective HDAC6 inhibitors. *European journal of medicinal chemistry* **2018,** *143*, 1406-1418.

25. Alam, N.; Zimmerman, L.; Wolfson, N. A.; Joseph, C. G.; Fierke, C. A.; Schueler-Furman, O., Structure-Based Identification of HDAC8 Non-histone Substrates. *Structure (London, England : 1993)* **2016,** *24* (3), 458-68.

26. Olson, D. E.; Udeshi, N. D.; Wolfson, N. A.; Pitcairn, C. A.; Sullivan, E. D.; Jaffe, J. D.; Svinkina, T.; Natoli, T.; Lu, X.; Paulk, J.; McCarren, P.; Wagner, F. F.; Barker, D.; Howe, E.; Lazzaro, F.; Gale, J. P.; Zhang, Y.-L.; Subramanian, A.; Fierke, C. A.; Carr, S. A.; Holson, E. B., An unbiased approach to identify endogenous substrates of "histone" deacetylase 8. *ACS chemical biology* **2014,** *9* (10), 2210-6.

27. Wolfson, N. A.; Pitcairn, C. A.; Sullivan, E. D.; Joseph, C. G.; Fierke, C. A., An enzyme-coupled assay measuring acetate production for profiling histone deacetylase specificity. *Analytical biochemistry* **2014,** *456*, 61-9.

28. Lopez, J. E.; Haynes, S. E.; Majmudar, J. D.; Martin, B. R.; Fierke, C. A., HDAC8 Substrates Identified by Genetically Encoded Active Site Photocrosslinking. *Journal of the American Chemical Society* **2017,** *139* (45), 16222-16227.

29. Gurard-Levin, Z. A.; Kim, J.; Mrksich, M., Combining mass spectrometry and peptide arrays to profile the specificities of histone deacetylases. *Chembiochem : a European journal of chemical biology* **2009,** *10* (13), 2159-61.

30. Castaneda, C. A.; Wolfson, N. A.; Leng, K. R.; Kuo, Y. M.; Andrews, A. J.; Fierke, C. A., HDAC8 substrate selectivity is determined by long- and short-range interactions leading to enhanced reactivity for full-length histone substrates compared with peptides. *The Journal of biological chemistry* **2017,** *292* (52), 21568-21577.

31. Tropea, J. E.; Cherry, S.; Waugh, D. S., Expression and purification of soluble His(6)-tagged TEV protease. *Methods Mol Biol* **2009,** *498*, 297-307.

32. Wolfson, N. A. Determining HDAC8 Substrate Specificity. Dissertation, University of Michigan, 2014.

33. Huang, X.; Hernick, M., A fluorescence-based assay for measuring N-acetyl-1-D-myo-inosityl-2-amino-2-deoxy-alpha-D-glucopyranoside deacetylase activity. *Analytical biochemistry* **2011,** *414* (2), 278-81.

34. London, N.; Raveh, B.; Cohen, E.; Fathi, G.; Schueler-Furman, O., Rosetta FlexPepDock web server--high resolution modeling of peptide-protein interactions. *Nucleic acids research* **2011,** *39* (Web Server issue), W249-53.

35. Raveh, B.; London, N.; Zimmerman, L.; Schueler-Furman, O., Rosetta FlexPepDock ab-initio: simultaneous folding, docking and refinement of peptides onto their receptors. *PloS one* **2011,** *6* (4), e18934.

36. Kuhlman, B.; Dantas, G.; Ireton, G. C.; Varani, G.; Stoddard, B. L.; Baker, D., Design of a novel globular protein fold with atomic-level accuracy. *Science* **2003,** *302* (5649), 1364-8.

37. Alford, R. F.; Leaver-Fay, A.; Jeliazkov, J. R.; O'Meara, M. J.; DiMaio, F. P.; Park, H.; Shapovalov, M. V.; Renfrew, P. D.; Mulligan, V. K.; Kappel, K.; Labonte, J. W.; Pacella, M. S.; Bonneau, R.; Bradley, P.; Dunbrack, R. L.; Das, R.; Baker, D.; Kuhlman, B.; Kortemme, T.; Gray, J. J., The Rosetta All-Atom Energy Function for Macromolecular Modeling and Design. *Journal of Chemical Theory and Computation* **2017,** *13* (6), 3031-3048.

38. Hornbeck, P. V.; Zhang, B.; Murray, B.; Kornhauser, J. M.; Latham, V.; Skrzypek, E., PhosphoSitePlus, 2014: mutations, PTMs and recalibrations. *Nucleic acids research* **2015,** *43* (Database issue), D512-20.

39. UniProt Consortium, T., UniProt: the universal protein knowledgebase. *Nucleic acids research* **2018,** *46* (5), 2699-2699.

40. Uhlen, M.; Zhang, C.; Lee, S.; Sjostedt, E.; Fagerberg, L.; Bidkhori, G.; Benfeitas, R.; Arif, M.; Liu, Z.; Edfors, F.; Sanli, K.; von Feilitzen, K.; Oksvold, P.; Lundberg, E.; Hober, S.; Nilsson, P.; Mattsson, J.; Schwenk, J. M.; Brunnstrom, H.; Glimelius, B.; Sjoblom, T.; Edqvist, P. H.; Djureinovic, D.; Micke, P.; Lindskog, C.; Mardinoglu, A.; Ponten, F., A pathology atlas of the human cancer transcriptome. *Science* **2017,** *357* (6352).

41. Alberty, R. A.; Hammes, G. G., Application of the Theory of Diffusion-controlled Reactions to Enzyme Kinetics. *The Journal of Physical Chemistry* **1958,** *62* (2), 154-159.

42. Valenzuela-Fernandez, A.; Cabrero, J. R.; Serrador, J. M.; Sanchez-Madrid, F., HDAC6: a key regulator of cytoskeleton, cell migration and cell-cell interactions. *Trends in cell biology* **2008,** *18* (6), 291-7.

43. Kunze, M. B.; Wright, D. W.; Werbeck, N. D.; Kirkpatrick, J.; Coveney, P. V.; Hansen, D. F., Loop interactions and dynamics tune the enzymatic activity of the human histone deacetylase 8. *Journal of the American Chemical Society* **2013,** *135* (47), 17862-8.

44. Casasola, A.; Scalzo, D.; Nandakumar, V.; Halow, J.; Recillas-Targa, F.; Groudine, M.; Rincón-Arano, H., Prelamin A processing, accumulation and distribution in normal cells and laminopathy disorders. *Nucleus (Austin, Tex.)* **2016,** *7* (1), 84-102.

45. Arbustini, E.; Pilotto, A.; Repetto, A.; Grasso, M.; Negri, A.; Diegoli, M.; Campana, C.; Scelsi, L.; Baldini, E.; Gavazzi, A.; Tavazzi, L., Autosomal dominant dilated cardiomyopathy with atrioventricular block: a lamin A/C defect-related disease. *Journal of the American College of Cardiology* **2002,** *39* (6), 981-90.

46. Mattioli, E.; Andrenacci, D.; Garofalo, C.; Prencipe, S.; Scotlandi, K.; Remondini, D.; Gentilini, D.; Di Blasio, A. M.; Valente, S.; Scarano, E.; Cicchilitti, L.; Piaggio, G.; Mai, A.; Lattanzi, G., Altered modulation of lamin A/C-HDAC2 interaction and p21 expression during oxidative stress response in HGPS. *Aging cell* **2018,** *17* (5), e12824.

47. Liu, Y.; Peng, L.; Seto, E.; Huang, S.; Qiu, Y., Modulation of histone deacetylase 6 (HDAC6) nuclear import and tubulin deacetylase activity through acetylation. *The Journal of biological chemistry* **2012,** *287* (34), 29168-74.

48. Depreux, F. F.; Puckelwartz, M. J.; Augustynowicz, A.; Wolfgeher, D.; Labno, C. M.; Pierre-Louis, D.; Cicka, D.; Kron, S. J.; Holaska, J.; McNally, E. M., Disruption of the lamin A and matrin-3 interaction by myopathic LMNA mutations. *Human molecular genetics* **2015,** *24* (15), 4284-95.

49. Guo, W.; Naujock, M.; Fumagalli, L.; Vandoorne, T.; Baatsen, P.; Boon, R.; Ordovas, L.; Patel, A.; Welters, M.; Vanwelden, T.; Geens, N.; Tricot, T.; Benoy, V.; Steyaert, J.; Lefebvre-Omar, C.; Boesmans, W.; Jarpe, M.; Sterneckert, J.; Wegner, F.; Petri, S.; Bohl, D.; Vanden Berghe, P.; Robberecht, W.; Van Damme, P.; Verfaillie, C.; Van Den Bosch, L., HDAC6 inhibition reverses axonal transport defects in motor neurons derived from FUS-ALS patients. *Nature communications* **2017,** *8* (1), 861.

50. Boyault, C.; Zhang, Y.; Fritah, S.; Caron, C.; Gilquin, B.; Kwon, S. H.; Garrido, C.; Yao, T. P.; Vourc'h, C.; Matthias, P.; Khochbin, S., HDAC6 controls major cell response pathways to cytotoxic accumulation of protein aggregates. *Genes Dev* **2007,** *21* (17), 2172-81.

51. Reed, N. A.; Cai, D.; Blasius, T. L.; Jih, G. T.; Meyhofer, E.; Gaertig, J.; Verhey, K. J., Microtubule acetylation promotes kinesin-1 binding and transport. *Current biology : CB* **2006,** *16* (21), 2166-72.

52. Galindo-Moreno, M.; Giraldez, S.; Saez, C.; Japon, M. A.; Tortolero, M.; Romero, F., Both p62/SQSTM1-HDAC6-dependent autophagy and the aggresome pathway mediate CDK1 degradation in human breast cancer. *Scientific reports* **2017,** *7* (1), 10078.

53. Wang, Z.-T.; Chen, Z.-J.; Jiang, G.-M.; Wu, Y.-M.; Liu, T.; Yi, Y.-M.; Zeng, J.; Du, J.; Wang, H.-S., Histone deacetylase inhibitors suppress mutant p53 transcription via HDAC8/YY1 signals in triple negative breast cancer cells. *Cellular signalling* **2016,** *28* (5), 506-515.

54. Scroggins, B. T.; Robzyk, K.; Wang, D.; Marcu, M. G.; Tsutsumi, S.; Beebe, K.; Cotter, R. J.; Felts, S.; Toft, D.; Karnitz, L.; Rosen, N.; Neckers, L., An Acetylation Site in the Middle Domain of Hsp90 Regulates Chaperone Function. *Molecular Cell* **2007,** *25* (1), 151-159.

CHAPTER V

Conclusions and Future Directions

Overview

The research summarized in this dissertation is part of an on-going effort in the field of protein post-translational acetylation to better understand the intricacies of this important PTM, its function in biological systems, and the enzymes responsible for its regulation. The focus of this research has centered on the family of metal-dependent human deacetylases, the HDACs. Specifically, HDAC8 and HDAC6 are the targets of this research, which not only seeks to investigate and characterize their function and regulation, but also to develop tools and establish paradigms for HDAC research. HDAC8 and HDAC6 share commonalities and divergencies that serve to enlighten the field about shared functionality among HDACs and key differences in their regulation. Both HDAC8 and HDAC6 share canonical deacetylase domains with conserved active sites and divalent metal ion coordination.[1-4] Both have proposed functions in the cytoplasm and the nucleus of the cell, some of which, like cytoskeletal dynamics regulation, are shared, and the two enzymes even display overlap in putative substrates and/or interacting partners including Arid1A[5-6], Hsp90[7-8], and α-tubulin.[9] Additionally, HDAC8 and HDAC6 appear to play a role in some of the same disease pathologies, such as invasive breast cancer.[10-12] However, the two enzymes exhibit many differences. HDAC8 is a class I enzyme, sharing structural homology with yeast Rpd3, and the second smallest isozyme, with short C- and N-terminal sequences flanking its deacetylase domain.[13-15] On the other hand, HDAC6 is a class II enzyme, with homology to yeast Hda1, and the largest deacetylase, containing multiple domains including a second catalytic domain with different substrate specificity.[13-15] These structural differences allude to significantly different cellular roles. Indeed, HDAC8 and HDAC6 do not share many protein substrates, and are involved in numerous different physiological and disease pathologies.[16-17] Understanding the shared and unique functions of HDAC8 and HDAC6 is a priority in the field and will help us obtain a clearer picture of their specific roles and, more

importantly, inform us about key aspects of their function and regulation that may be used to our advantage to improve the quality of life for those afflicted with disorders caused or exacerbated by HDAC misregulation and dysfunction.

This dissertation discusses research into aspects of HDAC function and regulation concerning the impact of post-translational modifications and substrate structure and sequence on the activity of HDAC8 and HDAC6. Here, I have described new details regarding HDAC8 post-translational phosphorylation and how it may regulate substrate binding and activity through slight shifts in structure. I also share the results of a study to investigate differences between peptide and full-length protein substrates and reported a methodology for doing so that can be adapted to other HDACs and protein substrates. And finally, I have revealed the development of a new structure-based computational tool to screen and identify novel HDAC6 substrates. This chapter summarizes key findings and conclusions from each chapter and discusses their implications in the field and future approaches for furthering the study on these topics.

The Impact of HDAC8 Post-Translational Phosphorylation on Structure and Function

In chapter II, we share a study on HDAC8 phosphorylation and its impact on HDAC8 substrate selectivity. We use HDAC8 S39E as a phosphomimetic, where the serine residue targeted for phosphorylation is replaced with a bulky and negatively charged glutamate residue, to model the effect of the PTM in *in vitro* activity and structure. We also implement molecular dynamics simulations to compare and contrast the structures of native HDAC8, phosphorylated HDAC8 and the phosphomimetic HDAC8 mutant. Previously, PKA was identified as the kinase responsible for the unique phosphorylation of HDAC8 at position 39.[18] However, less is known about the impact of phosphorylation on HDAC8 function other than apparent downregulation for a few substrates. Several studies have reported on changes due to HDAC8 phosphorylation, such as increasing HDAC8 affinity for the protein human ever- shorter telomeres 1B (hEST1B), but no prior in-depth analyses have been performed on HDAC8 phosphorylation.[8]

Here, we have reported that the phosphomimetic mutant both decreases deacetylase activity and alters substrate selectivity, suggesting that phosphorylation at S39 serves as a means of regulating targets of HDAC8-catalyzed deacetylation. Crystallographic analyses of the phosphomimetic mutant provide an explanation for the decreased activity and altered selectivity. Crystal structures of S39E reveal minor alterations in the structure due to lost and altered

interactions, increased loop dynamics at the peptide binding interface, and structural differences at the active site, thus altering both the substrate binding interface and the active site. Molecular dynamics simulations demonstrated that similar changes were observed for the peptide binding interface in both the phosphomimetic mutant and the modeled phosphorylated enzyme that result in less favorable binding interactions and less efficient deacetylation. In summary, these data suggest that phosphorylation causes slight shifts in the structure that subtly alters the peptide binding groove and the active site. These changes affect peptide substrates differentially, thus altering HDAC8 substrate selectivity and potentially altering both HDAC8 activity and the regulation of HDAC8-specific cellular substrates. These results further our understanding of HDAC8 phosphorylation by providing evidence that HDAC8 phosphorylation may be used as a means of altering HDAC8 substrate selectivity in the cell and thus warranting further study to tease out specific cellular changes due to HDAC8 phosphorylation.

Firstly, although molecular dynamics simulations provide support for the similarities between the phosphomimetic mutant and phosphorylated wild-type enzyme and support the use of the S39E mutant as a viable surrogate, the analysis of phospho-HDAC8 would be ideal. Obtaining sufficient quantities of fully phosphorylated HDAC8 to crystallize and perform enzymatic activities has not been achieved thus far. However, several approaches may prove to yield the desired results. The first includes enzymatically phosphorylating HDAC8 through incubation with PKA followed by a phospho-enrichment step, most often used in phospho-proteomics studies.[19] It has yet to be determined if this will provide sufficient quantities and purity of phospho-HDAC8 rapidly enough to maintain HDAC8 structure and activity; however, an anti-phosphotyrosine antibody immobilized agarose resin was used to successfully separate phospho-calmodulin from non-phosphorylated calmodulin.[20] Another technique recently reported by Jason Chin, is the use of a similar method to what was described in Chapter III to incorporate a phosphoserine residue during protein expression by means of non-natural amino acid incorporation.[21] Although non-natural amino acid incorporation often decreases protein expression, this would yield HDAC8 with the desired modification. Additionally, this technique could be used to express phospho-HDAC8 in mammalian cells thus allowing for analysis under more physiological relevant conditions.

Secondly, profiling additional substrates, both peptides and proteins as in Chapter III, would be necessary to investigate whether phosphorylation of HDAC8 leads to even larger

changes in substrate selectivity. Developing a model of peptide binding to phospho-HDAC8, facilitated by the available crystal structure of S39E, may accelerate this process by identifying peptides that might bind more favorably to phospho-HDAC8 than to wild type. Future crystal structures using the same ligand for both wild-type and phospho-/S39E HDAC8 would enhance the development of the structural model. Additionally, analysis of activity changes with acetylated protein substrates are needed to further clarify the functional role of phosphorylation of HDAC8.

Lastly, to establish relevant connections between the altered activity observed with peptides *in vitro* and changes to HDAC8 cellular function, recently reported approaches and methods currently under development may be implemented to study HDAC8 phosphorylation in a cellular context. One method is the use of active-site directed chemical covalent capture to identify HDAC8 substrates by genetically incorporating a photocrosslinker, such as p-benzoyl-L-phenylalanine (Bpa), into the structure of phospho- or S39E HDAC8 to capture transient interactions in cell lysates and live cells.[22] This method was used to identify 119 putative substrates of wild-type HDAC8 in HEK293 cell lysates.[22] Briefly, HDAC8 harboring an amber codon mutation at a selected location adjacent to the active site is co-expressed with an orthogonal p-benzoyl-L-phenylalanyl-tRNA synthetase (BpaRS)-tRNATyrCUA pair in E. coli supplemented with Bpa. When combined with cell lysates and exposed to light, HDAC8 photocrosslinks with interactors near the photocrosslinker site, and these interactors can be detected and identified using mass spectrometry. A similar approach adapted for use in live cells is currently under development. Comparing the photocrosslinking results of phospho- or S39E HDAC8 with that of wild-type could provide deeper insight into the regulatory role of HDAC8 phosphorylation.

A second method is to use mass spectrometry to measure changes in acetylated proteins in cells upon perturbation of HDAC8.[6] This method was used to identify multiple HDAC8 putative substrates, including SMC3, in MCF-7 cells treated with HDAC8-specific inhibitor PCI-34051.[6] Briefly, HDAC8 was expressed in MCF-7 cells grown in different media types containing normal, heavy, or light arginine and lysine and treated with the inhibitor PCI-34051 and with a structurally similar non-inhibitor BRD3811 and DMSO as negative controls. Using SILAC(stable isotope labeling of amino acids in cell culture)-based mass spectrometry, relative amounts of acetylated proteins were quantified and compared between the three groups to

identify putative HDAC8 substrates demonstrating hyperacetylation in the inhibitor treatment group. This approach could be adapted to look for changes due to phospho- or S39E HDAC8 by comparing the results from wild-type HDAC8 to results obtained with cells expressing phospho- or S29E HDAC8 or cells treated with a PKA activator. In place of SILAC-based mass spectrometry, an alternative approach is to use a proximity ligation assay (described in the next section) to identify putative substrates and quantify changes in acetylation.[23]

These methods may be used to determine whether phosphorylation of HDAC8 affects sister chromatid cohesion through SMC3 hyperacetylation, since the S39E mutation nearly abolished HDAC8 activity with an SMC3 peptide. Phosphorylation is often used by the cell to regulate protein function and is common among the HDACs.[24] However, phosphorylation within the deacetylase domain as a negative regulator of activity is unique to HDAC8 and serves as an opportunity to better understand HDAC8-specific function and cellular regulation and also to highlight potential approaches for HDAC8-specific targeting with small molecule modulators.[18]

Comparing Protein and Peptide Substrates and the Impact of Structure on HDAC8

In chapter III, HDAC8 deacetylase activity for three acetyl-lysine residues located on the N-terminal tail of Histone H3, H3K9ac, H3K14ac, and H3K56ac, in several different contexts was measured and compared. Using the acetate assay, HDAC8-catalyzed deacetylation of histone H3 was measured for 7-mer, 13-mer, and 17-mer sequences, and a mass spectrometry assay optimized for quantification of specific post-translationally modified histone residues was used to measure full-length tetrameric, octameric, and nucleosomal histone H3. Comparison of the catalytic efficiencies measured for peptides compared to proteins revealed that changing the size and structure of the substrate enhanced activity, with 30-300-fold enhanced catalytic efficiency and activities up to 10^4 M^{-1} s^{-1} for tetrameric H3K9ac compared to its corresponding peptides. Although the reactivity trends differed slightly, K9ac was a better substrate than K14ac for both peptides and full-length substrates. K9 is located only 4 residues away from K14 and both are within the unstructured region of the H3 tail. This differential reactivity provides compelling evidence that the local sequence affects HDAC8 substrate selectivity even in the context of a protein and supports the use of peptides to determine substrate selectivity.

Although the reactivity of HDAC8 with the peptide containing K56ac is similar to that of K9ac (within 2-fold), in the context of the tetrameric H3/H4 protein, K56ac reactivity did not increase to the same extent as that of K9ac (~50-fold for K56ac and ~300-fold for K9ac). K56

lies within a more structured region of the first α-helix in histone H3 thus suggesting that the structural context of the acetylated lysine also plays a pronounced role in determining HDAC8 substrate selectivity. Finally, introducing DNA into the octameric H3K9ac structure drastically reduced the catalytic efficiency compared to tetrameric and octameric H3K9ac, possibly due to the altered electrostatic charge or any changes in the structure or dynamics of the complex due to DNA incorporation. In contrast to the DNA-free protein complexes, HDAC8 catalytic efficiency for the nucleosome H3K9ac substrate was within the same order of magnitude as the acetylated peptide substrates thus underscoring the importance of local enzyme-substrate interactions in determining substrate selectivity. These results also suggest that for efficient HDAC8-catalyzed deacetylation of histones, remodeling factors may be necessary to alter chromatin reorganization and enhance DNA-histone dissociation.

This is the first time HDAC activity has been directly measured for full-length substrates and the first time the validity of using peptide substrates to draw conclusions about HDAC activity with proteins has been tested. This study marks an important milestone in HDAC research, allowing for in-depth analysis of HDAC activity with full-length substrates. However, several challenges remain. First, this method has been optimized for the analysis of single histone protein post-translational modifications, and while this approach can be easily adapted for use with any HDAC isozyme and any histone acetyl-lysine, expanding beyond single histone modifications will take further optimization. Since histones are often modified in more than one location, one question that remains to be answered is how multiple PTMs affect the substrate recognition of HDACs. Comparing HDAC-catalyzed deacetylation of substrates with two or more genetically incorporated acetyl-lysines (or other modification) could provide answers to these questions. Second, the methods for preparing full-length, singly acetylated substrates using non-natural amino acid incorporation is currently limited mainly to proteins that can be expressed and purified from *E. coli*. This limits analysis of many putative HDAC substrates due to large sizes, insolubility, and poor stability. Finally, as this study is designed to look specifically at a single interaction in isolation, important factors may be missed, such as protein concentration, substrate PTMs including multiple acetylation sites, cell status, and the presence of binding partners, that would otherwise be present in a normal functioning cell.

While some of these challenges are inherent in this type of research, this does highlight the need for new and improved methodologies for measuring HDAC-mediated deacetylation of

cellular substrates that can be easily adapted to a wide variety of substrates. One such method that is currently under development is the proximity ligation assay.[23, 25] This assay is performed in living cells, allowing for the study of multiple cell lines and therefore different contexts of HDAC activity, and utilizes HDAC-specific inhibition (small molecules), knock-down (RNAi), or knock-out (gene deletion/silencing) to measure changes in the acetylation levels of HDAC-specific substrates. The method for studying these changes in acetylation levels combines specific targeting of a given substrate and acetyl-lysine PTM using two antibodies, one against the substrate of interest and one against acetyl-lysine, with sensitive quantification of the acetylated substrate. In order to quantify the levels of the target acetylated protein, the two antibodies are modified with complementary segments of DNA such that when the two antibodies are within close proximity to each other, as would be the case when the antibodies targeting the protein and the acetyl-lysine are bound to the same molecule, the two complementary segments ligate together (method under development). These ligated segments can be sensitively quantified using real-time quantitative reverse transcription PCR (qRT-PCR) thus providing the acetylation status of a protein of interest that can be compared under different conditions, such as HDAC-specific inhibition.[26]

However, this approach does not demonstrate direct activity, since the signal (increased acetylation) is merely the response to the cue (HDACi). Additional control experiments would be necessary to test direct HDAC deacetylation. Inhibition of the other HDACs, for example, can be used to verify that the observed response is due to the activity of one isozyme. Moreover, the photocrosslinking method described in the previous section can be implemented to provide evidence of direct interactions between HDAC and substrate.[22] There is still much to be done to fully develop these tools to be used in place of or as an orthogonal approach to study direct HDAC activity with cellular substrates. In the meantime, the data presented in chapter III supports the continued use of peptide surrogates to screen and test HDAC activity as well as the adaption of the mass spectrometry approaches described in this chapter to measure HDAC-catalyzed deacetylation of other histone and non-histone substrates.

Profiling HDAC6 Substrate Specificity

In chapter IV, we report on the development of a structure-based approach to predict HDAC6 binding and activity using *in vitro* HDAC6 activity measurements and computer-based modeling of HDAC6-substrate interactions. Measurements of HDAC6-catalyzed deacetylation

of short, 6-mer, singly-acetylated peptide substrates are used to calibrate and optimize computational calculations in order to develop a structural model of peptide binding capable of distinguishing between HDAC6 peptide binders and non-binders and therefore between excellent and poor peptide substrates. Using such a model, large volumes of sequences can be rapidly screened to identify candidate HDAC6 substrates. Such a model has been developed using HDAC8 capable of reliably predicting HDAC8 activity *in vitro* with peptides.[27] Recently published crystal structures of HDAC6 have allowed for the development of a similar tool to study HDAC6 interactions thus accelerating the process of identifying relevant HDAC6 substrates.[14-15] Profiling HDAC6 activity with a library of peptides has revealed a wide array of catalytic efficiencies ranging from 12 to 220,000 M^{-1} s^{-1}. This indicates that HDAC6 has strong local sequence structural determinants that alter reactivity. Comparing the sequences of the best substrates with those of the poorest substrates does not reveal any obvious patterns, so a computational model was developed to identify the most energetically favorable sequences for HDAC-peptide binding.

Using the Rosetta framework and modules developed for modeling peptide binding, a starting template structure was identified of the best substrate docked into the catalytic pocket of HDAC6 using FlexPepDock. The screening module FlexPepBind was used to calibrate binding to identify the structure that yielded the best correlation between computational score and HDAC6 activity. The resulting model has successfully been able to identify good HDAC6 substrates. However, since the median activity for tested sequences is 2,500 M^{-1} s^{-1} indicating that, depending on what *in vitro* activity correlates to HDAC6 activity in cells, there are more good substrates than bad substrates in our peptide library and HDAC6 may show more substrate promiscuity than other isozymes, the model is still being optimized to identify poor binders. However, with peptide substrates measured thus far, the correlation between the interface score and measured peptide reactivity is promising and statistically significant with a correlation of R= -0.62 and p = <0.0001. This study represents the first report of such a wide dynamic range for HDAC6 activity as well as the first computational structure-based binding model for HDAC6 to identify novel HDAC6 substrates. Once the model is optimized to the point of identifying sequences with favorable and unfavorable interactions, the model can be used to screen the human acetylome using sequences deposited into the PhosphoSitePlus database.[28]

Moving forward, the highest rated hits will be selected as putative substrates from the best-documented sequences with strong evidence for acetylation (i.e. >5 reports including references to both high and low throughput studies with independent validation) and special attention paid towards known disease-related residues, sequences, and/or modifications. With putative substrates in-hand, we will begin efforts towards validating our findings and providing further evidence for HDAC6 interaction as described in Chapter IV using *in vitro* analysis of acetylated peptides and proteins. HDAC6 activity with the putative substrates can be further investigated in cells using HDAC6-specific inhibition or genetic knockout cell lines to observe changes in target protein acetylation either through simpler and less-sensitive methods such as western blot analysis or more sensitive methods such as mass spectrometry or the chemical ligation assay described above.[6, 23, 29-30] Additionally, the active-site directed covalent capture in cell lysates and live cells, as described above, could be implemented to identify HDAC6-specific interactions under physiological conditions.

One challenge to these approaches is isolating the contribution of HDAC6 activity to the regulation of a specific protein or pathway from that of other deacetylases. As previously mentioned, overlapping activity between isozymes is common, and the regulation of HDAC6 activity is not well documented.[31] We do not yet understand how one HDAC may compensate for the loss of activity of another, whether multiple isozymes react interchangeably and to the same extent given isozyme availability, or whether HDAC-specific activity is tissue- or organelle-specific. This is an ongoing question in the field. Expanding tools such as computational modeling of HDAC activity to encompass the whole family of histone deacetylases may elucidate the extent of the overlap of substrate selectivity and identify the functional contributions of each enzyme. In tandem with the development of potent isozyme-specific inhibitors, rational decisions can be made to identify which isozyme or isozymes would be most effective to target in a given disease pathology while maintaining the activity of the other isozymes and thus reducing toxicity from unnecessary loss of activity and expanding the therapeutic window of a treatment based on HDAC inhibition.

Concluding Remarks

Since the first mention of protein acetylation in the mid-20th century, we have sought to understand the purpose and regulation of this PTM, especially in light of the association of aberrant acetylation with human disease.[32-33] Advances during the last 50+ years, and in

particular over the past decade, have allowed discovery of the broad impact of protein acetylation. Studying the regulatory enzymes behind this modification provides a window into the tightly regulated process and the complexity of the impact acetylation has in maintaining cellular homeostasis. The family of histone deacetylases has been a central focus in acetylation research. The field has solved their crystal structures, elucidated their mechanisms, developed potent inhibitors for them, and studied their function in normal and disordered cells, tissues, and animals. However, there is much left to do to complete our understanding of these enzymes and of acetylation as a whole. As is often the case in research, when one question is answered, many new questions arise, and the more we discover about acetylation, the enzymes that regulate it, and the processes it regulates, the more we realize how much we have left to understand. The drive to find the answers to these questions is what makes the field of acetylation so compelling, and it fuels our continued search into the function of these fascinating enzymes.

References

1. Buggy, J. J.; Sideris, M. L.; Mak, P.; Lorimer, D. D.; McIntosh, B.; Clark, J. M., Cloning and characterization of a novel human histone deacetylase, HDAC8. *The Biochemical journal* **2000,** *350 Pt 1*, 199-205.

2. Hu, E.; Chen, Z.; Fredrickson, T.; Zhu, Y.; Kirkpatrick, R.; Zhang, G. F.; Johanson, K.; Sung, C. M.; Liu, R.; Winkler, J., Cloning and characterization of a novel human class I histone deacetylase that functions as a transcription repressor. *The Journal of biological chemistry* **2000,** *275* (20), 15254-64.

3. Van den Wyngaert, I.; de Vries, W.; Kremer, A.; Neefs, J.; Verhasselt, P.; Luyten, W. H.; Kass, S. U., Cloning and characterization of human histone deacetylase 8. *FEBS letters* **2000,** *478* (1-2), 77-83.

4. Grozinger, C. M.; Hassig, C. A.; Schreiber, S. L., Three proteins define a class of human histone deacetylases related to yeast Hda1p. *Proc Natl Acad Sci U S A* **1999,** *96* (9), 4868-73.

5. Bitler, B. G.; Wu, S.; Park, P. H.; Hai, Y.; Aird, K. M.; Wang, Y.; Zhai, Y.; Kossenkov, A. V.; Vara-Ailor, A.; Rauscher, F. J., III; Zou, W.; Speicher, D. W.; Huntsman, D. G.; Conejo-Garcia, J. R.; Cho, K. R.; Christianson, D. W.; Zhang, R., ARID1A-mutated ovarian cancers depend on HDAC6 activity. *Nature cell biology* **2017,** *19* (8), 962-973.

6. Olson, D. E.; Udeshi, N. D.; Wolfson, N. A.; Pitcairn, C. A.; Sullivan, E. D.; Jaffe, J. D.; Svinkina, T.; Natoli, T.; Lu, X.; Paulk, J.; McCarren, P.; Wagner, F. F.; Barker, D.; Howe, E.; Lazzaro, F.; Gale, J. P.; Zhang, Y. L.; Subramanian, A.; Fierke, C. A.; Carr, S. A.; Holson, E. B., An unbiased approach to identify endogenous substrates of "histone" deacetylase 8. *ACS chemical biology* **2014,** *9* (10), 2210-6.

7. Bali, P.; Pranpat, M.; Bradner, J.; Balasis, M.; Fiskus, W.; Guo, F.; Rocha, K.; Kumaraswamy, S.; Boyapalle, S.; Atadja, P.; Seto, E.; Bhalla, K., Inhibition of histone deacetylase 6 acetylates and disrupts the chaperone function of heat shock protein 90: a novel basis for antileukemia activity of histone deacetylase inhibitors. *The Journal of biological chemistry* **2005,** *280* (29), 26729-34.

8. Lee, H.; Sengupta, N.; Villagra, A.; Rezai-Zadeh, N.; Seto, E., Histone deacetylase 8 safeguards the human ever-shorter telomeres 1B (hEST1B) protein from ubiquitin-mediated degradation. *Mol Cell Biol* **2006,** *26* (14), 5259-69.

9. Vanaja, G. R.; Ramulu, H. G.; Kalle, A. M., Overexpressed HDAC8 in cervical cancer cells shows functional redundancy of tubulin deacetylation with HDAC6. *Cell Communication and Signaling* **2018,** *16* (1), 20.

10. Chakrabarti, A.; Oehme, I.; Witt, O.; Oliveira, G.; Sippl, W.; Romier, C.; Pierce, R. J.; Jung, M., HDAC8: a multifaceted target for therapeutic interventions. *Trends in pharmacological sciences* **2015,** *36* (7), 481-92.

11. Seidel, C.; Schnekenburger, M.; Dicato, M.; Diederich, M., Histone deacetylase 6 in health and disease. *Epigenomics* **2015,** *7* (1), 103-18.

12. Park, S. Y.; Jun, J. A.; Jeong, K. J.; Heo, H. J.; Sohn, J. S.; Lee, H. Y.; Park, C. G.; Kang, J., Histone deacetylases 1, 6 and 8 are critical for invasion in breast cancer. *Oncol Rep* **2011,** *25* (6), 1677-81.

13. Vannini, A.; Volpari, C.; Filocamo, G.; Casavola, E. C.; Brunetti, M.; Renzoni, D.; Chakravarty, P.; Paolini, C.; De Francesco, R.; Gallinari, P.; Steinkuhler, C.; Di Marco, S., Crystal structure of a eukaryotic zinc-dependent histone deacetylase, human HDAC8, complexed with a hydroxamic acid inhibitor. *Proc Natl Acad Sci U S A* **2004,** *101* (42), 15064-9.

14. Miyake, Y.; Keusch, J. J.; Wang, L.; Saito, M.; Hess, D.; Wang, X.; Melancon, B. J.; Helquist, P.; Gut, H.; Matthias, P., Structural insights into HDAC6 tubulin deacetylation and its selective inhibition. *Nature chemical biology* **2016,** *12* (9), 748-54.

15. Hai, Y.; Christianson, D. W., Histone deacetylase 6 structure and molecular basis of catalysis and inhibition. *Nature chemical biology* **2016,** *12* (9), 741-7.

16. Wolfson, N. A.; Pitcairn, C. A.; Fierke, C. A., HDAC8 substrates: Histones and beyond. *Biopolymers* **2013,** *99* (2), 112-26.

17. Simoes-Pires, C.; Zwick, V.; Nurisso, A.; Schenker, E.; Carrupt, P. A.; Cuendet, M., HDAC6 as a target for neurodegenerative diseases: what makes it different from the other HDACs? *Mol Neurodegener* **2013,** *8*, 7.

18. Lee, H.; Rezai-Zadeh, N.; Seto, E., Negative Regulation of Histone Deacetylase 8 Activity by Cyclic AMP-Dependent Protein Kinase A. *Molecular and Cellular Biology* **2004,** *24* (2), 765-773.

19. Schmidt, S. R.; Schweikart, F.; Andersson, M. E., Current methods for phosphoprotein isolation and enrichment. *Journal of chromatography. B, Analytical technologies in the biomedical and life sciences* **2007,** *849* (1-2), 154-62.

20. Palomo-Jimenez, P. I.; Hernandez-Hernando, S.; Garcia-Nieto, R. M.; Villalobo, A., A method for the purification of phospho(Tyr)calmodulin free of nonphosphorylated calmodulin. *Protein Expr Purif* **1999,** *16* (3), 388-95.

21. Beranek, V.; Reinkemeier, C. D.; Zhang, M. S.; Liang, A. D.; Kym, G.; Chin, J. W., Genetically Encoded Protein Phosphorylation in Mammalian Cells. *Cell Chem Biol* **2018,** *25* (9), 1067-1074.e5.

22. Lopez, J. E.; Haynes, S. E.; Majmudar, J. D.; Martin, B. R.; Fierke, C. A., HDAC8 Substrates Identified by Genetically Encoded Active Site Photocrosslinking. *Journal of the American Chemical Society* **2017,** *139* (45), 16222-16227.

23. Jiao, J.; Han, R.; Hancock, W. W.; Beier, U. H., Proximity Ligation Assay to Quantify Foxp3 Acetylation in Regulatory T Cells. In *HDAC/HAT Function Assessment and Inhibitor Development: Methods and Protocols*, Krämer, O. H., Ed. Springer New York: New York, NY, 2017; pp 287-293.

24. Brandl, A.; Heinzel, T.; Kramer, O. H., Histone deacetylases: salesmen and customers in the post-translational modification market. *Biology of the cell / under the auspices of the European Cell Biology Organization* **2009,** *101* (4), 193-205.

25. Bellucci, A.; Fiorentini, C.; Zaltieri, M.; Missale, C.; Spano, P., The "in situ" proximity ligation assay to probe protein-protein interactions in intact tissues. *Methods Mol Biol* **2014,** *1174*, 397-405.

26. Heid, C. A.; Stevens, J.; Livak, K. J.; Williams, P. M., Real time quantitative PCR. *Genome research* **1996,** *6* (10), 986-94.

27. Alam, N.; Zimmerman, L.; Wolfson, N. A.; Joseph, C. G.; Fierke, C. A.; Schueler-Furman, O., Structure-Based Identification of HDAC8 Non-histone Substrates. *Structure (London, England : 1993)* **2016,** *24* (3), 458-68.

28. Hornbeck, P. V.; Zhang, B.; Murray, B.; Kornhauser, J. M.; Latham, V.; Skrzypek, E., PhosphoSitePlus, 2014: mutations, PTMs and recalibrations. *Nucleic acids research* **2015,** *43* (Database issue), D512-20.

29. Wieczorek, M.; Guhrs, K. H.; Heinzel, T., Assessment of HDACi-Induced Acetylation of Nonhistone Proteins by Mass Spectrometry. *Methods Mol Biol* **2017,** *1510*, 313-327.

30. de Zoeten, E. F.; Wang, L.; Butler, K.; Beier, U. H.; Akimova, T.; Sai, H.; Bradner, J. E.; Mazitschek, R.; Kozikowski, A. P.; Matthias, P.; Hancock, W. W., Histone deacetylase 6 and heat shock protein 90 control the functions of Foxp3(+) T-regulatory cells. *Mol Cell Biol* **2011,** *31* (10), 2066-78.

31. Seto, E.; Yoshida, M., Erasers of histone acetylation: the histone deacetylase enzymes. *Cold Spring Harbor perspectives in biology* **2014,** *6* (4), a018713-a018713.

32. Timmermann, S.; Lehrmann, H.; Polesskaya, A.; Harel-Bellan, A., Histone acetylation and disease. *Cellular and molecular life sciences : CMLS* **2001,** *58* (5-6), 728-36.

33. Haberland, M.; Montgomery, R. L.; Olson, E. N., The many roles of histone deacetylases in development and physiology: implications for disease and therapy. *Nature reviews. Genetics* **2009,** *10* (1), 32-42.